The role of water in hydrogen electrocatalysis
Ledezma Yanez, I.D.

Citation
Ledezma Yanez, I. D. (2016, June 9). *The role of water in hydrogen electrocatalysis*. Retrieved from https://hdl.handle.net/1887/40161

Cover Page

Universiteit Leiden

The handle http://hdl.handle.net/1887/40161 holds various files of this Leiden University dissertation

Author: Ledezma Yanez, Isis
Title: The role of water in hydrogen electrocatalysis
Issue Date: 2016-06-09

THE ROLE OF WATER IN HYDROGEN ELECTROCATALYSIS

PROEFSCHRIFT

ter verkrijging van
de graad van Doctor aan de Universiteit Leiden,
op gezag van de Rector Magnificus prof. mr. C. J. J. M. Stolker,
volgens besluit van het College voor Promoties
te verdedigen op donderdag 9 juni 2016
klokke 16:15 uur

door

Isis Ledezma Yanez

geboren te Barquisimeto (Venezuela) in 1983

Be resilient.

Contents

1. Introduction

1.1. Motivation

This work is part of a larger project from our research group, focused on a better understanding of the role of the solvent in electrocatalytic reactions. The main project is subdivided in the following three different approaches: the first project involves the use of ultra-high vacuum techniques (UHV) for the study of H_2 and O_2 dissociation on stepped platinum surfaces covered with water. The research is carried by MSc. Cansin Badan, as his PhD project in the UHV section of the group, under the supervision of Dr. Ludo Juurklink. The second project comprises a detailed computational study, to be found in the PhD thesis entitled: "Water Related Adsorbates on Stepped Platinum Surfaces", by MSc. Manuel Kolb. The third project is presented in this thesis, and pertains to the study of the role of the solvent in the electrocatalysis of hydrogen evolution and oxidation in a "wet" non-aqueous solvent and in alkaline solutions, joining the efforts for a future sustainable hydrogen production and conversion.

Currently, we produce H_2 primarily from the steam-reforming process[1], and from water electrolysis[2] in a less prominent way. The hydrogen produced is mainly used for processes such as oil refining and in the Haber-Bosch reaction for ammonia synthesis. The ideal picture contemplates a far-reaching use: a hydrogen-based economy[3], where electrolysers driven by renewable energy (solar and wind) are used for splitting water into hydrogen and oxygen with low energy losses. These fuels would be piped to the industry, cities and fuel stations as feedstock for chemical reactors, and for the built-in fuel cells for domestic appliances and cars[3b], replacing the use of fossil fuels in a large sector of human activities. The excess could be stored when the supply exceeds the demand. As an extra positive outcome, we would have attained environmental progress by diminishing the greenhouse gas emissions.

The truth is that the sustainable water splitting technologies are still far from scalable and affordable. The electrolyser technologies use rather expensive

catalysts for the anodic oxygen evolution, based on rare metal oxides such as IrO_2 and RuO_2 in acidic environment, which also yield a good turnover for hydrogen production whenever the cathode is made out of platinum. On the other hand, several theoretical[4] and experimental[5] efforts have been put forward for the scalability of the oxygen evolution in alkaline media, allowing the use of anodes made from perovskites or earth-abundant metal oxides, such as Ni, Mn and Fe, lowering the cost of production and improving reaction rates, since these metal oxides and perovskites are proven to be stable and cost-efficient. However, the hydrogen evolution in alkaline solutions presents slow reaction rates[6], leading to an overpotential at the cathode, which translates into energy losses.

Although the hydrogen evolution reaction has been intensely studied, the efforts have been consistently focused on the design of good catalysts, overlooking the role of the solvent. Consequently, a systematic study of the electrolyte interactions in the hydrogen electrocatalysis seems appropriate. We strongly believe that a better understanding of the solvent-intermediates, solvent-electrolyte and solvent-catalyst interactions is fundamental for improving the hydrogen electrocatalysis, and could be extended to several other electrocatalytic reactions involving water, contributing to a more realistic description of the processes occurring at the electrode-electrolyte interface.

1.2. Hydrogen electrocatalysis on platinum

In 1928, Bowden[7] described an adsorbed layer of hydrogen near the equilibrium potential for H_2/H^+, deposited on the surface of a thin layer of Pt on a Hg electrode. Later, in 1934, Frumkin and Shalygin[8] gave evidence of the adsorption of hydrogen on a platinum electrode before the equilibrium potential, i.e. at potentials positive to the H_2/H^+ equilibrium potential. It was until 1956 when Breiter *et al.*[9] identified two different forms of hydrogen adsorbed on platinum, coming back seven years after with a well-defined model for the strongly and

weakly adsorbed hydrogen on platinum electrodes[10]. The model was based on Langmuir and Frumkin isotherms. The species identified were the hydrogen deposited positive of the equilibrium potential, known as underpotential deposited hydrogen, or H-UPD, and another type of hydrogen deposited negative of the equilibrium potential, commonly called overpotential deposited hydrogen or H-OPD.

Once these adsorbed forms of hydrogen on platinum were identified, questions were redirected towards their kinetics of formation and their role in the hydrogen oxidation and evolution reactions. From the early studies, we pay special attention to those reported by Conway on kinetics[6a], followed by the structure sensitivity of the reaction[11], the kinetics of H-UPD/H-OPD in alkaline media[12] and the consequences of the coadsorption of anionic species[13]. More recently, Yan *et al.* reported[14] that the binding energy of hydrogen atoms to the polycrystalline platinum surface is the sole descriptor for the hydrogen oxidation and evolution in aqueous media. These studies refuelled the discussion on the origin of the pH dependence of the hydrogen evolution, for which a plausible explanation is still missing.

In acid media, the overall electrochemical hydrogen reaction is

$$2H^+ + 2e^- \rightarrow H_2 \tag{Eq. 1}$$

Whereas for alkaline media we write

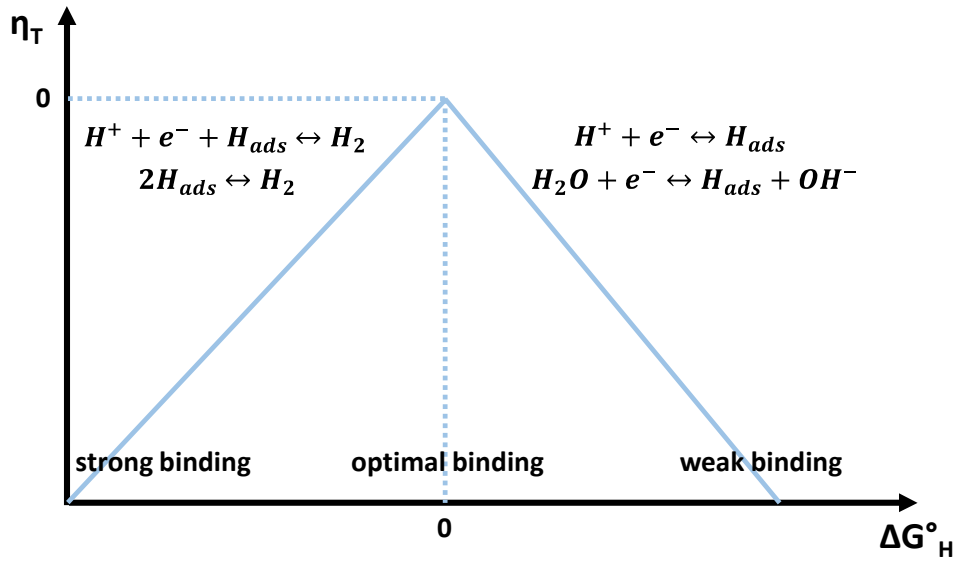$$2H_2O + 2e^- \rightarrow H_2 + 2OH^- \tag{Eq. 2}$$

The key step for the hydrogen evolution reaction is the adsorption of atomic hydrogen on the electrode surface (Volmer step), with one electron transfer:

$$H^+ + e^- + * \rightarrow H_{ADS} \tag{Eq. 3}$$

It is known that from (Eq. 3) to hydrogen evolution, two routes should be considered; i) the combination of two H_{ADS} on the electrode surface to produce H_2, known as the Tafel step, or ii) the combination of H_{ADS} with one proton and one electron transfer to give H_2, known as the Heyrovsky step[15].

In the overall mechanism for hydrogen evolution, there will be one step with the least favourable reduction potential, or the least favourable thermodynamics (in case of a chemical step), and this step is usually identified as the rate-determining step (or rather potential-determining step) for the hydrogen evolution to proceed. In the simplest model, the thermodynamics of these steps depends on only a single parameter, or "descriptor", namely the free binding energy of hydrogen to the catalyst, ΔG_H°.

In Figure 1 we illustrate the relationship between the thermodynamic overpotential, η, which corresponds to the potential difference between the equilibrium potential of the H_2/H^+ redox couple and the extra driving force (potential) necessary for the reaction to proceed; and the binding energy of the atomic hydrogen to the metal, ΔG_H° . The plot is based on the Sabatier principle[16], which predicts that the ideal catalyst binds the intermediate in a balanced way; neither too strongly nor too weakly. In an ideal catalyst, the zero overpotential is achieved when each reaction step is thermodynamically neutral, because the reaction does not need to overcome energetic barriers (the optimal binding energy at the top of the volcano). So far, this relationship is the most accepted descriptor for the hydrogen electrocatalysis, and ΔG_H° is considered as the sole descriptor of the hydrogen evolution rate. However, the question remains how the solvent influences the rate-determining step; in other words, the impact of the solvent interactions on the already established descriptor, or if solvent effects should be considered as an additional separate descriptor.

Inside the figure:

$$\eta_T$$

$$0$$

$$H^+ + e^- + H_{ads} \leftrightarrow H_2$$
$$2H_{ads} \leftrightarrow H_2$$

$$H^+ + e^- \leftrightarrow H_{ads}$$
$$H_2O + e^- \leftrightarrow H_{ads} + OH^-$$

strong binding **optimal binding** **weak binding**

$$0$$

$$\Delta G°_H$$

Figure 1. Volcano plot depicting the thermodynamic overpotential, η, versus the binding energy, $\Delta G_H^°$. Adapted from Ref.[17] The top of the volcano indicates an optimal binding energy of the intermediates with zero overpotential.

It has been reported[18] that from the Sabatier principle one cannot extract a sole descriptor for the hydrogen evolution because the reaction chooses the pathway with the lowest activation energy, and it does not always depend on stability. Therefore, the transition states should also be considered. It is clear that the potential at which Eq. 3 takes place will strongly depend on the binding energy associated to the adsorbed atomic hydrogen. What is not clear yet is how other molecules in the interface such as solvent molecules and electrolyte could influence the energetic requirements and the activation energies for the separate steps in the hydrogen evolution mechanism. From transient measurements, Conway and co-workers[6a] have discussed the difference in reactivity between H-UPD and H-OPD; the former being strongly adsorbed on the electrode surface as an spectator for the HER, whereas the latter has been ascribed as the real intermediate in the hydrogen evolution. It has also been stated[19] that the H-UPD is

also sitting in the platinum subsurface, in order to leave some surface available for the H-OPD to react. From these observations we understand that H-UPD does not intervene in the hydrogen evolution/oxidation reaction, although the interplay between the kinetics of both types of hydrogen and the solvent present at the interface has not been discussed.

Since there is little agreement about the molecular nature of reaction descriptors in the hydrogen evolution other than ΔG_H°, in this work we study the contribution of the solvent to the kinetics of hydrogen adsorption and evolution on platinum and gold, by means of electrochemical and spectroelectrochemical studies in a non-aqueous and aqueous solvents. We focus on the solvation of protons and the solvent-proton, solvent-electrode interactions at the electrode interface.

1.3. Acetonitrile as a solvent

Acetonitrile is one of the preferred solvents in electrochemistry due to some of its physicochemical properties: high dielectric constant (37.5), miscibility with water and amphoteric properties. The free electron pair in the nitrogen interacts strongly with cations and electrode surfaces[20], whereas the anions seem to interact, although not specifically, with the methyl groups of the solvent. Since acetonitrile is both a weak acid and base, acids tend to be weaker in acetonitrile than in water[21]. For instance, perchloric acid has been reported as the strongest acid in acetonitrile, although the measured pk_a=1.57[22] indicates that it does not dissociate completely[23]. Most acids are weak in acetonitrile, meaning that they only dissociate partially. When this is the case, the base formed from the partial deprotonation associates with the conjugated acid. The process is called homoconjugation and is observed in many aprotic solvents[23b]. It is due to the fact that the solvent molecules do not confer enough stability to the anions, instead, these anions prefer to go for

the partially shared charge of the proton with another molecule of acid, seeking a better stability.

1.4. Proton solvation

It is obvious that the proton solvation depends on the nature of the solvent and the acid itself. In addition to the capability of the solvent to stabilize the proton, homoconjugation and partial dissociation may depend on how stable the configuration of the solvated proton and the corresponding anion is. On the other hand, aprotic solvents like acetonitrile solvate protons in a different way than protic solvents. For instance, the absolute free energy of solvation of a proton in acetonitrile is -1089 kJ.mol^{-1} [24], whereas for water it is -1104.5 kJ.mol^{-1} [25]. Given these solvation energies, it is not surprising that for the solvation of protons in acetonitrile/water mixtures it has been found that, even at trace levels of water, the preferred solvation spheres are attributed to protons surrounded by water[26]. Furthermore, it has been shown[26-27] that water tends to form clusters in the mixture[28]. Other works suggest [29] that, in mixtures of water and aprotic solvents, both electrostatic and steric interactions play an important role in whether the proton is solvated by water or by the aprotic solvent molecules. Steric effects would contribute to the preferential solvation of protons in water, since water molecules are smaller than those of organic nature. While these studies are directed to the understanding of solvation processes, our main interest here focuses on the impact of proton solvation from the electrocatalytic perspective, which has not been evaluated in great detail in the literature.

1.5. Outline of the thesis

This work aims at gathering fundamental insight in the role of the solvent in the electrocatalysis of hydrogen, by revisiting the benchmarking systems; i.e. hydrogen evolution and oxidation on platinum and gold electrodes. Since the study is focused on solvation processes and the interactions between solvent, electrolyte and reaction intermediates at the electrolyte-electrode interface, the techniques used span from *in situ* Fourier-Transform InfraRed Spectroscopy (FTIR) and Surface Enhanced Raman Spectroscopy (SERS) to Electrochemical Impedance Spectroscopy (EIS) and Laser-Induced Temperature Jump method, as well as the classic cyclic voltammetry. Our findings highlight the role of water in the hydrogen electrochemistry, and opens a new perspective towards electrocatalytic processes oriented to the production of alternative energy sources by means of electrocatalytic reactions.

We make our first exploration in Chapter 2, where we studied the hydrogen oxidation and evolution reactions on a polycrystalline platinum electrode in acetonitrile. In this work we compare the voltammetric response of the system in presence of a metallic, hydrophilic cation and a lipophilic, organic cation, to show the sensitivity of the reaction kinetics to the presence of water in the organic-based electrolytes. In this first approach, we used *in situ* FTIR and SERS to demonstrate that the hydrogen oxidation and evolution is mediated by water, as protons and small cations are preferentially solvated by water. The importance of our findings impacts on the difficulty to establish a reference electrode for organic solvents due to the high sensitivity of the reaction to trace amounts of water, reflecting on several studies on molecular catalysts which use a non-protic solvent as test systems. Furthermore, these limitations make us realize the difficulty to establish reliable comparisons between catalytic activities of these different compounds in different solvents, especially if they contain different trace amounts of water.

In the same vein, Chapter 3 presents a study on the influence of water on the hydrogen evolution reaction on a polycrystalline gold electrode in acetonitrile, since it is a non-ideal system due to the fact that gold does not catalyse the hydrogen oxidation. In this chapter we follow the migration of ions and water using *in situ* FTIR spectroscopy, revealing that water accumulates at the interface in presence of protons, which again exhibit preferential solvation, as proposed in Chapter 2. Remarkably, the Tafel plot analysis shows that the hydrogen evolution on polycrystalline gold and platinum present the same rate-determining step, which consists of the first electron transfer and the consequent adsorption of hydrogen.

Since the role of water as a solvent has proved to be crucial for the electrocatalysis of hydrogen, we present a study in aqueous electrolytes in Chapter 4. The study covers a thorough spectroelectrochemical study of the kinetics of H-UPD and hydrogen evolution in a wide pH range, on a Pt(111) single crystal. The study elucidates the molecular origin of the slow reaction rates for the hydrogen evolution reaction in alkaline solutions. We show that the kinetic limitations are linked to the energetic penalty associated to the reorganization of water and the migration of charges through the water networks at the electrode-electrolyte interface. We also present a model based on the displacement of the potential of zero charge closer to the equilibrium potential of the H^+/H_2 redox couple by using submonolayer amounts of Ni deposited on the electrode surface.

1.6. References

1. Van Hook, J. P., Methane-Steam Reforming. *Catalysis Reviews* **1980,** *21* (1), 1-51.

2. Ni, M.; Leung, M. K. H.; Leung, D. Y. C.; Sumathy, K., A review and recent developments in photocatalytic water-splitting using for hydrogen production. *Renewable and Sustainable Energy Reviews* **2007,** *11* (3), 401-425.

3. (a) Turner, J. A., A Realizable Renewable Energy Future. *Science* **1999,** *285* (5428), 687-689; (b) Bockris, J. O. M., The origin of ideas on a Hydrogen Economy and its solution to the decay of the environment. *International Journal of Hydrogen Energy* **2002,** *27* (7–8), 731-740.

4. Man, I. C.; Su, H.-Y.; Calle-Vallejo, F.; Hansen, H. A.; Martínez, J. I.; Inoglu, N. G.; Kitchin, J.; Jaramillo, T. F.; Nørskov, J. K.; Rossmeisl, J., Universality in Oxygen Evolution Electrocatalysis on Oxide Surfaces. *ChemCatChem* **2011,** *3* (7), 1159-1165.

5. (a) Diaz-Morales, O.; Ledezma-Yanez, I.; Koper, M. T. M.; Calle-Vallejo, F., Guidelines for the Rational Design of Ni-Based Double Hydroxide Electrocatalysts for the Oxygen Evolution Reaction. *ACS Catalysis* **2015,** *5* (9), 5380-5387; (b) Suntivich, J.; May, K. J.; Gasteiger, H. A.; Goodenough, J. B.; Shao-Horn, Y., A Perovskite Oxide Optimized for Oxygen Evolution Catalysis from Molecular Orbital Principles. *Science* **2011,** *334* (6061), 1383-1385.

6. (a) Bai, L.; Harrington, D. A.; Conway, B. E., Behavior of overpotential—deposited species in Faradaic reactions—II. ac Impedance measurements on H2 evolution kinetics at activated and unactivated Pt cathodes. *Electrochimica Acta* **1987,** *32* (12), 1713-1731; (b) Schouten, K. J. P.; van der Niet, M. J. T. C.; Koper, M. T. M., Impedance spectroscopy of H and OH adsorption on stepped single-crystal platinum electrodes in alkaline and acidic media. *Physical Chemistry Chemical Physics* **2010,** *12* (46), 15217-15224.

7. Bowden, F. P.; Rideal, E. K., The Electrolytic Behaviour of Thin Films. Part I. Hydrogen. *Proceedings of the Royal Society of London A: Mathematical, Physical and Engineering Sciences* **1928,** *120* (784), 59-79.

8. Frumkin, A. N., Shlygin, AI, On Platinum Electrode. *Dokl. Akad. Nauk. SSSR* **1934,** *2*.

9. Becker, M.; Breiter, M., Untersuchung der Sauerstoffbelegung an Edelmetallelektroden mit Hilfe von Impedanzmessungen und kathodischen Ladekurven I. Glatte Platinelektroden. *Zeitschrift für Elektrochemie, Berichte der Bunsengesellschaft für physikalische Chemie* **1956,** *60* (9-10), 1080-1089.

10. Breiter, M. W.; Breiter, M. W., ELECTROCHEMICAL STUDY OF HYDROGEN ADSORPTION ON CLEAN PLATINUM METAL SURFACES. *Annals of the New York Academy of Sciences* **1963,** *101* (3), 709-721.

11. Barber, J.; Morin, S.; Conway, B. E., Specificity of the kinetics of H2 evolution to the structure of single-crystal Pt surfaces, and the relation between opd and upd H. *Journal of Electroanalytical Chemistry* **1998,** *446* (1–2), 125-138.

12. Barber, J. H.; Conway, B. E., Structural specificity of the kinetics of the hydrogen evolution reaction on the low-index surfaces of Pt single-crystal electrodes in 0.5 M dm−3 NaOH1. *Journal of Electroanalytical Chemistry* **1999,** *461* (1–2), 80-89.

13. Qian, S. Y.; Conway, B. E.; Jerkiewicz, G., Comparative effects of adsorbed S-species on H sorption into Pd from UPD and OPD H: a kinetic analysis. *International Journal of Hydrogen Energy* **2000,** *25* (6), 539-550.

14. Sheng, W.; Zhuang, Z.; Gao, M.; Zheng, J.; Chen, J. G.; Yan, Y., Correlating hydrogen oxidation and evolution activity on platinum at different pH with measured hydrogen binding energy. *Nature communications* **2015,** *6*, 5848.

15. D. Pletcher, R. G., R. Peat, L. M. Peter, J. Robinson, *Instrumental Methods in Electrochemistry*. Woodhead Publishing Limited: Cambridge, UK, 2010; p 666.

16. Sabatier, P., Hydrogénations et déshydrogénations par catalyse. *Berichte der deutschen chemischen Gesellschaft* **1911,** *44* (3), 1984-2001.

17. Koper, M. T. M.; Bouwman, E., Electrochemical Hydrogen Production: Bridging Homogeneous and Heterogeneous Catalysis. *Angewandte Chemie International Edition* **2010,** *49* (22), 3723-3725.

18. Quaino, P.; Juarez, F.; Santos, E.; Schmickler, W., Volcano plots in hydrogen electrocatalysis – uses and abuses. *Beilstein Journal of Nanotechnology* **2014,** *5*, 846-854.

19. Marković, N. M.; Sarraf, S. T.; Gasteiger, H. A.; Ross, P. N., Hydrogen electrochemistry on platinum low-index single-crystal surfaces in alkaline solution. *Journal of the Chemical Society, Faraday Transactions* **1996,** *92* (20), 3719-3725.

20. (a) Gu, R. A.; Cao, P. G.; Sun, Y. H.; Tian, Z. Q., Surface-enhanced Raman spectroscopy studies of platinum surfaces in acetonitrile solutions. *Journal of Electroanalytical Chemistry* **2002,** *528* (1–2), 121-126; (b) Markovits, A.; Minot, C., Theoretical Study of the Acetonitrile Flip-Flop with the Electric Field Orientation: Adsorption on a Pt(111) Electrode Surface. *Catalysis Letters* **2003,** *91* (3-4), 225-234; (c) Coetzee, J. F.; Campion, J. J., Solute-solvent interactions. I. Evaluations of relative activities of reference cations in acetonitrile and water. *Journal of the American Chemical Society* **1967,** *89* (11), 2513-2517; (d) Ledezma-Yanez, I.; Díaz-Morales, O.; Figueiredo, M. C.; Koper, M. T. M., Hydrogen Oxidation and Hydrogen Evolution on a Platinum Electrode in Acetonitrile. *ChemElectroChem* **2015,** *2* (10), 1612-1622.

21. McCarthy, B. D.; Martin, D. J.; Rountree, E. S.; Ullman, A. C.; Dempsey, J. L., Electrochemical Reduction of Brønsted Acids by Glassy Carbon in Acetonitrile— Implications for Electrocatalytic Hydrogen Evolution. *Inorganic chemistry* **2014,** *53* (16), 8350-8361.

22. Izutsu, K., *Acid-Base Dissociation Constants in Dipolar Aprotic Solvents*. Blackwell Science: Oxford, U.K., 1990

13

23. (a) Felton, G. A. N.; Glass, R. S.; Lichtenberger, D. L.; Evans, D. H., Iron-Only Hydrogenase Mimics. Thermodynamic Aspects of the Use of Electrochemistry to Evaluate Catalytic Efficiency for Hydrogen Generation. *Inorganic chemistry* **2006,** *45* (23), 9181-9184; (b) Fourmond, V.; Jacques, P. A.; Fontecave, M.; Artero, V., H2 evolution and molecular electrocatalysts: determination of overpotentials and effect of homoconjugation. *Inorganic chemistry* **2010,** *49* (22), 10338-47.

24. Kelly, C. P.; Cramer, C. J.; Truhlar, D. G., Single-Ion Solvation Free Energies and the Normal Hydrogen Electrode Potential in Methanol, Acetonitrile, and Dimethyl Sulfoxide. *The journal of physical chemistry. B* **2007,** *111* (2), 408-422.

25. Tissandier, M. D.; Cowen, K. A.; Feng, W. Y.; Gundlach, E.; Cohen, M. H.; Earhart, A. D.; Coe, J. V.; Tuttle, T. R., The Proton's Absolute Aqueous Enthalpy and Gibbs Free Energy of Solvation from Cluster-Ion Solvation Data. *The Journal of Physical Chemistry A* **1998,** *102* (40), 7787-7794.

26. Mestdagh, J. M.; Binet, A.; Sublemontier, O., Solvation shells of the proton surrounded by acetonitrile, ethanol, and water molecules. *The Journal of Physical Chemistry* **1989,** *93* (26), 8300-8303.

27. Jamroz, D.; Stangret, J.; Lindgren, J., An infrared spectroscopic study of the preferential solvation in water-acetonitrile mixtures. *Journal of the American Chemical Society* **1993,** *115* (14), 6165-6168.

28. Kovacs, H.; Laaksonen, A., Molecular dynamics simulation and NMR study of water-acetonitrile mixtures. *Journal of the American Chemical Society* **1991,** *113* (15), 5596-5605.

29. Stace, A. J., Preferential solvation of hydrogen ions in mixed water-amine ion clusters. *Journal of the American Chemical Society* **1984,** *106* (8), 2306-2315.

2. Hydrogen oxidation and hydrogen evolution on a platinum electrode in acetonitrile

ABSTRACT

This work discusses the kinetics of the hydrogen oxidation and evolution on a polycrystalline platinum electrode in acetonitrile, in presence of two different electrolytes. Our findings point out the sensitivity of the kinetics of these reactions to the presence of small amounts of water. In situ Infrared Spectroscopy (FTIR) reveals the ion migration owing to the preferential solvation of protons in residual water, whereas the Surface Enhanced Raman Spectroscopy (SERS) confirms that the water leaves the interface under hydrogen oxidation conditions. These observations imply that the kinetic sensitivity of this electrocatalytic reaction towards the preferential solvation processes presents a serious constraint in the establishment of a reference electrode for non-aqueous solvents based on the HOR/HER on platinum, and on the comparison of its catalysis in various non-aqueous solvents.

2.1. Introduction

The hydrogen oxidation reaction (HOR) and hydrogen evolution reaction (HER) are key reactions in electrochemistry,[1] as well as in the development of technologies towards clean energy and fuel cells. The majority of the electrochemical studies of HOR/HER have pertained to aqueous electrolytes. With the search for new, cheap, and efficient catalysts for HER, studies of molecular catalysts often employ non-aqueous solvents, such as acetonitrile, for activity testing.[2] Having a standard activity test in the same solvent then becomes desirable, including detailed insight into the molecular mechanisms involved in this standard system. Platinum would be the most suitable electrode material for such a benchmark activity test, as it is for tests in aqueous electrolytes. Although several studies on the HER and HOR in acetonitrile[3] have been carried out, comparatively little has been settled about the mechanism involved, such as the role of cations, anions and residual water, leading to an incomplete understanding of the process and its catalysis.

Acetonitrile is an aprotic solvent that has proved to be convenient for use in electrochemistry,[4] primarily related to its miscibility with water, combined with a relatively high dielectric constant (37.5), giving excellent solvation properties for a variety of electrolytes. However, ion pairs can form in acetonitrile[5] and, under certain conditions, they can also adsorb strongly or even dissociate on the electrode surface,[6] under the influence of an electrode potential. These features make acetonitrile especially sensitive to the use of different supporting electrolytes for hydrogen oxidation and hydrogen evolution, leading to voltammetric responses that have proved difficult to interpret.

Early work by Chambers[1f] and Sawyer[7] demonstrated the high sensitivity and even irreproducibility to electrolyte parameters of HER and HOR activity on a platinum electrode in acetonitrile. More recent findings reported by Suárez-Herrera *et al.*[3c] highlighted the role of the nature of cations and the presence of water on

the HOR activity on single-crystal platinum electrodes in acetonitrile. Their *in situ* infrared data revealed that chemisorption of hydrogen, acetonitrile and cyanide takes place only when water is present in the interface. Interestingly, they propose that hydrogen oxidation on platinum in acetonitrile is mediated by hydroxyl groups present on the electrode surface, as formed by the oxidation of residual water. According to their results, the proton released in this process is stabilized by forming an ion pair with the electrolyte anion. This proposition is in agreement with the earlier observation that oxidation of Pt activates the surface for the HOR in acetonitrile.[7] Those conclusions lead to the intriguing apparent paradox that in acetonitrile, HOR takes place on an oxygen-covered Pt surface, whilst in aqueous electrolyte, HOR takes place on hydrogen-covered Pt surface.[8] It also raises the question whether Pt is really a suitable activity standard for HOR/HER in acetonitrile.

In this work, we present a combined electrochemical and *in situ* spectroscopic study of the HOR/HER reaction on platinum in acetonitrile. We aim to understand (i) how the interaction of the acetonitrile with the electrolyte ions and with platinum[6,9] affects the catalytic activity, and (ii) how a small amount of water interferes with the catalytic activity in the presence of two different cations, i.e. tetrabutylammonium TBA^+ and lithium Li^+, expecting the latter to have a stronger specific interaction with water. Our results show that the HOR/HER on Pt is a reversible process in acetonitrile, but also that there is a crucial role of water and cations. According to our findings, the role of water seems to be primarily in the preferential solvation of protons and other small cations, rather than in the activation of the platinum surface.

2.2. Experimental Section

Solutions were prepared using acetonitrile as received (Anhydrous 99.8%, from Sigma-Aldrich). As proton source, we used perchloric acid (70% *Suprapur®*

Merck). LiClO$_4$ and tetrabutylammonium perchlorate for electrochemical analysis (99.0% from Sigma-Aldrich) were used as supporting electrolytes. Ferrocenium hexafluorophosphate (97%, from Sigma-Aldrich) and ferrocene (99%, from Alfa Aesar) were used in equimolar concentration to calibrate the equilibrium potential of the Ag/AgClO$_4$ reference electrode used in this work. All the solutions were purged with argon (purity grade 6.0), whereas for the experiments performed under hydrogen atmosphere we used a constant hydrogen flux (purity grade 5.6). No further attempts were made to dry the electrolyte solutions.

Prior to experiments, the glassware was rinsed with water (Milipore® MiliQ; resistivity >18.2 MΩ.cm), then rinsed with acetone (Sigma-Aldrich), and placed in the oven over night, at 120 °C.

For the electrochemical measurements we used an Ivium potentiostat/galvanostat (IviumStat) connected to a one-compartment, three-electrode cell. The working electrode (WE) was a platinum wire with a diameter of 120 μm and a real surface area of $(5,9 \pm 0,1) \times 10^{-4}$ cm^2, measured from the hydrogen adsorption/desorption in aqueous solution,[10] assembled to a glass stem and flame annealed before each measurement. The counter electrode (CE) consisted of a platinum spiral, while the reference electrode (RE) was a home-made Ag/AgClO$_4$ in acetonitrile. The RE consisted on a silver wire immersed in a glass tube, filled with a 1 mM Ag/AgClO$_4$ solution in acetonitrile. The tube has a glass-junction, allowing the free transport of ions from the luggin into the electrolyte. A 10 μF capacitor was connected between the RE and a platinum wire immersed in the solution, as a noise filter. In order to calibrate the zero in the Ag/AgClO$_4$ RE scale respect the SHE scale, we prepared a ferrocene/ferrocenium solution in an equimolar concentration (10 mM), as the accepted internal standard for electrochemical measurements in non-aqueous solutions, and measured its cyclic voltammetry against the Ag/AgClO$_4$ RE. The equilibrium potential of the redox couple Fc^0/Fc$^+$ was calculated as the half wave potential in the cyclic voltammetry and the measured value is 0.038 V.

Surface Enhanced Raman Spectroscopy (SERS) measurements were performed with a confocal Raman microscope (LabRam HR, Horiba Yobin Yvon), equipped with a He/Ne laser (633 nm) and a 50X objective. The electrochemical measurements were controlled with a METROHM µAUTOLABIII potentiostat/galvanostat, using an electrochemical cell with one compartment and three electrodes: a platinum wire as CE, $Ag/AgClO_4$ in acetonitrile as RE, whereas the working electrode consisted of 2 ML of platinum deposited galvanostatically from an aqueous 100 mM H_2PtCl_6 solution on a roughened gold surface.[11] The gold surface was previously polished with alumina (different mesh; e.g. 1 µm, 0.3 µm and 0.05 µm), rinsed with ultrapure water and sonicated during ten minutes to remove any alumina residues remaining. The roughening procedure has been reported in the literature[12] and consists on immersing the electrode in a 100 mM KCl solution and perform 25 oxidation-reduction cycles, between -0.30 V and 1.20 V vs. SCE, by holding the cathodic potential for 30 s and the anodic potential for 1.3 s.

The Fourier Transform Infra-Red Spectroscopy (FTIRS) measurements were carried out in a three electrode cell coupled to a CaF_2 prism slanted at 60 degrees, and connected to a Bruker Vertex80V IR spectrophotometer. The WE was a platinum disc settled in a thin layer configuration, the CE was a platinum wire and the RE was $Ag/AgClO_4$ in acetonitrile. Hundred interferograms were averaged for each spectrum, with a resolution of 8 cm^{-1}, as well as for the measurement of the transmission spectra, whose reference spectrum was taken from pure acetonitrile. The spectra in this work are reported as difference spectra with respect to a background spectrum, and normalized against such reference, $(T-T_0)/T_0$. Hence, bands pointing upwards correspond to the depletion of species at the electrode surface and will be called positive bands, while bands pointing downwards indicate the adsorption of species and will be assigned as negative bands.

2.3. Results

2.3.1. Reference scale: from Ag^0/Ag$^+$ to SHE.

In this work we employ a practical reference scale suitable for the H$^+$/H$_2$ couple in acetonitrile. Fourmond et al.[2d] have recently reconsidered the standard potential of the hydrogen couple in acetonitrile, E_{SHE}^{MeCN}, measured using a molecular catalyst, and reporting an estimated value of -0.070 V vs Fc^0/Fc$^+$, which corresponds to -0.033 V vs. our Ag/AgClO$_4$ electrode in acetonitrile. However, standard conditions are generally not achievable due to the low dissociation constant of acids in organic solvents, including perchloric acid in acetonitrile (pk$_a$=1.57)[13]

Therefore,

$$E_{H^+/H_2}^{eq,MeCN} = E_{H^+/H_2}^{0,MeCN} + \frac{RT}{2F} ln \frac{[H^+]^2}{pH_2} \qquad \text{(Eq. 1)}$$

$$E_{\frac{H^+}{H_2}}^{eq,MeCN} = E_{SHE}^{MeCN} + \frac{RT}{2F} ln \frac{(\alpha c)^2}{pH_2} \qquad \text{(Eq. 2)}$$

where α is the degree of dissociation, and *c* is the nominal concentration of the HA acid.

We note that there is still considerable uncertainty in the "real" value of E_{SHE}^{MeCN}. The estimated value quoted by Fourmond *et al.* deviates from previous values, and is also ca. 0.1 - 0.2 V different from theoretical estimates by Fawcett[14]. In the voltammetric curves shown below, V$_{SHE}$ is understood as the electrode potential referred to E_{SHE}^{MeCN}.

2.3.2. Voltammetry for HOR/HER in acetonitrile

Figures 1 and 2 show the cyclic voltammograms for polycrystalline platinum in acetonitrile, using tetrabutylammonium perchlorate (TBAP; black solid line) or
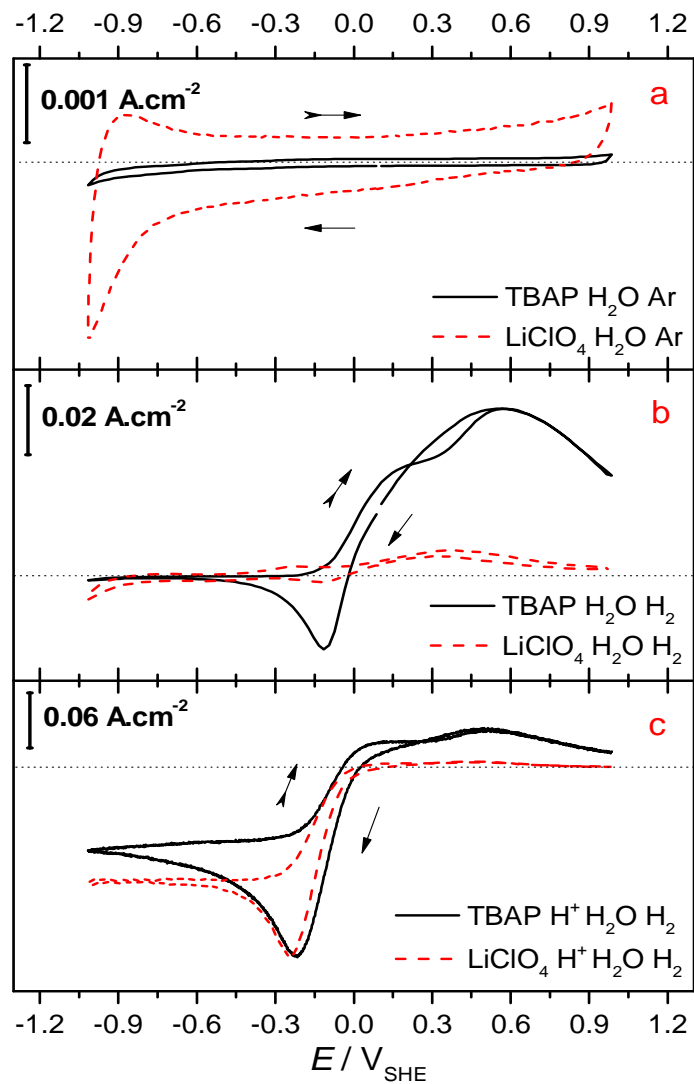
LiClO$_4$ (red dashed line) as supporting electrolytes. Fig. 1a shows the hydrogen oxidation in the base electrolyte in the absence of proton donor. Fig. 1b shows the hydrogen evolution in the presence of 10 mM HClO$_4$ in an Ar saturated electrolyte. Finally, Fig.1c combines HOR and HER in the presence of 10 mM HClO$_4$ in a H$_2$ saturated electrolyte. In each subfigure (a to c), we present the last cycle out of 200 scans between 1.0 and -1.0 V$_{SHE}$, starting the sweep at 0.1 V$_{SHE}$ in the cathodic direction. The blank voltammetry of Pt in both electrolytes is rather featureless and is shown in the Appendix A, Figure A1. In both electrolytes, there is a pair of reduction/oxidation peaks that is observed clearly in the first scan but disappears quickly in subsequent scans. The HER/HOR currents are sensitive to the scan rate in both electrolytes (Fig.A2). Especially, the HOR current lowers with lower scan rates, whereas the system with TBAP exhibits a larger HER current in the acidic solution. In general, the HER/HOR becomes more reversible at high scan rates for both electrolytes, suggesting the presence of a slow deactivation process in the system.

Figure 1a shows the voltammetry recorded for the solution saturated with hydrogen, with the peak for the hydrogen oxidation presenting a similar current and shape for both electrolytes. In the negative-going scan, the proton reduction peak is observed, and is somewhat larger for the LiClO$_4$ electrolyte. In Figure 1b, the voltammetries for solutions containing 10 mM HClO$_4$ for each electrolyte, saturated with Ar, should have a real proton concentration of 2.1 mM as calculated from the pK$_a$ of the acid. Obviously, the proton reduction peak in Figure 1b has a higher current compared to the same peak in Figure 1a. A small current is observed in the positive-going scan, corresponding to the oxidation of H$_2$ formed in the previous cathodic scan. Evaluation of the HER/HOR couple in Figure 1c shows a similarly shaped proton reduction peak in comparison with Figure 1b, (though the current is slightly larger in Figure 1c, due to proton formation in the oxidation of molecular hydrogen). However, the HOR current is considerably smaller than in the proton-free electrolyte solution depicted in Figure 1a.

22

Figure 2 shows the cyclic voltammetries for polycrystalline platinum in acetonitrile, using TBAP (black solid line) or $LiClO_4$ (red dashed line) as supporting electrolytes, in presence of 50 mM H_2O. Figure 2a compares the blank voltammetries for both electrolytes and shows that the background current for the solution with $LiClO_4$ is one order of magnitude larger compared with the solution containing TBAP. For the $LiClO_4$ electrolyte, the onset potential for water reduction is ca. -0.750 V_{SHE} (see Figure A1a). In the anodic sweep, there is a corresponding oxidation peak, which, however, cannot be due to hydrogen oxidation, since that is expected to occur only at much more positive potentials (see Figure 1a). For the TBAP electrolyte, no significant water reduction current is observed in this potential window. After saturating the solutions with hydrogen, Figure 2b depicts the HOR process in the presence of water. The voltammetry obtained for TBAP electrolyte is very similar to the voltammetry presented in Figure 1a for the HOR in absence of added water, although the hydrogen oxidation current is slightly smaller than in Figure 1a, while the reduction current peak is comparatively larger. A much more significant influence of water is observed for the $LiClO_4$ electrolyte. Figure 2b shows an irreversible behavior and a much lower redox current. Addition of 10 mM $HClO_4$ to the solutions with water and saturating them with hydrogen gas, leads to the voltammetric responses shown in Figure 2c. Remarkably, the proton reduction wave is very similar for both electrolytes, and not significantly different from the system in Figure 1c, but the hydrogen oxidation is significantly inhibited by the combination of Li^+ and water.
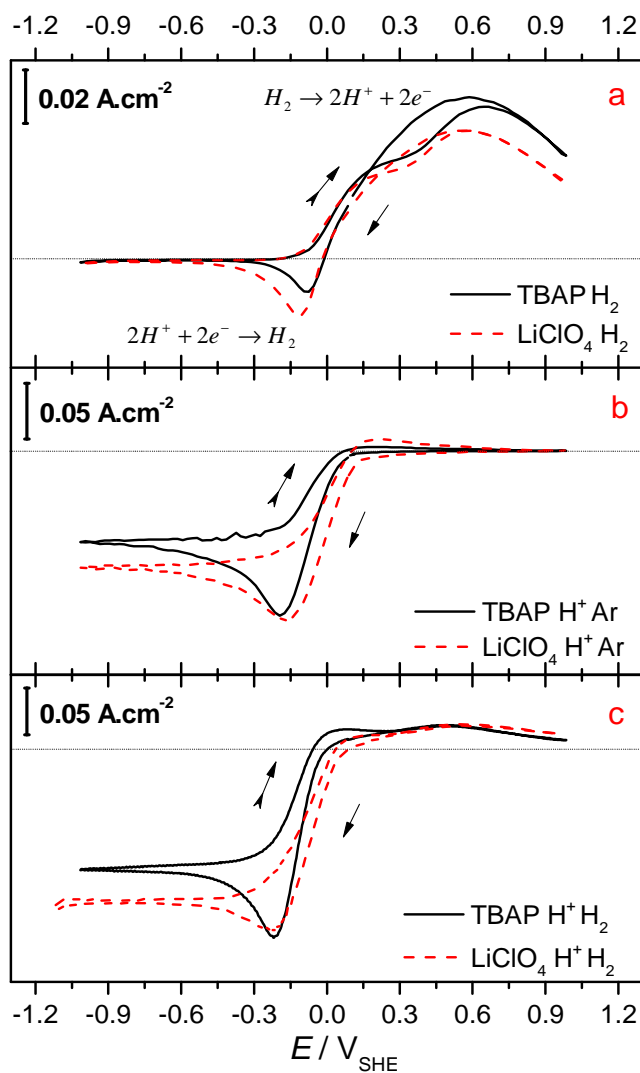
Figure 1. Cyclic voltammetries for a polycrystalline platinum wire in acetonitrile, containing 100 mM LiClO₄ (red dashed line) or 100 mM TBAP (black solid line), as supporting electrolytes. a) Hydrogen saturated; b) After adding 10 mM HClO₄; argon saturated; c) After adding 10 mM HClO₄; hydrogen saturated. Scan rate: 500 mV/s, in order to minimize gradual solvent decomposition[15]. The horizontal dotted lines mark zero current.

Figure 2. Cyclic voltammetries for a polycrystalline platinum wire in acetonitrile, containing 100 mM LiClO$_4$ (red dashed line) or 100 mM TBAP (black solid line), as supporting electrolytes, in presence of 50 mM H$_2$O. a) Argon saturated; b) Hydrogen saturated; c) Adding 10 mM HClO$_4$; hydrogen saturated. Scan rate: 500 mV/s. The horizontal dotted lines mark zero current.

2.3.3. Fourier Transform InfraRed Spectroelectrochemistry.
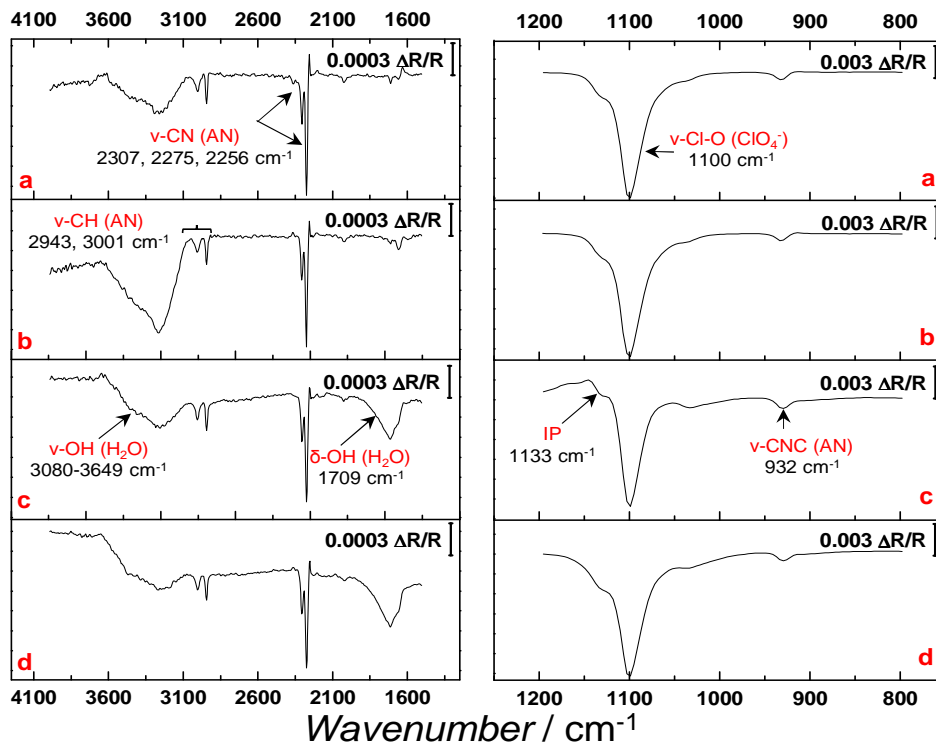### 2.3.3.1.   Transmission spectra.

In order to properly evaluate the relevant interactions between solvent and other electrolyte components, we first measured the transmission spectra for acetonitrile in the presence of $LiClO_4$ or TBAP as supporting electrolytes, in an Ar-saturated electrolyte, in an H_2-saturated electrolyte, in an Ar-saturated electrolyte containing 10 mM $HClO_4$, and finally in an H_2-saturated electrolyte containing 10 mM $HClO_4$. Results are shown in Figures 3 (for $LiClO_4$) and 4 (for TBAP). These spectra are difference spectra, i.e. the spectrum for pure acetonitrile was subtracted from the electrolyte spectra. The bands identified in the spectra will be discussed according to the relevant solution components, i.e. acetonitrile, perchlorate and water, in agreement with the bands reported in the literature[16].

Acetonitrile (AN) shows bands in the 2940-3000 cm^{-1} range, ascribed to the v-CH modes,[17] and in the 2260-2340 cm^{-1} range, corresponding to the C-N bending and stretching modes. The C-H modes are naturally more prominent in presence of TBAP, due to the butyl chains of the TBA cation. The most remarkable difference is in the 2260-2340 cm^{-1} region for the two electrolytes. The spectra for the system containing $LiClO_4$ show two clear bands pointing downwards at 2307 and 2275 cm^{-1}, and one band pointing upwards at 2256 cm^{-1} ascribed to the CN bending and the CN stretching modes. These bands are essentially undisturbed by the presence of H_2 and protons (or water) in the transmission spectra. On the other hand, for the solution with TBAP (Figure 4) we observe the bands in the 2260-2340 cm^{-1} window to point upwards in presence of argon or molecular hydrogen. These bands present a blue shift when compared to the equivalent spectra in Figure 3. In addition, the presence of $HClO_4$ (and water) changes the nature of these bands in TBAP.

The perchlorate ion is characterized by the Cl-O stretching vibration around 1100 cm^{-1}. High- and low-frequency shoulders on the main band at 1100 cm^{-1} have

been ascribed to perchlorate involved in the formation of contact ion pairs (CIP). Barthel and Deser have shown the existence of such ion pairs in (more concentrated) $LiClO_4$ solutions in AN.[16a] These CIP are due to interactions between perchlorate anions and the cations, surrounded by solvent molecules. The observation of a shoulder near 1130 cm^{-1} in the $LiClO_4$ electrolyte confirms the existence of ion pairs in this electrolyte. In TBAP, these features are much less prominent.

Finally, water bands between 3100-3750 cm^{-1} (O-H stretching region) and 1550-1900 cm^{-1} (O-H bending region) are observed. This illustrates that we must count on the presence of trace amounts of water in "dry" AN with added electrolyte, and substantial amounts of water in AN acidified with $HClO_4$. No significant differences were observed between the blank solutions saturated with argon and saturated with hydrogen.

Figure 3. Transmission spectra for acetonitrile, containing 100 mM LiClO$_4$ as supporting electrolyte: a) Argon-saturated; b) Hydrogen saturated; c) After adding 10 mM HClO$_4$, Ar-saturated and d) After adding 10 mM HClO$_4$, H$_2$-saturated. The spectrum for pure acetonitrile was subtracted and the spectra in the figures correspond to difference spectra. (IP stands for ion pairs).
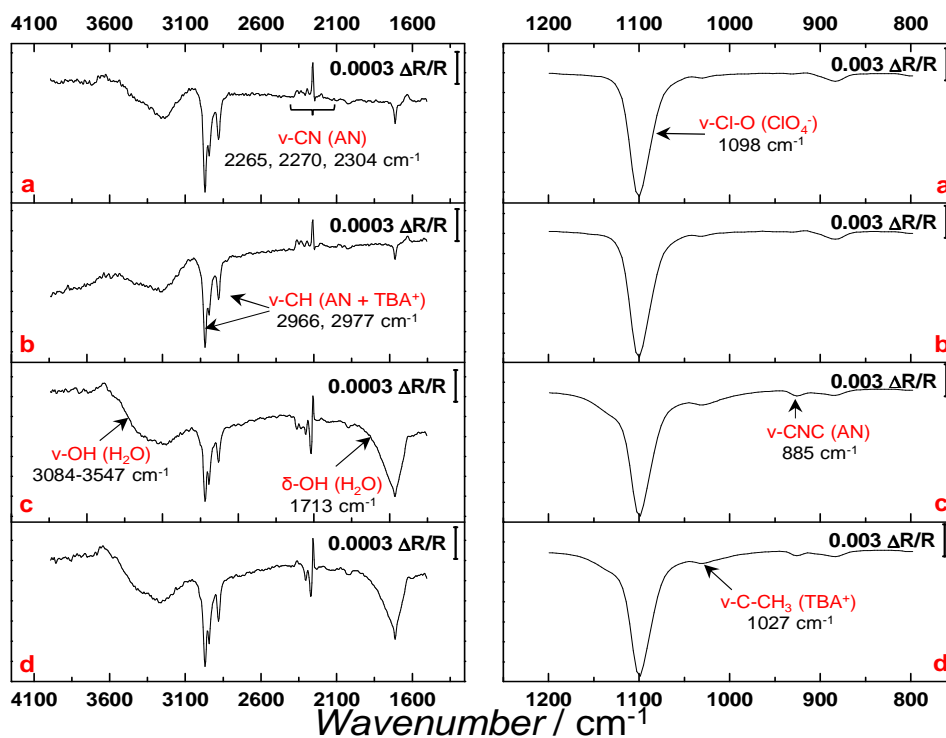
Figure 4. Transmission spectra for acetonitrile, containing 100 mM TBAP as supporting electrolyte: a) Argon-saturated; b) Hydrogen saturated; c) After adding 10 mM HClO$_4$, Ar-saturated and d) After adding 10 mM HClO$_4$, H$_2$-saturated. The spectrum for pure acetonitrile was subtracted and the spectra in the figures correspond to difference spectra.

### 2.3.3.2. Substractively Normalized Interfacial Fourier Transform Infrared Spectroscopy (SNIFTIRS).

Figures 5 and 6 show the potential-dependent SNIFTIR spectra for platinum in acetonitrile, containing 100 mM TBAP or $LiClO_4$ respectively, under different conditions. The spectra were taken from negative towards positive potentials (bottom to top in each subfigure), and plotted as difference spectra with the reference spectrum taken at -0.314 V_{SHE}. By convention, the bands pointing upwards are ascribed as positive bands, whereas the bands pointing downwards correspond to negative bands. Some of the characteristic bands from the acetonitrile electrolyte described in the previous section are present in the spectra shown in Figures 5 and 6.

Figure 5a (top panels) shows the spectra for the TBAP-acetonitrile electrolyte in the absence of H_2 or proton donor. As depicted in the figure, the C-H and C-N vibrations are potential dependent, due to a change in orientation of the near-surface AN as a result of the applied potential.[9] Under conditions of hydrogen oxidation at the platinum electrode (Fig.5b, middle panels), we observe two important changes: the appearance of a positive band in the O-H stretching region (3300 – 3750 cm^{-1}) and O-H bending region (tail observed at 1633 cm^{-1}), indicating that water is depleting from the electrode surface; and the development of a negative band in the Cl-O stretching region around 1130 cm^{-1}, indicating that perchlorate anions are attracted or migrating to the electrode surface. In the presence of $HClO_4$ the same bands are observed. The most likely interpretation of these results is that the protons generated by H_2 oxidation are preferentially solvated by water. Under oxidation conditions, these water-solvated protons move away from the surface (hence the observed depletion by water) and the perchlorate ions migrate towards the surface. No significant difference was found between the features for the system with and without acid, in presence of H_2, other than that the water-related band appear at lower potentials in the presence of acid.

Figure 6 shows the FTIR spectra for platinum in acetonitrile, containing 100 mM LiClO$_4$, under the same conditions as in Figure 5. Qualitatively, the spectra are similar to Figure 5 but some significant differences can nevertheless be observed. In the system saturated with argon (Fig. 6a, top panels) we observe the CN stretching modes for acetonitrile. In presence of hydrogen (Fig. 6b, middle panels) we observe the occurrence of a third shoulder around 3469 cm^{-1} in the O-H stretching region (3300 – 3750 cm^{-1}), which may be attributed to the interaction of water with the Li$^+$, since it is not observed for the systems with TBAP (compare Figures 5 and 6). These observations are complementary to the observations in Figure 5, since the lithium cation shows preferential solvation in presence of water[18] and implies that the water is leaving the surface by solvating and migrating with Li$^+$ and the H$^+$ formed during the hydrogen oxidation
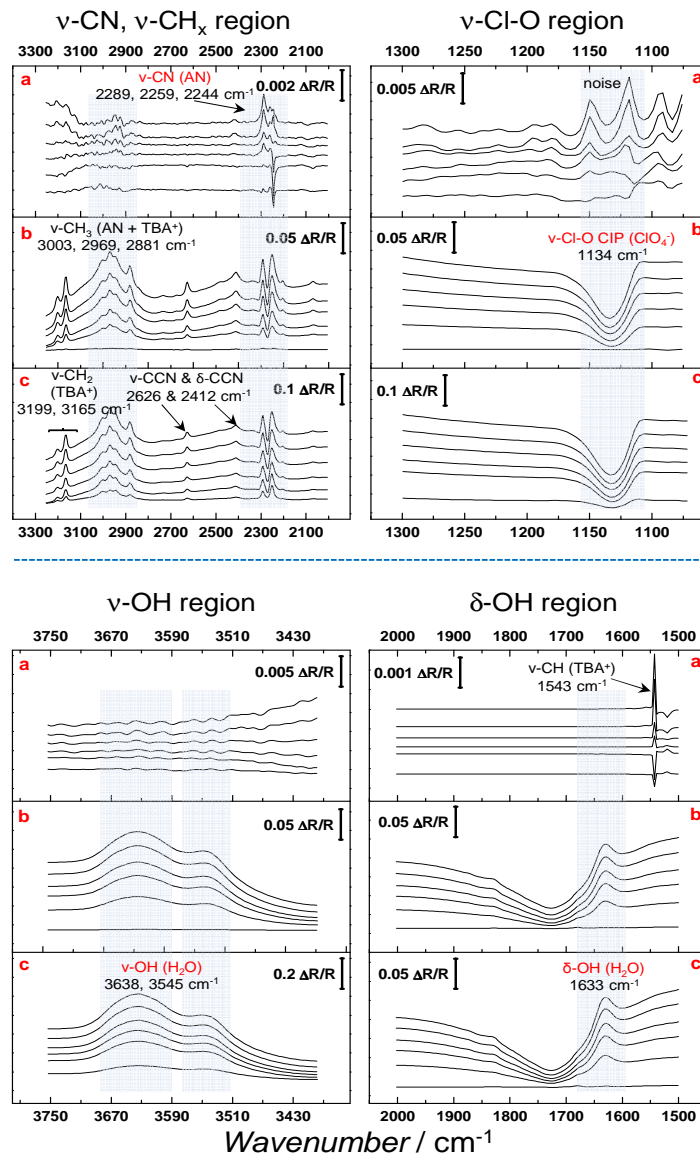
ν-CN, ν-CHₓ region

ν-Cl-O region

ν-OH region

δ-OH region

Wavenumber / cm⁻¹

Figure 5. Potential-dependent SNIFTIR spectra for a polycrystalline platinum electrode in acetonitrile, containing 100 mM TBAP as supporting electrolyte: a) Argon atmosphere; b) Hydrogen atmosphere; c) After adding 10 mM HClO$_4$ under hydrogen atmosphere. Reference spectrum: -0.500 V$_{Ag^0/Ag^+}$ (corresponding to -0.314 V$_{SHE}$).

ν-CN, ν-CHₓ region

ν-Cl-O region

ν-OH region

δ-OH region

Wavenumber / cm⁻¹
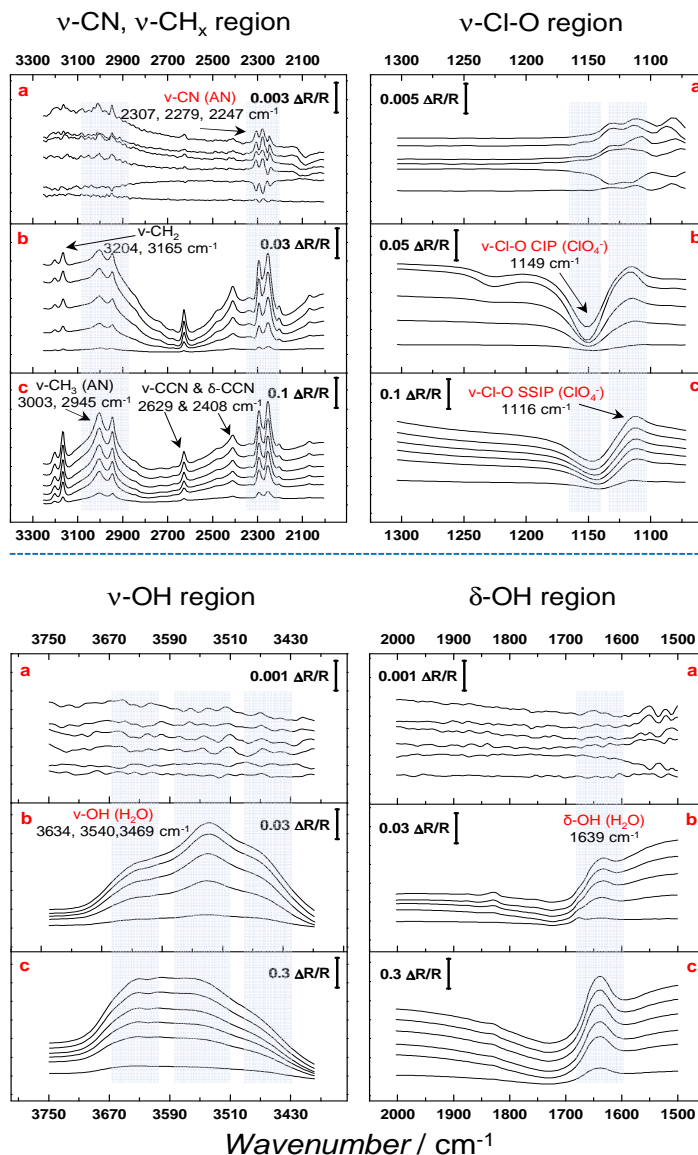
Figure 6. Potential-dependent SNIFTIR spectra for a polycrystalline platinum electrode in acetonitrile, containing 100 mM LiClO$_4$ as supporting electrolyte: a) Argon atmosphere; b) Hydrogen atmosphere; c) After adding 10 mM HClO$_4$ under hydrogen atmosphere. Reference spectrum: -0.500 V$_{Ag^0/Ag^+}$ (corresponding to -0.314 V$_{SHE}$).

33

2.3.4. Surface Enhanced Raman Spectroscopy (SERS).

The potential-dependent SER spectra for platinum in acetonitrile containing 100 mM electrolyte are shown in Figures 7 and 8. The spectra from 100 to 2250 cm^{-1} are shown in the Figures A3 and A4. The Figures presented below correspond to the region 2000 to 2200 cm^{-1}. The bands depicted here appear around 2070 cm^{-1} and 2140-2160 cm^{-1} and have been reported[6] as the v-CN vibrations from isocyanide adsorbed on the surface of the electrode, i.e. with N binding to the Pt. In agreement with the report by Tian and coworkers,[6] this suggests that acetonitrile decomposes on the platinum surface, especially at more negative potential (the potential window in their measurements was 0.7 V more negative than ours). They also observed that the presence of water inhibits the acetonitrile decomposition. Interestingly, under conditions of water removal from the surface (H_2 oxidation) at positive potential, the (iso)cyanide bands at 2050-2150 cm^{-1} appear. The bands are much weaker (and even absent in TBAP electrolyte in our potential window) when no hydrogen oxidation/proton generation takes place. This could be interpreted as a "protective layer" of water on the Pt surface under unreactive conditions, which is removed by the generation of protons that are preferentially solvated by water.

The band positions are potential dependent, as observed by Tian *et al.*,[6] and also cation dependent. The (iso-)cyanide bands are not present in the system containing TBA^+ saturated with argon (see Figure 7, top panel), while in presence of Li^+ and argon-saturated, only one of the bands attributed to the isocyanide stretching can be observed, but with a low intensity (see Figure 8, top panel). As mentioned, we ascribe the enhancement of these bands in both systems saturated with hydrogen to the removal of water from the interface by hydrogen oxidation.

34
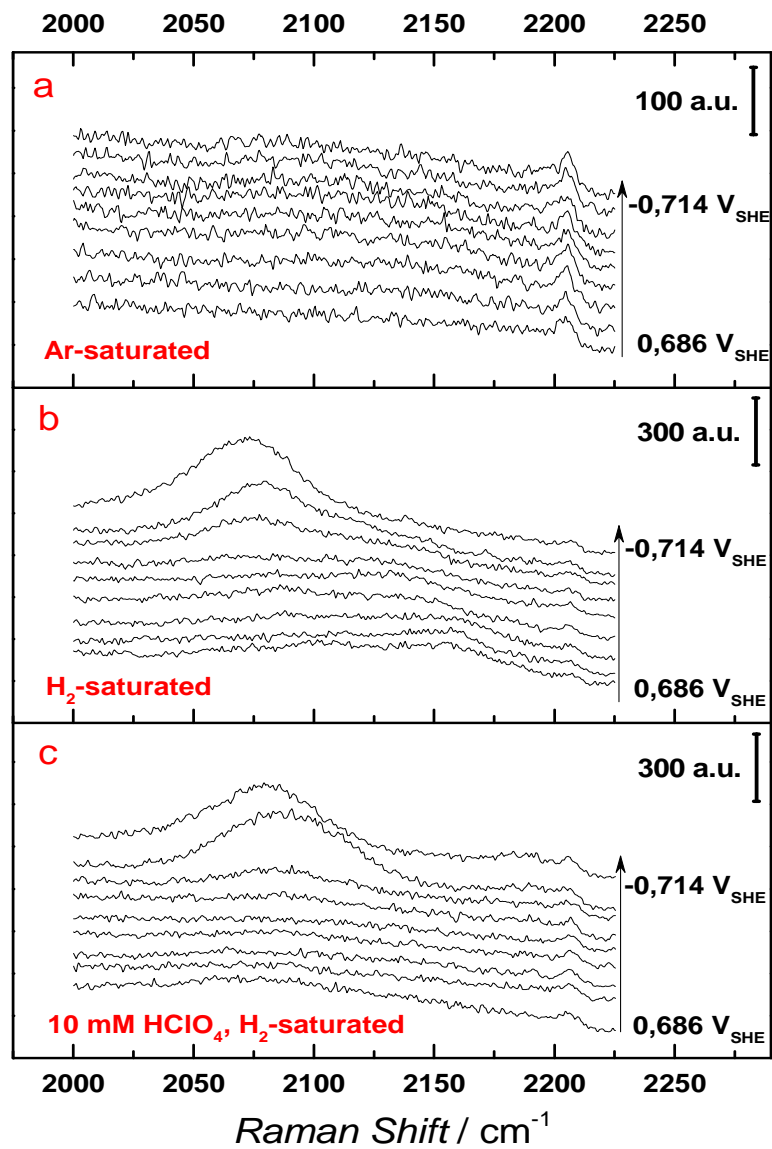
Figure 7. Potential-dependent SER spectra for acetonitrile, containing 100 mM TBAP as supporting electrolyte: a) Argon atmosphere; b) Hydrogen atmosphere; c) After adding 10 mM $HClO_4$; hydrogen atmosphere.
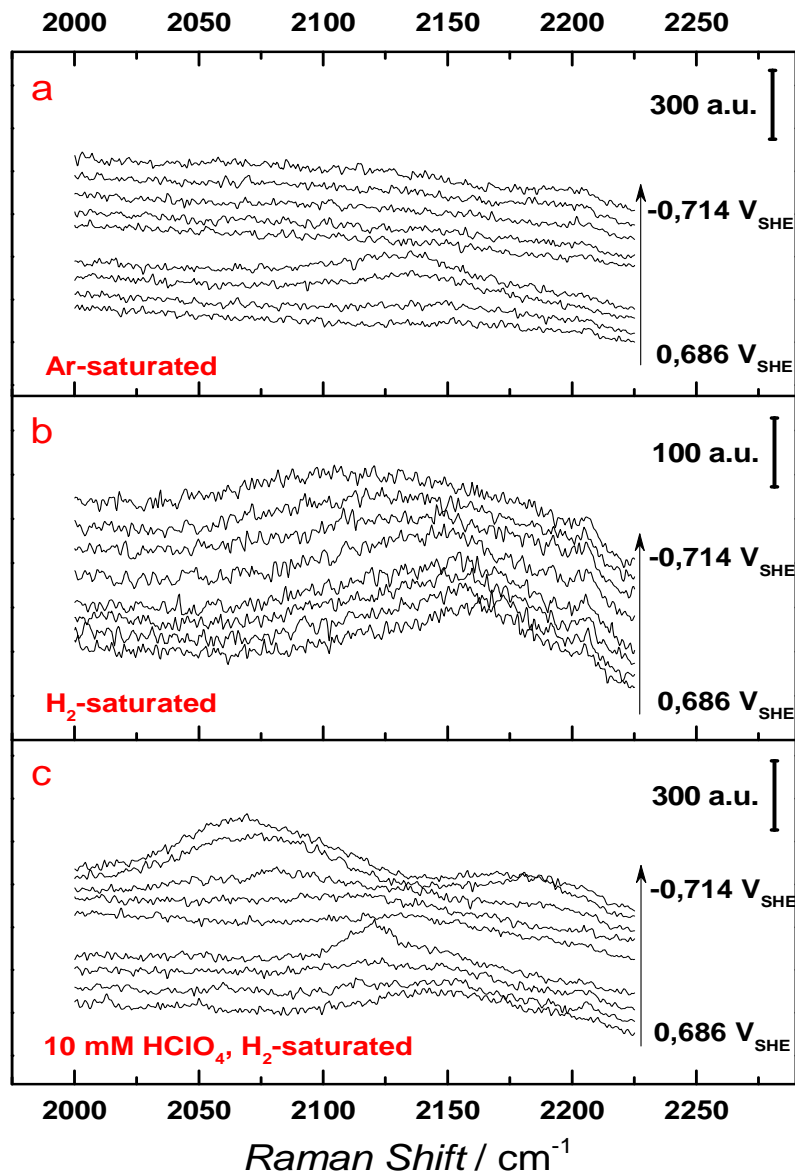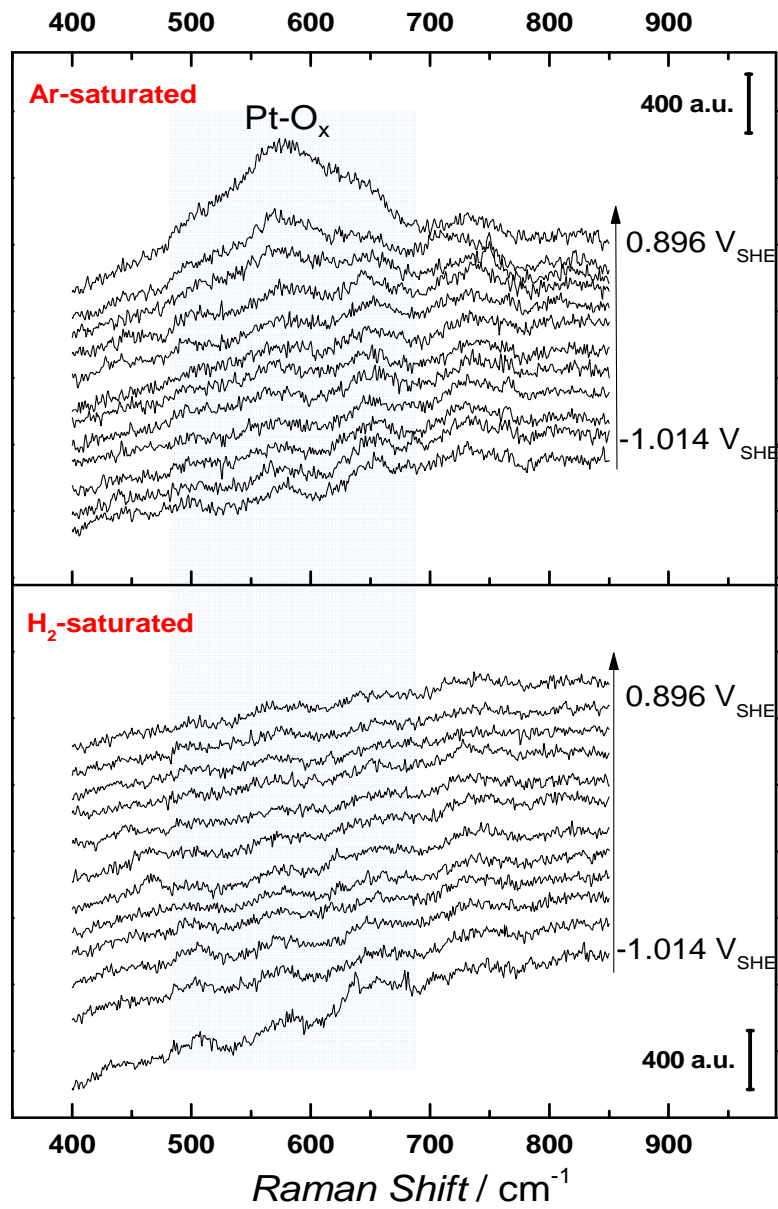
Figure 8. Potential-dependent SER spectra for acetonitrile, containing 100 mM LiClO$_4$ as supporting electrolyte: a) Argon atmosphere; b) Hydrogen atmosphere; c) After adding 10 mM HClO$_4$; hydrogen atmosphere.

Finally, Figure 9 shows the SER spectra of the region 400-850 cm^{-1} for acetonitrile in presence of TBAP and 50 mM of water. The spectra from 100 to 3500 cm^{-1} are shown as Figure A4 in the Appendix A. In the top panel we observe the formation of a broad band at high potentials of ca. 0.8-0.9 V$_{SHE}$ centered ca. 570 cm^{-1}, reported[19] as a mixture of Pt-O and α-PtO$_2$. Again, this suggests that water is present at the Pt-acetonitrile interface, and it becomes oxidized at sufficiently positive potential. However, the platinum oxide band is not observed for the hydrogen-saturated solution, as shown in the bottom panel of Figure 9. This is consistent with our conclusion that water is removed from the interface under conditions of hydrogen oxidation. We note that these experiments were performed only in a solution containing TBAP as supporting electrolyte, since the LiClO$_4$ forms visible aggregates on the electrode surface in presence of 50 mM of water, presumably due to the formation of LiOH.[20]

Figure 9. Potential-dependent SER spectra for acetonitrile, containing 100 mM TBAP as supporting electrolyte, in presence of 50 mM of water.

2.4. Discussion

Our aim in this paper was to categorize and ultimately understand the differences and similarities in kinetics of the HOR/HER in acetonitrile in the presence of two supporting electrolytes, their main difference being the nature of the cation, i.e. the tetrabutylammonium cation, as a hydrophobic/lipophilic cation, vs. Li^+ as a metallic, hydrophilic cation. Since our solutions contained trace amounts of water from different sources (primarily from the electrolyte and the acid), we purposefully added a controlled amount of water to evaluate its effect more clearly. Our results point out the high sensitivity of the HOR/HER kinetics in acetonitrile towards the presence of even small amounts of water.

The voltammetry of HOR and HER in acetonitrile (Figure 1) shows that their kinetics is relatively insensitive to the nature of the electrolyte cation. The reaction is reversible and the observed equilibrium potential corresponds well with the expected reversible potential. From the voltammetry, the addition of water (Figure 2) appears to have a limited influence, with the exception of a significant lowering of the HOR current in the Li^+-containing electrolyte. It has been reported that Li^+ can associate with hydroxyl groups from water to form LiOH aggregates on the electrode surface[20], which can block the active sites for HOR/HER. Even though no visible aggregates were observed on the μ-electrode surface, we cannot discard its formation.

Both in situ FTIR and SERS experiments show that (a trace amount of) water plays a crucial role. These experiments suggest that water is present at the Pt-acetonitrile interface initially, but is not observable until the oxidation current is flowing, in presence of molecular hydrogen. When H_2 is oxidized, the protons generated are preferentially solvated by water molecules, and leave the interface by migration of the solvated protons. Simultaneously, perchlorate ions migrate towards the surface. The SER spectra showed that the platinum oxides are formed

only in presence of water, at high positive potentials, and their formation is suppressed under hydrogen oxidation conditions.

The preferential solvation of protons by water in acetonitrile, leading to the migration of water away from the electrode surface once the protons are generated, is in good agreement with earlier conclusions about protons in acetonitrile-water mixtures. The preferential solvation of protons by water in water-acetonitrile mixtures follows from thermodynamic studies.[18, 21] Sublemontier and coworkers[5c] studied protons surrounded by solvent shells, following the mass spectra of supersonic beams containing hydrogen-bonded clusters of acetonitrile and water molecules. Their results showed that the protons, in presence of acetonitrile and small amounts of water, form solvation shells with the structure $(CH_3CN)_n(H_2O)_{n-2}H^+$. Furthermore, the stability of these clusters is granted by the formation of hydrogen bonds, and the arrangement of acetonitrile molecules in the outer coordination sphere is related to the acetonitrile as an acceptor of hydrogen bonds. A study by Benoit and Domain[22] reported the enthalpy of solvation of protons for several solvents, including water and acetonitrile. In their work, the heat of solvation for a proton in acetonitrile is -251 kcal.mol^{-1}, whereas for water it is -270 kcal.mol^{-1}. As stated by Burger,[23] these findings correlate well with the Gutmann donicities of both solvents (i.e. their ability to solvate cations) and endorse our observations of preferential solvation.

Regarding the low HOR currents registered in presence of Li$^+$ (see figure 1), we propose that the effect is related to the strong lithium-water interaction. Like protons, lithium is preferentially solvated by water in water-acetonitrile mixtures.[18] Water is a source of hydroxyl species, whose formation is promoted by the presence of Li$^+$.[20] As mentioned, in the presence of a larger amount of water in LiClO$_4$, a deposit was observed on the electrode surface. On the other hand, it has been reported[24] that the TBA$^+$ is solvated by acetonitrile; moreover, it can form hydrophobic clusters with the solvent, even at high water concentrations.

From our observations, we conclude that the hydrogen oxidation and evolution in acetonitrile are mediated by the presence of water, and this sensitivity towards the nature of the cations is attributed to preferential solvation effects. Therefore, we propose that the overall reaction of HOR/HER on platinum in acetonitrile should be written as:

$$H_2 + 2nH_2O(AN) \leftrightarrow 2H^+(H_2O)_n(AN) + 2e^-$$
(Eq. 3)
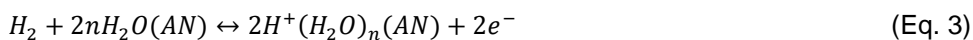
It is worth mentioning that the detailed structure of the solvation shells for the cations escapes the scope of this study. Like our present work, many previous reports on the HOR/HER on Pt in acetonitrile did not use rigorously water-free acetonitrile in combination with rigorously water-free electrolytes. In the light of our results, the practical meaning of the Hydrogen Electrode as a potential reference or activity benchmark in acetonitrile has its limitations because protons are preferentially solvated by water, at least under the experimental conditions described in this work. In general, the HOR/HER electrode kinetics in acetonitrile is highly sensitive towards the presence of water traces, even to the extent that purposefully adding water makes no apparent difference.

2.5. Conclusions

In this paper we studied the hydrogen oxidation and hydrogen evolution reactions on a platinum electrode in an acetonitrile-based electrolyte, by a combination of voltammetry and *in situ* Infrared and Raman Spectroscopy. From these spectroelectrochemical measurements in absence and presence of added water, we conclude that the hydrogen oxidation and evolution in acetonitrile is strongly mediated by (trace amounts of) water, as the protons generated by hydrogen oxidation are preferentially solvated by water. These water-carrying protons migrate away from the electrode surface during the anodic reaction. Therefore, the reversibility of HOR/HER in acetonitrile depends, to a certain extent,

on the solvation degree of the species involved in the electrocatalytic reaction, specifically on the presence of water. We also conclude that water is not involved in the electrochemical reaction, but it acts as a co-solvent to the cations in solution. This makes it difficult to establish a proper hydrogen reference electrode for non-aqueous solvents, and impacts on comparing catalysts of the HOR/HER reaction in different solvents. The implications of our conclusions could be extended to other systems under similar conditions, such as dimethylformamide and dimethylsulfoxide, which are also widely used in test systems for the development of new catalysts for hydrogen evolution.

2.6. Acknowledgments

2.7. References

1. (a) Strmcnik, D.; Uchimura, M.; Wang, C.; Subbaraman, R.; Danilovic, N.; van der, V.; Paulikas, A. P.; Stamenkovic, V. R.; Markovic, N. M., Improving the hydrogen oxidation reaction rate by promotion of hydroxyl adsorption. *Nat Chem* **2013,** *5* (4), 300-306; (b) Subbaraman, R.; Tripkovic, D.; Strmcnik, D.; Chang, K.-C.; Uchimura, M.; Paulikas, A. P.; Stamenkovic, V.; Markovic, N. M., Enhancing Hydrogen Evolution Activity in Water Splitting by Tailoring Li+-Ni(OH)2-Pt Interfaces. *Science* **2011,** *334* (6060 %U http://www.sciencemag.org/content/334/6060/1256.abstract), 1256-1260; (c) Hoshi, N.; Asaumi, Y.; Nakamura, M.; Mikita, K.; Kajiwara, R., Structural Effects on the Hydrogen Oxidation Reaction on n(111)–(111) Surfaces of Platinum. *The Journal*

of Physical Chemistry C **2009,** *113* (39), 16843-16846; (d) Juodkazis, K. s.; Juodkazytė, J.; Šebeka, B.; Juodkazis, S., Reversible hydrogen evolution and oxidation on Pt electrode mediated by molecular ion. *Applied Surface Science* **2014,** *290*, 13-17; (e) Kunimatsu, K.; Senzaki, T.; Samjeské, G.; Tsushima, M.; Osawa, M., Hydrogen adsorption and hydrogen evolution reaction on a polycrystalline Pt electrode studied by surface-enhanced infrared absorption spectroscopy. *Electrochimica Acta* **2007,** *52* (18), 5715-5724; (f) Lanning, J. A.; Chambers, J. Q., Voltammetric study of the hydrogen ion/hydrogen couple in acetonitrile/water mixtures. *Analytical Chemistry* **1973,** *45* (7), 1010-1016; (g) Roubelakis, M. M.; Bediako, D. K.; Dogutan, D. K.; Nocera, D. G., Proton-coupled electron transfer kinetics for the hydrogen evolution reaction of hangman porphyrins. *Energy & Environmental Science* **2012,** *5* (7), 7737-7740; (h) Schmidt, T. J.; Ross Jr, P. N.; Markovic, N. M., Temperature dependent surface electrochemistry on Pt single crystals in alkaline electrolytes: Part 2. The hydrogen evolution/oxidation reaction. *Journal of Electroanalytical Chemistry* **2002,** *524–525* (0), 252-260.

2. (a) Angamuthu, R.; Bouwman, E., Reduction of protons assisted by a hexanuclear nickel thiolate metallacrown: protonation and electrocatalytic dihydrogen evolution. *Phys Chem Chem Phys.* **2009,** *11* (27), 1463-9076; (b) Baffert, C.; Artero, V.; Fontecave, M., Cobaloximes as Functional Models for Hydrogenases. 2. Proton Electroreduction Catalyzed by Difluoroborylbis(dimethylglyoximato)cobalt(II) Complexes in Organic Media. *Inorganic chemistry* **2007,** *46* (5), 1817-1824; (c) Felton, G. A. N.; Glass, R. S.; Lichtenberger, D. L.; Evans, D. H., Iron-Only Hydrogenase Mimics. Thermodynamic Aspects of the Use of Electrochemistry to Evaluate Catalytic Efficiency for Hydrogen Generation. *Inorganic chemistry* **2006,** *45* (23), 9181-9184; (d) Fourmond, V.; Jacques, P. A.; Fontecave, M.; Artero, V., H2 evolution and molecular electrocatalysts: determination of overpotentials and effect of homoconjugation. *Inorganic chemistry* **2010,** *49* (22), 10338-47; (e) Helm, M. L.; Stewart, M. P.; Bullock, R. M.; DuBois, M. R.; DuBois, D. L., A Synthetic Nickel

Electrocatalyst with a Turnover Frequency Above 100,000 s−1 for H2 Production. *Science* **2011,** *333* (6044), 863-866; (f) Lee, C. H.; Dogutan, D. K.; Nocera, D. G., Hydrogen Generation by Hangman Metalloporphyrins. *Journal of the American Chemical Society* **2011,** *133* (23), 8775-8777; (g) Roberts, J. A. S.; Bullock, R. M., Direct Determination of Equilibrium Potentials for Hydrogen Oxidation/Production by Open Circuit Potential Measurements in Acetonitrile. *Inorganic chemistry* **2013,** *52* (7), 3823-3835; (h) Valdez, C. N.; Dempsey, J. L.; Brunschwig, B. S.; Winkler, J. R.; Gray, H. B., Catalytic hydrogen evolution from a covalently linked dicobaloxime. *Proceedings of the National Academy of Sciences* **2012,** *109* (http://www.pnas.org/content/109/39/15589.abstract), 15589-15593.

3. (a) McCarthy, B. D.; Martin, D. J.; Rountree, E. S.; Ullman, A. C.; Dempsey, J. L., Electrochemical Reduction of Brønsted Acids by Glassy Carbon in Acetonitrile—Implications for Electrocatalytic Hydrogen Evolution. *Inorganic chemistry* **2014,** *53* (16), 8350-8361; (b) Rudnev, A. V.; Molodkina, E. B.; Danilov, A. I.; Polukarov, Y. M.; Berna, A.; Feliu, J. M., Adsorption behavior of acetonitrile on platinum and gold electrodes of various structures in solution of 0.5 M H2SO4. *Electrochimica Acta* **2009,** *54* (14), 3692-3699; (c) Suárez-Herrera, M. F.; Costa-Figueiredo, M.; Feliu, J. M., Voltammetry of Basal Plane Platinum Electrodes in Acetonitrile Electrolytes: Effect of the Presence of Water. *Langmuir* **2012,** *28* (11), 5286-5294; (d) Szklarczyk, M.; Sobkowski, J., The behaviour of high polar organic solvents at platinum electrode — II. Adsorption and electrode reactions of acetonitrile. *Electrochimica Acta* **1980,** *25* (12), 1597-1601; (e) Zieja, J.; Gadomska-Trzos, J.; Stojek, Z., Electrooxidation and Electroreduction of Undiluted Acetonitrile at Platinum Microelectrodes. In Situ Determination of Water in Acetonitrile. *Electroanalysis* **2001,** *13* (8-9), 621-625.

4. (a) Klunker, J.; Schäfer, W., Anodic behavior of copper in acetonitrile: the influence of carbon dioxide and dimethylamine. *Journal of Electroanalytical Chemistry* **1999,** *466* (1), 107-116; (b) Kütt, A.; Leito, I.; Kaljurand, I.; Sooväli, L.; Vlasov, V. M.; Yagupolskii, L. M.; Koppel, I. A., A Comprehensive Self-Consistent

Spectrophotometric Acidity Scale of Neutral Brønsted Acids in Acetonitrile. *The Journal of Organic Chemistry* **2006,** *71* (7), 2829-2838; (c) Lv, W.; Zhang, R.; Gao, P.; Gong, C.; Lei, L., Electrochemical reduction of carbon dioxide with lead cathode and zinc anode in dry acetonitrile solution. *Journal of Solid State Electrochemistry* **2013,** *17* (11), 2789-2794; (d) Pavlishchuk, V. V.; Addison, A. W., Conversion constants for redox potentials measured versus different reference electrodes in acetonitrile solutions at 25°C. *Inorganica Chimica Acta* **2000,** *298* (1), 97-102; (e) Wasmus, S.; Cattaneo, E.; Vielstich, W., Reduction of carbon dioxide to methane and ethene—an on-line MS study with rotating electrodes. *Electrochimica Acta* **1990,** *35* (4), 771-775.

5. (a) Barthel, J.; Buchner, R.; Wismeth, E., FTIR Spectroscopy of Ion Solvation of LiClO4 and LiSCN in Acetonitrile, Benzonitrile, and Propylene Carbonate. *J Solution Chem* **2000,** *29* (10), 937-954; (b) Eberspächer, P.; Wismeth, E.; Buchner, R.; Barthel, J., Ion association of alkaline and alkaline-earth metal perchlorates in acetonitrile. *Journal of Molecular Liquids* **2006,** *129* (1-2), 3-12; (c) Mestdagh, J. M.; Binet, A.; Sublemontier, O., Solvation shells of the proton surrounded by acetonitrile, ethanol, and water molecules. *The Journal of Physical Chemistry* **1989,** *93* (26), 8300-8303; (d) Marcus, Y.; Hefter, G., Ion Pairing. *Chemical Reviews* **2006,** *106* (11), 4585-4621.

6. Gu, R. A.; Cao, P. G.; Sun, Y. H.; Tian, Z. Q., Surface-enhanced Raman spectroscopy studies of platinum surfaces in acetonitrile solutions. *Journal of Electroanalytical Chemistry* **2002,** *528* (1–2), 121-126.

7. Barrette, W. C.; Sawyer, D. T., Determination of dissolved hydrogen and effects of media and electrode materials on the electrochemical oxidation of molecular hydrogen. *Analytical Chemistry* **1984,** *56* (4), 653-657.

8. Strmcnik, D.; Tripkovic, D.; van der Vliet, D.; Stamenkovic, V.; Marković, N. M., Adsorption of hydrogen on Pt(1 1 1) and Pt(1 0 0)

surfaces and its role in the HOR. *Electrochemistry Communications* **2008,** *10* (10), 1602-1605.

9. Markovits, A.; Minot, C., Theoretical Study of the Acetonitrile Flip-Flop with the Electric Field Orientation: Adsorption on a Pt(111) Electrode Surface. *Catalysis Letters* **2003,** *91* (3-4), 225-234.

10. Trasatti, S.; Petrii, O. A., Real surface area measurements in electrochemistry. *Journal of Electroanalytical Chemistry* **1992,** *327* (1–2), 353-376.

11. Zou, S.; Weaver, M. J., Surface-Enhanced Raman Scattering on Uniform Transition-Metal Films: Toward a Versatile Adsorbate Vibrational Strategy for Solid-Nonvacuum Interfaces? *Analytical Chemistry* **1998,** *70* (11), 2387-2395.

12. Gao, P.; Gosztola, D.; Leung, L.-W. H.; Weaver, M. J., Surface-enhanced Raman scattering at gold electrodes: dependence on electrochemical pretreatment conditions and comparisons with silver. *Journal of Electroanalytical Chemistry and Interfacial Electrochemistry* **1987,** *233* (1–2), 211-222.

13. Izutsu, K., *Acid-Base Dissociation Constants in Dipolar Aprotic Solvents*. Blackwell Science: Oxford, U.K., 1990

14. Fawcett, W. R., The Ionic Work Function and its Role in Estimating Absolute Electrode Potentials. *Langmuir* **2008,** *24* (17), 9868-9875.

15. Angerstein-Kozlowska, H.; Macdougall, B.; Conway, B. E., Electrochemisorption and reactivity of nitriles at platinum electrodes and the anodic H desorption effect. *Journal of Electroanalytical Chemistry and Interfacial Electrochemistry* **1972,** *39* (2), 287-313.

16. (a) Barthel, J.; Deser, R., FTIR study of ion solvation and ion-pair formation in alkaline and alkaline earth metal salt solutions in acetonitrile. *J Solution Chem* **1994,** *23* (10), 1133-1146; (b) Fawcett, W. R.; Fedurco, M.; Opallo, M., The

inhibiting effects of tetraalkylammeonium cations on simple heterogeneous electron transfer reactions in polar aprotic solvents. *The Journal of Physical Chemistry* **1992,** *96* (24), 9959-9964; (c) Loring, J. S.; Fawcett, W. R., Ion–Solvent Interactions in Acetonitrile Solutions of Lithium, Sodium, and Tetraethylammonium Perchlorate Using Attenuated Total Reflectance FTIR Spectroscopy. *The Journal of Physical Chemistry A* **1999,** *103* (19), 3608-3617.

17. Kizhakevariam, N.; Villegas, I.; Weaver, M. J., Model electrochemical interfaces in ultra-high vacuum: solvent-induced surface potential profiles on Pt(111) from work-function measurements and infrared Stark effects. *Surface Science* **1995,** *336* (1–2), 37-54.

18. Marcus, Y., *Ion solvation.* Wiley: Chichester; New York, 1985.

19. (a) Zou, S.; Chan, H. Y. H.; Williams, C. T.; Weaver, M. J., Formation and Stability of Oxide Films on Platinum-Group Metals in Electrochemical and Related Environments As Probed by Surface-Enhanced Raman Spectroscopy: Dependence on the Chemical Oxidant. *Langmuir* **2000,** *16* (2), 754-763; (b) Chan, H. Y. H.; Zou, S.; Weaver, M. J., Mechanistic Differences between Electrochemical and Gas-Phase Thermal Oxidation of Platinum-Group Transition Metals As Discerned by Surface-Enhanced Raman Spectroscopy. *The Journal of Physical Chemistry B* **1999,** *103* (50), 11141-11151; (c) Luo, H.; Park, S.; Chan, H. Y. H.; Weaver, M. J., Surface Oxidation of Platinum-Group Transition Metals in Ambient Gaseous Environments: Role of Electrochemical versus Chemical Pathways. *The Journal of Physical Chemistry B* **2000,** *104* (34), 8250-8258.

20. Irr, L. G., Voltammetric studies of lithium salt-acetonitrile solutions containing traces of water. *Electrochimica Acta* **1984,** *29* (1), 1-5.

21. Hefter, G., Ion solvation in aqueous–organic mixtures. In *Pure and Applied Chemistry*, 2005; Vol. 77, p 605.

22. Domain, R.; Benoit, M., Basicity of Aprotonic Dipolar Solvents. *Canadian Journal Of Chemistry Revue Canadienne De Chimie* **1976,** *54* (13), 2101-2109.

23. Burger, K., *Solvation, ionic and complex formation reactions in non-aqueous solvents.* Elsevier Scientific: Amsterdam ; Oxford, United Kingdom, 1983; p 268 p.

24. Saielli, G.; Scorrano, G.; Bagno, A.; Wakisaka, A., Solvation of tetraalkylammonium chlorides in acetonitrile-water mixtures: mass spectrometry and molecular dynamics simulations. *Chemphyschem : a European journal of chemical physics and physical chemistry* **2005,** *6* (7), 1307-15.

3. Influence of water on the hydrogen evolution reaction on a gold electrode in acetonitrile solution

ABSTRACT

Here we discuss the importance of water in the proton solvation for the hydrogen evolution on polycrystalline gold microelectrodes. We perform cyclic voltammetry in acetonitrile electrolyte, in presence and absence of added amounts of water, with the interfacial movement of water and ions monitored by means of in situ Fourier Transform InfraRed (FTIR) spectroscopy. Our results show that the small trace amounts of water accumulate at the gold-acetonitrile interface, and that in the absence of protons this water leaves the interface with more negative potential. On the other hand, in the presence of protons in solution, protons exhibit a preferential solvation by water and water accumulates at the electrode surface under conditions of hydrogen evolution. Tafel plot analysis shows that the hydrogen evolution on gold in acetonitrile presents the same rate-determining step as for polycrystalline platinum, implying that the first electron transfer to yield adsorbed hydrogen is the rate-determining step of the reaction.

3.1. Introduction

Hydrogen evolution in non-aqueous solvents has been subject of study for many years, with a general focus on the dependence of the catalytic activity on the nature of the catalyst and the proton donor[1]. More recently, the influence of small or even trace amounts of water in acetonitrile solutions has been studied for a variety of electrochemical reduction or protonation reactions, such as hydrogen evolution, oxygen reduction, and carbon dioxide reduction[2]. In our previous work on hydrogen oxidation and proton reduction on the benchmark catalyst, i.e. platinum[2c], we showed by in situ Fourier-Transform Infrared (FTIR) spectroscopic analysis that the hydrogen oxidation and evolution (HOR/HER) in acetonitrile is assisted by a preferential solvation of protons in water. The HOR/HER appears to be so sensitive to the presence of water that even trace amounts influence the process. It would be important to characterize the role of water for non-ideal catalytic behavior, as it is the case with polycrystalline gold electrodes, on which the HOR does not proceed. An older study on the HER on platinum and gold can be found in literature[3], focusing on the solvation of two different acids (HCl and HPic) in acetonitrile. Their main findings pointed out the homoconjugation effect between the acid and the acetonitrile, due to incomplete dissociation of the acids, as well as the electrosorption of the solvent on the electrode surface, leading to irreversible behavior. However, the influence of water was not taken into account.

Here we present a spectroelectrochemical study, combining cyclic voltammetry and FTIR experiments, of the hydrogen evolution reaction in acetonitrile with 0.1 M tetrabutylammonium electrolyte, in presence and absence of 10 mM of perchloric acid as proton donor, under argon and hydrogen atmosphere. The experiments were also performed in presence of a small amount of added water (50 mM), in order to evaluate the importance of the water-proton and water-electrode interactions. The cyclic voltammetry and FTIR spectroscopy show that the hydrogen evolution on gold is mediated by the presence of water due to a preferential solvation of protons, in a similar fashion to what has been observed on

platinum electrodes. This behaviour appears to play an important role already at very low water concentrations.

3.2. Experimental Section

Prior to experiments, the glassware was rinsed with water (Milipore® MiliQ; resistivity >18.2 MΩ.cm), rinsed thoroughly with acetone (Sigma-Aldrich) and placed in the oven overnight at 120 °C. Acetonitril e (Anhydrous 99.8%, from Sigma-Aldrich) with tetrabutylammonium perchlorate (99.0% from Sigma-Aldrich) were used as received for preparing the electrolyte solutions. Ferrocenium hexafluorophosphate (97%, from Sigma-Aldrich) and ferrocene (99%, from Alfa Aesar) were used for preparing an equimolar solution in order to calibrate the equilibrium potential of the home-made $Ag/AgClO_4$ (97% from Sigma-Aldrich) reference electrode. The solutions were purged with argon (purity grade 6.0). For the experiments under hydrogen atmosphere we used a constant hydrogen flux (purity grade 5.6). All solutions used in this work are considered "wet", since we did not treat the reactants to reduce their characteristic water content.

Cyclic voltammetry was measured in a one-compartment, three-electrode cell connected to an Ivium potentiostat/galvanostat (IviumStat). The working electrode (WE) consisted of a gold wire, with a diameter of 120 µm and a real surface area of $(4.2 \pm 0.2) \times 10^{-2}$ cm^2 (obtained by measuring the area of the reduction peak from the gold oxides in aqueous electrolyte), assembled into a glass stem. The gold microelectrode was flame-annealed and rinsed with water and acetone before each measurement. We used a gold spiral as the counter electrode (CE) and a $Ag/AgClO_4$ electrode in acetonitrile as the reference electrode (RE). A 10 µF capacitor was connected between the RE and a platinum wire immersed in the solution, as a noise filter. The equilibrium potential of the redox couple Fc^0/Fc^+ was calculated as the half wave potential using cyclic voltammetry with a measured value of 0.038 V vs. $Ag/AgClO_4$.

The Fourier Transform Infra-Red Spectroscopy measurements were performed in a three electrode cell coupled to a CaF_2 prism slanted at 60 degrees, and connected to a Bruker Vertex80V IR spectrophotometer. A gold disk was mechanically polished with alumina of three different mesh (Alfa-Aesar), rinsed in an ultrasonic bath, flame-annealed and settled in the cell in a thin layer configuration, by pressing it against the prism. The CE was a gold wire and the RE was the $Ag/AgClO_4$. Hundred interferograms were averaged for each spectrum, with a resolution of 8 cm^{-1}. The transmission spectra used for the elucidation of bands in "dry" electrolyte were reported previously[2c], whereas the transmission spectra for the solutions containing electrolyte and added water were recorded using a SeZn window with an incident angle of 60°. One hundred scans were collected with a resolution of 8 cm^{-1} using p-polarized light. The reference spectrum was acquired from pure acetonitrile. All spectra in this work are reported as absorbance spectra, according to the approximation $A \approx \Delta R / R_0$ where R and R_0 are the reflectance corresponding to the single spectra obtained for the sample potential and the reference potential at their respective potentials. The interpretation of the bands is as follows: bands pointing upwards correspond to the formation of species at the surface at the sample potential with respect to the reference potential, and are called positive bands, while bands pointing downwards indicate the depletion of species from the electrode surface and are called negative bands.

3.3. Results

3.3.1. Characterization of the hydrogen evolution on polycrystalline gold in acetonitrile by cyclic voltammetry

Figures 1a and 1b depict the voltammograms collected for a polycrystalline gold microelectrode in acetonitrile solutions, containing 0.1 M of tetrabutylammonium perchlorate (TBAP) used as received and in presence of 50

mM of water, respectively. We present the second and last scan out of 200 voltammograms, recorded at a scan rate of 500 mV.s^{-1}. The dashed lines correspond to electrolytes under Ar-saturated conditions, whereas the solid lines represent the voltammograms for the H$_2$-saturated solutions. For the electrolyte with argon (Fig. 1a) we observe a reduction current at ca. -0.8 V$_{Ag/Ag+}$ and an adsorption/desorption process at ca. 0.5 V$_{Ag/Ag+}$. These peaks decrease and stabilize after the sixth scan (not shown), reaching the size and shape presented in the 200th scan. In the same subfigure, it is shown that the main difference in the second and last scan for the electrolyte in presence of H$_2$ is a smaller current corresponding to the peak at ca. 0.5 V$_{Ag/Ag+}$, suggesting that this process is hindered under H$_2$ saturation. This smaller current is probably due to a higher water availability at the electrode surface, as suggested by the blanks obtained in presence of added water, shown in Figure 1b, top panel, indicating that bubbling H$_2$ brings (a small amount of) water into the cell. The second scans recorded in presence of argon or hydrogen also show the reduction peak at -0.8 V$_{Ag/Ag+}$ as well as the oxidation-reduction peaks at ca. 0.5 V$_{Ag/Ag+}$, but with a smaller current compared to the voltammograms observed in the electrolyte without added water. In the 200th scan for the water-containing acetonitrile, in presence of argon or hydrogen, we observe a redox peak at 0.84 V$_{Ag/Ag+}$, presumably corresponding to the formation of gold (hydr)oxides [4]. These observations suggest that the gold-electrolyte interface is affected by the presence of water, and leads to oxide formation in the presence of considerable amounts of water. Our results also show that the hydrogen oxidation does not proceed on gold under the conditions studied.

In Figure 1a, bottom panel, we present the hydrogen evolution reaction (HER) current observed with the addition of 10 mM of HClO$_4$, in presence and absence of hydrogen. The two voltammograms are similar in current and shape, with an onset for proton reduction at ca. -0.50 V$_{Ag/Ag+}$. No significant differences are observed between the HER in presence and absence of hydrogen. We also present the same voltammograms after adding 50 mM of water in Figure 1b, bottom panel.
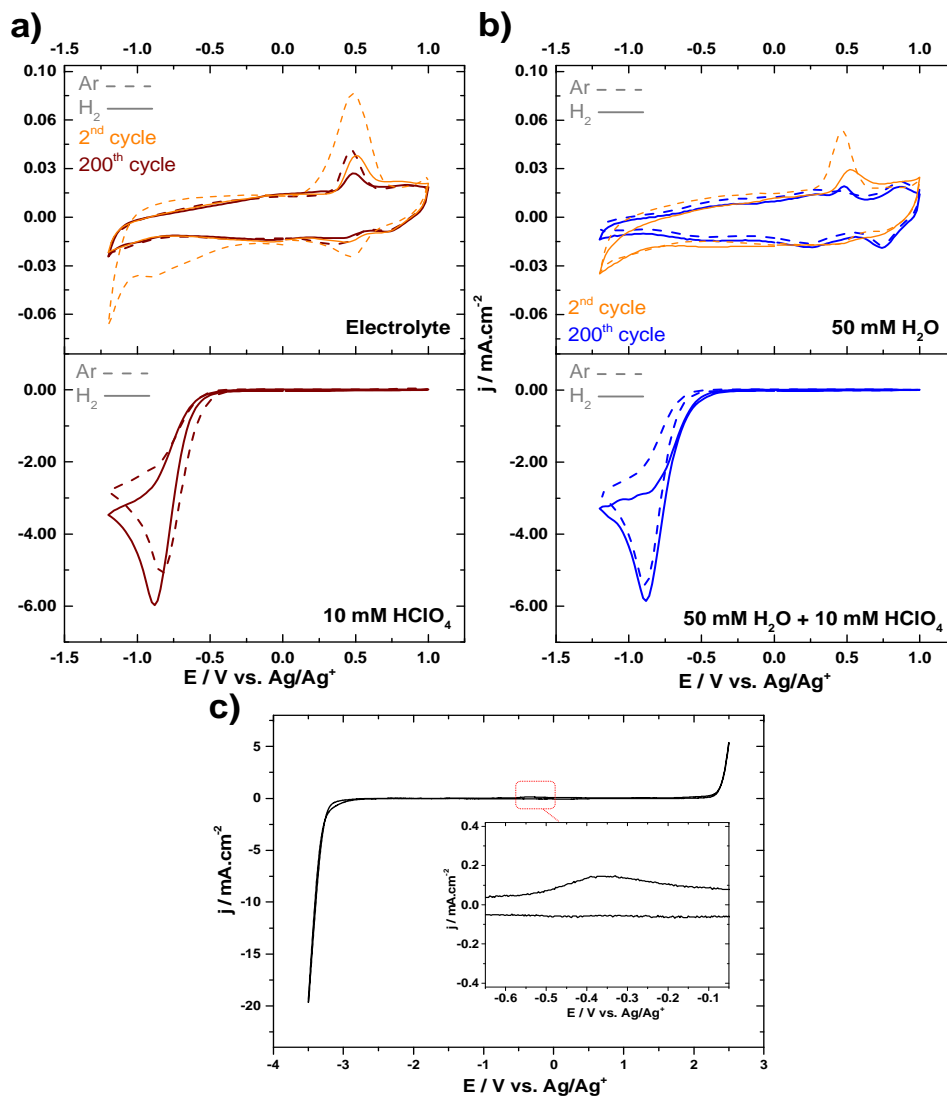
Figure 1. Cyclic voltammograms for a polycrystalline gold microelectrode in acetonitrile, containing 0.1 M TBAClO$_4$ as supporting electrolyte, with and without 10 mM of HClO$_4$. a) Using acetonitrile and supporting electrolyte as received, scan rate: 500 mV/s; b) After adding 50 mM of water, scan rate: 500 mV/s; c) In a wider working window in presence of 50 mM of water and argon saturation, scan rate: 50 mV.s^{-1}; insert: zoom in of the potential window -0.7 – -0.2 V$_{Ag/Ag+}$.

Still, no significant changes in current or features were observed when compared to the voltammetries obtained from the electrolytes without added water.

Finally, Figure 1c shows the last scan out of 50 voltammograms recorded in a much wider potential window at 50 mV.s^{-1}, for the electrolyte in presence of added water and argon, in order to ensure that no solvent decomposition is observed in the working window chosen for this work. No water reduction is observed; only solvent decomposition at ca. -2.9 V$_{Ag/Ag+}$. A small oxidation peak is observed at ca. -0.35 V$_{Ag/Ag+}$, probably related to the electrolyte adsorption at the electrode surface, as consequence of the lower scan rate used. This large potential window of (apparent) electrolyte stability is in agreement with what was previously reported by Gerischer and Wagner[5].

3.3.2. Evaluation of the water effect on the hydrogen evolution on polycrystalline gold using Fourier-Transform InfraRed spectroscopy

In order to study the interfacial processes occurring at the electrode interface, Fourier-Transform InfraRed (FTIR) spectroscopy was performed at a series of fixed potentials, for all the systems characterized in the previous section by cyclic voltammetry. The transmission spectra for these acetonitrile solutions have been discussed in our previous work[2c]; therefore, the interpretation of the main features shown in this work are based on the aforementioned study, in agreement with earlier reports from the literature[6].

We will discuss the features which are sensitive to the presence or absence of added water and hydrogen; namely, the acetonitrile bands, the water bands and the bands attributed to the supporting electrolyte, TBAP, i.e. TBA$^+$ cations and ClO$_4^-$ anions. The C-N bending and stretching modes from acetonitrile are observed in the range 2260-2340 cm^{-1}, and the C-H modes in the range 2900-3000

cm^{-1}. We note that the C-H modes are more intense in the presence of the electrolyte TBAP, due to the butyl chains present in the cation[2c]. The presence of water is characterized by bands in the O-H stretching region between 3100 and 3750 cm^{-1}, and by the bending modes in the 1500-1650 cm^{-1} range. Finally, the perchlorate ion presents a sharp band around 1130 cm^{-1}, from the Cl-O stretching mode. This vibration of the perchlorate anion has been reported previously[6a] by Barthel *et al.* to be susceptible to the formation of ion pairs in acetonitrile solutions, as manifested by the presence of low- and/or high-frequency shoulders.

The spectra were acquired from positive toward negative potentials (top to bottom in each figure), and the reference spectrum was recorded at 0 $V_{Ag/Ag+}$. The positive bands are related to the formation or accumulation of species at or near the electrode surface, whereas the negative bands indicate the depletion of species out of the double layer region, respectively.

Figure 2 shows the spectra collected for a gold electrode in acetonitrile electrolyte without added water, under argon atmosphere and hydrogen atmosphere. The spectra corresponding to the Ar-saturated solution is shown in figure 2a, along with an indication for the characteristic bands in the FTIR measurements. Figure 2a shows clearly the positive bands corresponding to C-N modes from acetonitrile in the region 2260-2340 cm^{-1}, as well as the C-H modes from TBA^+ at 2900-3000 cm^{-1}. The perchlorate band at 1133 cm^{-1} is also positive in the whole potential range studied. No signs of residual water are registered until -1 $V_{Ag/Ag+}$, in contrast to the hydrogen-saturated solution, presented in Figure 2b. The spectra for these solutions show a potential-dependent band pointing downwards in the range 3400-3750 cm^{-1}, with the corresponding bending tail at 1633 cm^{-1}, indicating the depletion of water from the electrode surface with increasingly negative potential. All the other bands have a diminished intensity in presence of molecular hydrogen (Figure 2b). These observations appear to be related to the observations made in Figures 1a and 1b, where the presence of H_2 brings water into the electrolyte. Figure 2 suggest that trace amounts of water accumulate at the

gold-electrolyte interface, with water depleting from the interface with more negative potential.

a) Electrolyte, Ar-saturated   **b) Electrolyte, H₂-saturated**
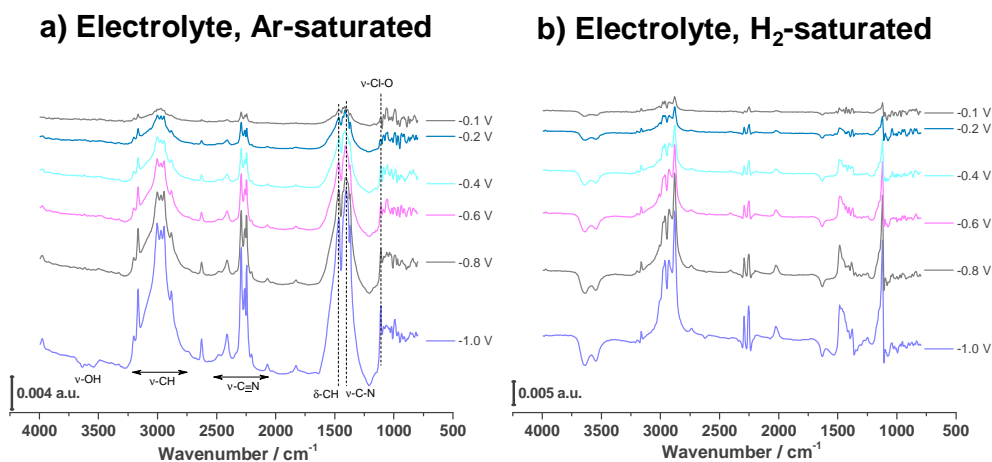
Figure 2. Potential-dependent absorbance spectra for a polycrystalline gold electrode in acetonitrile, containing 0.1 M tetrabutylammonium perchlorate as supporting electrolyte. Reference spectrum recorded at 0 $V_{Ag/Ag+}$.

Addition of 50 mM of water to the electrolyte in presence or absence of hydrogen leads to spectra shown in Figures 3a and 3b. In the transmission spectra we observe a small negative band around 2250 cm^{-1} from the CN stretching modes, indicating the interaction of the electrolyte with the acetonitrile. We also observe a positive band in the range 3000 – 3500 cm^{-1} from the water stretching mode and a displaced tail from the OH deformation at 1500 cm^{-1}. The perchlorate band can be found around 1100 cm^{-1}, next to the C-H modes from the TBAP (1250 cm^{-1}). No significant differences were observed between the transmission spectra from the solution saturated with argon and the one saturated with hydrogen. From the Ar-saturated solution we recorded the potential-dependent spectra shown in Figure 3a, in which most water and electrolyte bands are negative, suggesting migration away from the electrode surface. However, the spectra show two small positive bands at 1221 and 1713 cm^{-1}, presumably related to a C-N mode and a C-

O stretching mode, respectively [7], probably from the TBA$^+$ cation, since the acetonitrile does not decompose at these applied potentials. The spectra for the H$_2$-saturated solution can be found in Figure 3b. All the bands from water and electrolyte are pointing downwards, suggesting the migration of species away from the electrode surface. The results presented in Figures 2 and 3 suggest that the electrolyte TBAP interacts more strongly with the electrode when water is not present. The potential-dependent behaviour of the electrolyte ions in Figures 2 and 3 is somewhat difficult to interpret, but one must bear in my mind these measurements were performed in a thin-layer configuration, which was sometimes difficult to stabilize. Also, since no current is flowing, one would not expect any significant movement of ions, other than those adsorbing or desorbing, or moving in and out of the double layer. When a small amount of water is present or added to the electrolyte, and no apparent hydrogen evolution is proceeding, water leaves the electrode surface when a cathodic potential is applied, and this behaviour is independent of the saturation gas.
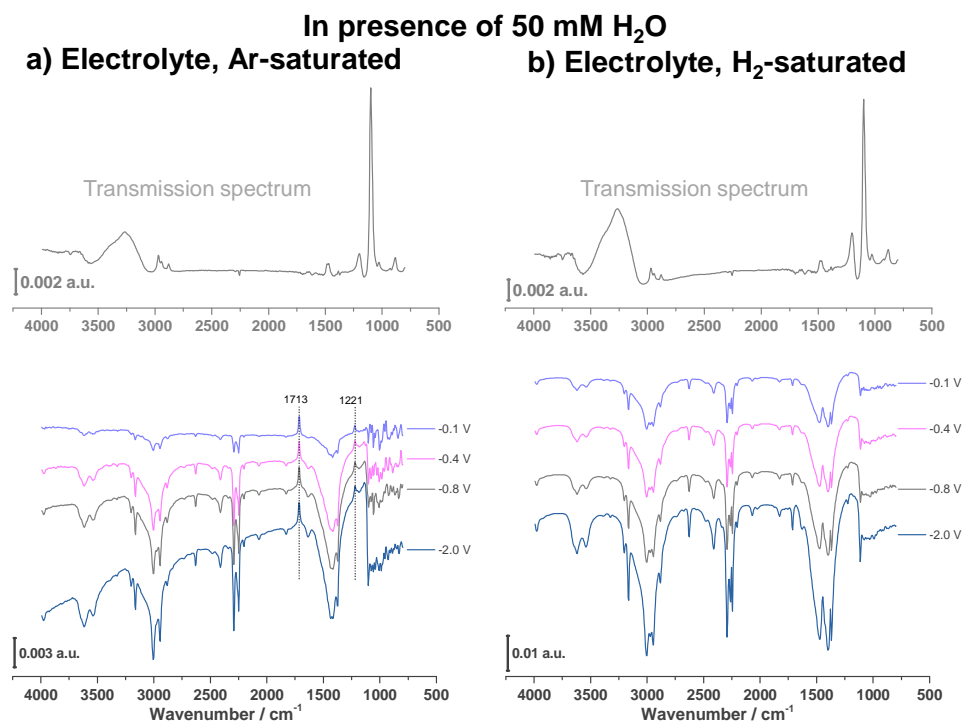
Figure 3. Potential-dependent absorbance spectra for a polycrystalline gold electrode in acetonitrile, containing 0.1 M tetrabutylammonium perchlorate as supporting electrolyte and in presence of 50 mM of added water. Reference spectrum recorded at 0 $V_{Ag/Ag+}$.

The blank spectra presented in Figures 2 and 3 showed the conditions of the interface in the absence of proton reduction. Now we proceed to evaluate the hydrogen evolution in the acetonitrile electrolyte in presence of a proton donor in the absence and presence of added water, both under argon or hydrogen saturated regime. The spectra obtained for the HER in the acetonitrile electrolytes in the presence of argon or hydrogen are shown in Figures 4a and 4b. In Figure 4a the accumulation of water at the electrode surface is illustrated by the potential dependence of the double band near 3500 cm^{-1} and the water bending mode at 1633 cm^{-1}. We also observe the migration of the TBA$^+$ and the acetonitrile towards

the electrode surface, described by the positive bands from the cation C-H at 2750 to 3250 cm^{-1} and the C-N stretching modes at 2450 cm^{-1}, respectively. On the other hand, the sharp perchlorate stretching mode at 1130 cm^{-1} depletes with more negative potentials. Saturation with molecular hydrogen leads to similar observations as in Figure 4a, without significant changes from what is observed in the Ar-saturated solution in presence of proton donor. These observations suggest that water accumulates at the electrode surface in presence of protons, and that perchlorate anions deplete from the surface, in agreement with Faradaic current flow.
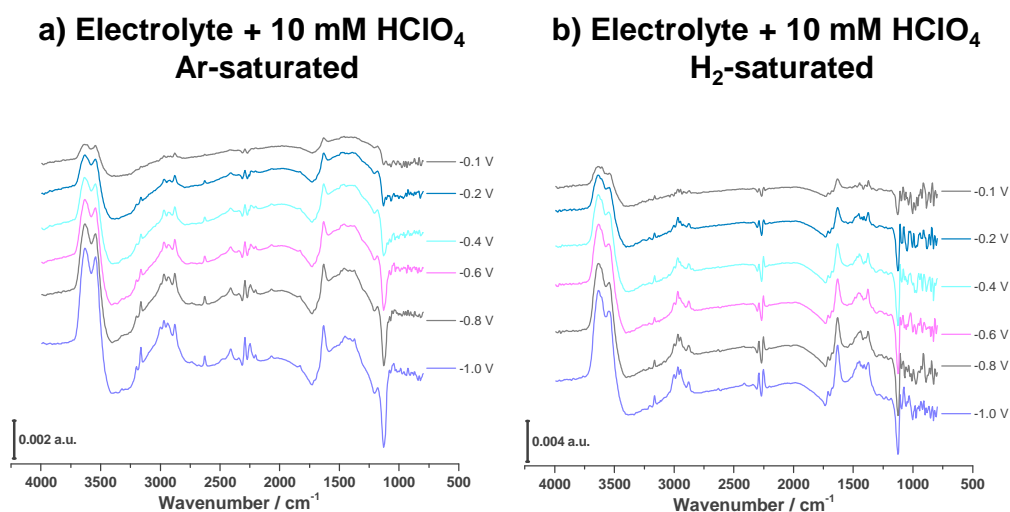
Figure 4. Potential-dependent absorbance spectra for the hydrogen evolution on a polycrystalline gold electrode in acetonitrile, containing 0.1 M tetrabutylammonium perchlorate as supporting electrolyte + 10 mM of $HClO_4$. Reference spectrum recorded at 0 $V_{Ag/Ag+}$.

In presence of added water and protons, the spectra from the Ar-saturated solution initially show a depletion of water from the interface until an inversion in the band orientation is observed at -0.4 $V_{Ag/Ag+}$ at the onset of HER. At this potential, the water bands turn positive, indicating accumulation of water at the

electrode surface. Acetonitrile and TBA⁺ are initially positive and then invert the configuration at -0.8 $V_{Ag/Ag+}$, indicating the migration of electrolyte-related species from the surface as we produce hydrogen, while water is present in the double layer. Under hydrogen-saturated conditions, Figure 5b shows all electrolyte-related bands and water migrating towards the electrode, except for the perchlorate, which leaves the surface. We also note that the C-N modes from TBA⁺ appear enhanced in this system.
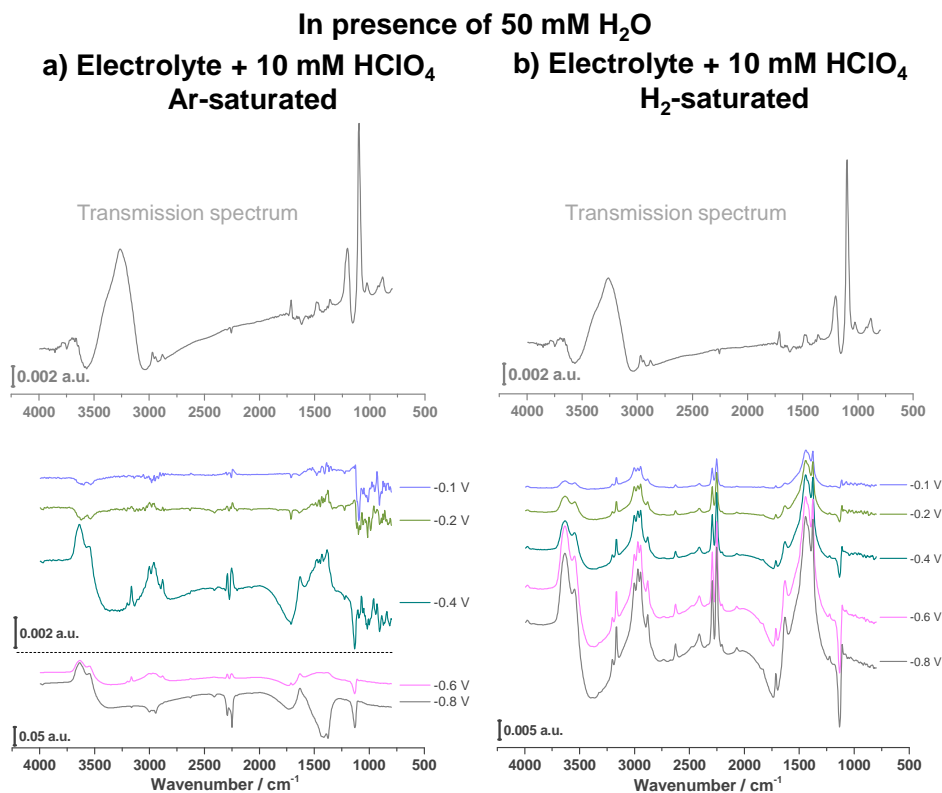
Figure 5. Potential-dependent absorbance spectra for the hydrogen evolution on a polycrystalline gold electrode in acetonitrile, containing 50 mM of water and 0.1 M tetrabutylammonium perchlorate as supporting electrolyte + 10 mM of $HClO_4$ as proton donor. Reference spectrum recorded at 0 $V_{Ag/Ag+}$.

Finally, we compare the HER on gold and platinum electrodes in acetonitrile solutions containing supporting electrolyte and 10 mM of $HClO_4$. Figure 6 shows the Tafel plots obtained at a scan rate of 10 mV.s^{-1}. We subtracted the non-Faradaic contributions from the voltammograms in order to obtain polarization curves shown in this work. The measurements in Figure 6 show a Tafel slope value of 132 mV.dec[-1] for a gold electrode and 137 mV.dec[-1] for a platinum electrode. The Tafel slopes indicate that the hydrogen evolution on gold and platinum in acetonitrile proceed through the same rate-determining step, namely that the first electron transfer step is rate-determining for the hydrogen evolution in acetonitrile solutions on both metals. Interestingly, this mechanism resembles the mechanism for HER in alkaline aqueous solution[8] and may suggest an important role of solvent reorganization in the hydrogen adsorption step.
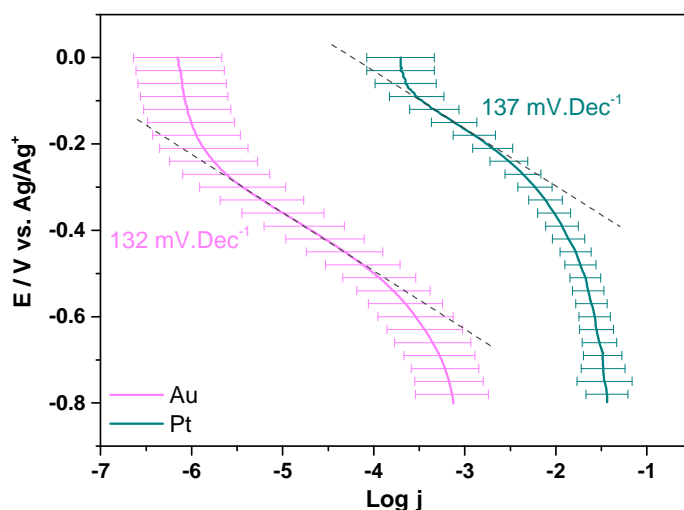
Figure 6. Tafel plots measured for gold and platinum microelectrodes in acetonitrile in presence of 0.1 M TBAP as supporting electrolyte and 10 mM $HClO_4$ as proton donor. Argon atmosphere.

3.4. Discussion and conclusions

In this paper, we have illustrated how important small amounts of water may be in the proper description and understanding of the hydrogen evolution reaction at a gold electrode in acetonitrile. The FTIR studies presented in this work reveal that trace amounts of water accumulate at the gold-acetonitrile interface. Previous work has shown that the largest source water is the electrolyte salt, not the acetonitrile itself, but also the bubbling of hydrogen appears to bring water into the solution. In absence of protons and Faradaic current, the water migrates away from the surface into the bulk with more negative potentials. On the other hand, in presence of added protons, under hydrogen evolution conditions, water accumulates at the electrode surface with more negative potential, indicating that protons carry water to the surface during their migration as a consequence of preferential solvation. This conclusion is underlined by experiments with purposefully added water. A very similar observation has been made previously for hydrogen evolution on platinum electrodes in acetonitrile [2c]. Regarding the migration of anions and cations in the acetonitrile solutions, under conditions of Faradaic current, they behave in accordance with the applied potential, i.e. TBA$^+$ cations migrate towards the surface and perchlorate anions move away at applied cathodic potentials. In the absence of Faradaic current, the behavior of the motion of ions is not fully understood but it should be noted that the thin-layer configuration under which the FTIR measurements were performed may not be stable enough to draw clear conclusions.

From the Tafel plot analysis we conclude that the hydrogen evolution on gold and platinum proceeds via the same mechanism in the sense that the rate-determining step for the hydrogen evolution in (water-containing) acetonitrile is the first electron transfer, leading to the adsorption of atomic hydrogen.

3.5. Acknowledgements

3.6. References

1. (a) Lanning, J. A.; Chambers, J. Q., Voltammetric study of the hydrogen ion/hydrogen couple in acetonitrile/water mixtures. *Analytical Chemistry* 1973, *45* (7), 1010-1016; (b) Felton, G. A. N.; Glass, R. S.; Lichtenberger, D. L.; Evans, D. H., Iron-Only Hydrogenase Mimics. Thermodynamic Aspects of the Use of Electrochemistry to Evaluate Catalytic Efficiency for Hydrogen Generation. *Inorganic chemistry* 2006, *45* (23), 9181-9184; (c) Baffert, C.; Artero, V.; Fontecave, M., Cobaloximes as Functional Models for Hydrogenases. 2. Proton Electroreduction Catalyzed by Difluoroborylbis(dimethylglyoximato)cobalt(II) Complexes in Organic Media. *Inorganic chemistry* 2007, *46* (5), 1817-1824; (d) Fourmond, V.; Jacques, P. A.; Fontecave, M.; Artero, V., H2 evolution and molecular electrocatalysts: determination of overpotentials and effect of homoconjugation. *Inorganic chemistry* 2010, *49* (22), 10338-47; (e) Treimer, S. E.; Evans, D. H., Electrochemical reduction of acids in dimethyl sulfoxide. CE mechanisms and beyond1. *Journal of Electroanalytical Chemistry* 1998, *449* (1–2), 39-48; (f) McCarthy, B. D.; Martin, D. J.; Rountree, E. S.; Ullman, A. C.; Dempsey, J. L., Electrochemical Reduction of Brønsted Acids by Glassy Carbon in Acetonitrile—Implications for Electrocatalytic Hydrogen Evolution. *Inorganic chemistry* 2014, *53* (16), 8350-8361.

2. (a) Suárez-Herrera, M. F.; Costa-Figueiredo, M.; Feliu, J. M., Voltammetry of Basal Plane Platinum Electrodes in Acetonitrile Electrolytes: Effect of the Presence of Water. *Langmuir* 2012, *28* (11), 5286-5294; (b) Staszak-Jirkovský, J.; Subbaraman, R.; Strmcnik, D.; Harrison, K. L.; Diesendruck, C. E.; Assary, R.;

Frank, O.; Kobr, L.; Wiberg, G. K. H.; Genorio, B.; Connell, J. G.; Lopes, P. P.; Stamenkovic, V. R.; Curtiss, L.; Moore, J. S.; Zavadil, K. R.; Markovic, N. M., Water as a Promoter and Catalyst for Dioxygen Electrochemistry in Aqueous and Organic Media. *ACS Catalysis* 2015, *5* (11), 6600-6607; (c) Ledezma-Yanez, I.; Díaz-Morales, O.; Figueiredo, M. C.; Koper, M. T. M., Hydrogen Oxidation and Hydrogen Evolution on a Platinum Electrode in Acetonitrile. *ChemElectroChem* 2015, *2* (10), 1612-1622; (d) Rudnev, A. V.; Zhumaev, U. E.; Kuzume, A.; Vesztergom, S.; Furrer, J.; Broekmann, P.; Wandlowski, T., The promoting effect of water on the electroreduction of CO2 in acetonitrile. *Electrochimica Acta* 2016, *189*, 38-44; (e) Figueiredo, M. C.; Ledezma-Yanez, I.; Koper, M. T. M., In situ spectroscopic study of CO2 electroreduction at copper electrodes in acetonitrile. *ACS Catalysis (Submitted)* 2016.

3. Sereno, R.; Macagno, V. A.; Giordano, M. C., Electrochemical behavior of acidic acetonitrile solutions at platinum and gold electrodes. *Journal of Electroanalytical Chemistry and Interfacial Electrochemistry* 1977, *76* (2), 199-216.

4. Wagner, D.; Gerischer, H., The influence of the water activity in acetonitrile on the formation and reduction of an oxide layer on gold. *Journal of Electroanalytical Chemistry and Interfacial Electrochemistry* 1989, *258* (1), 127-137.

5. Gerischer, H.; Wagner, D., The Underpotential Deposition of Lithium Ions from Acetonitrile Solutions with Small Amounts of Water. *Berichte der Bunsengesellschaft für physikalische Chemie* 1988, *92* (11), 1325-1330.

6. (a) Barthel, J.; Deser, R., FTIR study of ion solvation and ion-pair formation in alkaline and alkaline earth metal salt solutions in acetonitrile. *J Solution Chem* 1994, *23* (10), 1133-1146; (b) Loring, J. S.; Fawcett, W. R., Ion–Solvent Interactions in Acetonitrile Solutions of Lithium, Sodium, and Tetraethylammonium Perchlorate Using Attenuated Total Reflectance FTIR Spectroscopy. *The Journal of Physical Chemistry A* 1999, *103* (19), 3608-3617; (c) Fawcett, W. R.; Fedurco, M.; Opallo, M., The inhibiting effects of tetraalkylammonium cations on simple

heterogeneous electron transfer reactions in polar aprotic solvents. *The Journal of Physical Chemistry* 1992, *96* (24), 9959-9964.

7. Lambert, B., *Introduction to organic spectroscopy*. MacMillan: New York, 1987.

8. Ledezma-Yanez, I.; Wallace, W. D. Z.; Sebastián-Pascual, P.; Climent, V.; Feliu, J. M.; Koper, M. T. M., Enhancement of hydrogen evolution rates on platinum electrodes by controlling interfacial water reorganization. *(Submitted)* 2016.

4. Enhancement of hydrogen evolution rates on platinum electrodes by controlling interfacial water reorganization

ABSTRACT

The hydrogen evolution on platinum electrodes is a milestone reaction in electrocatalysis as well as an important reaction towards sustainable energy storage. Although the hydrogen evolution mechanism has been the subject of numerous studies, the pH dependent kinetics of this reaction is not yet fully understood. We present here a detailed kinetic study of the hydrogen adsorption and evolution reaction on Pt(111) in a wide pH range. Impedance measurements show that the hydrogen adsorption and hydrogen evolution are both slow in alkaline media, which is consistent with the observation of a shift in the rate-determining step for H_2 evolution with increasing pH value. Adding nickel to the Pt(111) surface lowers the barrier for the hydrogen adsorption rate and thereby enhances the hydrogen evolution rate. These observations are explained by a new model which highlights the role of interfacial water reorganization to accommodate charge transfer through the electric double layer, the energetics of which is controlled by how strongly water interacts with interfacial field. In alkaline media, the potential of zero charge is very positive compared the hydrogen evolution potential, leading to a higher activation energy for reorganizing water. Nickel lowers the potential of zero charge of Pt(111), as confirmed by laser-induced temperature jump experiments, and thereby lowers the barrier for hydrogen adsorption. Our findings and model shed new light on the origin of the slow kinetics for the hydrogen evolution reaction in alkaline media, solving a long-known problem toward efficient hydrogen production.

4.1. Introduction

There is a global call for industrial processes that combine economic progress with long-term preservation of natural resources. In terms of technological advances for sustainable energy production[1], there is a recent renewed interest to realize the so-called hydrogen economy[2] by photocatalytic water splitting or by the combination of photovoltaics with water electrolysis[3]. Methane steam-reforming[4] is currently the most cost-efficient technology available for hydrogen production, but unsustainable in the long run as it is still based on the deployment of fossil fuels. In order for the hydrogen economy to meet our future energy demands[5], there are, however, various fundamental bottlenecks to be overcome, such as that related to the efficient catalysis of the associated multi-proton multi-electron transfer reactions. Essentially, significant advances are required to lower the high inherent costs of electrocatalysts, by increasing the efficiency of water oxidation, by the replacement of scarce and expensive catalyst materials by earth-abundant alternatives, and by maximizing their durability and lifetime. Substantial efforts have thus been devoted to lowering the costs of the electrodes necessary for water splitting[6]. Recent theoretical works exposed the mechanistic features of the oxygen evolution reaction (OER)[7], taking place at the anodes of electrolyzers, in which water is oxidized to produce molecular oxygen and protons. These insights motivated several reports on earth-abundant and highly-efficient OER anode materials that typically work at high pH[8]. Unfortunately, the price to be paid for the use of alkaline conditions is a significant overpotential at the cathode, where the hydrogen evolution reaction (HER) takes place.

It has long been known in the electrochemistry literature that the kinetics of both the hydrogen evolution reaction (HER) and hydrogen oxidation reaction (HOR) on platinum are significantly slower in alkaline media than in acidic media[9]. The elucidation of the molecular-level origin of this problem would be of obvious importance for the further development of alkaline electrolysers and alkaline fuel cells. Marković *et al.* have recently shown[10] how the oxophylicity of the interface, as

modified by adsorbing a small amount of Ni(OH)$_2$ on Pt(111), may improve the kinetics of the HER/HOR, and ascribed this effect to the favorable interaction of surface adsorbed OH$_{ads}$ with the relevant intermediates. Mechanistic studies on the HER[10a-c, 11] have traditionally correlated reaction rates with thermodynamic descriptors, in particular the strength of the bond between hydrogen and the metal electrode, following the Sabatier principle[12]. Gasteiger *et al.* and Yan *et al.* have suggested[11c, 13] that a pH-dependent H-binding energy lies at the origin of the pH-dependent HER/HOR kinetics, and therefore they concluded that the H-binding energy is and remains the sole descriptor for the HER/HOR reaction. Specifically, Yan *et al.* have considered the pH-dependent shifts of the voltammetric peaks in the so-called "underpotential deposition" (UPD) hydrogen region of polycrystalline platinum as evidence for such a pH-dependent H-binding energy. However, the molecular-level origin of the pH-dependent H-binding energy has remained elusive. More importantly, we have recently argued[14] that the nature of the "hydrogen" peaks on polycrystalline platinum are unlikely to be associated with the adsorption of hydrogen only, but also include the effect of the adsorption of oxygenated species on (110) and (100) sites. Therefore, their peak potentials are not unambiguous indicators of H-binding energy. Moreover, on a Pt(111) electrode, there is no significant shift of the H-UPD with pH, but there is still a very significant pH-dependence of the HER/HOR kinetics (see below). Therefore, it appears that in spite of the undeniable success of the traditional models, they overlook important kinetic details, and that a consistent explanation of why HER/HOR on Pt is slow in alkaline media is still missing.

In this work, we present a detailed kinetic study of the hydrogen adsorption and evolution reaction on a Pt(111) single-crystal electrode, in a wide pH range, and in the absence and presence of a small amount of Ni(OH)$_2$ promoter. Electrochemical impedance spectroscopy is used to accurately measure the charge transfer kinetics of hydrogen adsorption. We present a new model for the rate of hydrogen adsorption step, based on the idea that the barrier for this reaction depends on how close or remote the electrode potential is in relation to the potential of zero

(free, see below) charge (pzc). The laser-induced temperature jump technique is then used to measure the potential of maximum entropy (pme), which is closely related to the pzc, to show that at pH 13, the addition of $Ni(OH)_2$ to Pt(111) indeed shifts the pme/pzc closer to the hydrogen adsorption region. We attribute the impact of the pzc on the activation barrier of hydrogen adsorption to the energy penalty associated with the reorganization of interfacial water to accommodate charge movement through the double layer. In acid media, the pzc/pme of Pt(111) is close to the hydrogen region, and the energy of reorganization of the interfacial water to move a proton through the double layer is relatively small. In alkaline media, the pzc/pme of Pt(111) is far from the hydrogen region (i.e. close to the OH_{ads} region) and the corresponding strong electric field existing at the electrode/electrolyte interface in the hydrogen region leads to a large reorganization energy for interfacial water when OH^- transfers through the double layer. In general terms, our results show how a cost-effective, earth-abundant metal as nickel, in the form of nickel hydroxide, promotes the reorganization of water networks at the electrode-electrolyte interface by shifting the pzc closer to the equilibrium potential of the HER reaction, thereby enhancing the reaction rate for the hydrogen evolution at high pH values. Our model also suggests a new strategy for designing new and better electrocatalysts in aqueous media, highlighting the role of the interfacial solvent reorganization on ion transfer steps.

4.2. Experimental Details

Experiments were carried out in a fluorinated ethylene propylene (FEP, Nalgene) electrochemical cell for alkaline solutions, whereas a glass cell was preferred for acidic solutions, using a three-electrode assembly at room temperature in both cases. The cells and glassware were initially cleaned by boiling in a 1:1 mixture of concentrated sulfuric acid and nitric acid, rinsed thoroughly and boiled with ultra clean water (Milipore® MiliQ; resistivity >18.2 MΩ.cm) five times

before each set of experiments. All the glassware and cells were kept in a permanganate/sulfuric acid mixture when not in use.

Solutions of different pH value were prepared as follows: for pH 1 we used solutions of 0.1 M $HClO_4$ (Merck 70%, Suprapur). In the preparation of pH 1.8 we used a mixture of 0.01 M $HClO_4$ + 0.090 M $NaClO_4$ (monohydrate, EMSURE), and for pH 2.5 the mixture was 0.001M $HClO_4$ + 0.099 M $NaClO_4$. Phosphate buffer solutions of 0.1 M were prepared for pH 4.3, 7, 9.1 and 9.8, using sodium dihydrogen phosphate and/or disodium hydrogen phosphate (Merck 99.99%, Suprapur) and ortho-phosphoric acid (Merck 85%, Suprapur) as indicated by the Henderson-Hesselbach equation for buffers. For pH 11 and 12 we prepared solutions of 0.001 M NaOH (Sigma-Aldrich, 99.99% trace metal basis) + 0.090 M $NaClO_4$, and 0.01M NaOH + 0.090 M $NaClO_4$ respectively. Solutions of 0.1 M NaOH were prepared for pH 13.

Bead-type single crystal platinum electrodes with a (111) orientation (<0.5 degrees) were used as working electrodes (WE). Before each experiment the electrode was flame-annealed for 1 min and cooled down to room temperature in a 3:1 proportion Ar + H_2 mixture (Linde 6.0). The electrode was transferred to the electrochemical cell with a protective droplet of deoxygenated water. All measurements were carried out with the Pt single crystal electrode in a hanging meniscus configuration. A platinum wire was used as counter electrode (CE). For the EIS measurements a home-made, self-contained hydrogen electrode (SCHE) was placed in the same electrolyte, with a Teflon connection in order to avoid contact between the solution and the glass. A 10 μF capacitor was connected, as a noise filter, between the RE and a platinum wire immersed in the solution. All potentials noted are referred to the reversible hydrogen electrode (RHE).

The argon was bubbled through a 3 M KOH trap before it entered the cell, in order to remove impurities which may be present from the tubing. The cell was placed inside a Faraday cage. Cyclic voltammetries and impedance spectra were

collected using a computer-controlled Ivium A06075 potentiostat (Iviumstat). Impedance spectra were measured with frequencies ranging from 10 kHz to 0.1 Hz and a peak-to-peak amplitude of 5 mV. The data was fitted to the equivalent electric circuit (EEC) shown in 2a, using a Python script, employing the Levenberg-Marquardt algorithm for non-linear least square regression.

For the deposition of a submonolayer of $Ni(OH)_2$ on the Pt(111) electrode we used a solution of 0.1M $NaClO_4$ and 5mM $Ni(NO_3)_2$ (Sigma-Aldrich 99.999%, trace metals basis). The solution was purged with Argon for 10 minutes and the Pt(111) electrode was modified via electroless instantaneous deposition, by placing the electrode in the deaerated solution for 10 s. After deposition, the Pt(111)-Ni electrode was rinsed with ultrapure water and brought to hanging meniscus configuration in a cell containing a 0.1 M NaOH solution, in order to perform cyclic voltammetry (3 cycles). The laser induced temperature jump experiment was performed as described elsewere[15]. Pulses of 5 ns of the second harmonic of a Nd-YAG laser (532 nm) were used as laser source, with an energy density around 8 $mJ.cm^{-2}$ (the laser beam diameter is 4 mm and the energy of the laser pulse is 1mJ), a value of energy small enough to prevent the damage of the $Ni(OH)_2$ deposit on the Pt(111) electrode. The laser energy was measured with a pyroelectric sensor head (Model M-935-10). The only effect from laser irradiation is the increase of the temperature of the interface.

4.3. Results and Discussion

Figure 1 illustrates the key observation that we wish to explain in this work, comparing the cyclic voltammetries for a Pt(111) electrode at pH 11 (blue line), pH 12 (red line), pH 13 (turquoise line) and pH 1 (black, dashed line). All the measurements were collected using a scan rate of 50 $mV.s^{-1}$. The voltammetric curves are very similar in current and shape for the alkaline pH, showing the typical features for the Pt(111) surface orientation: the hydrogen adsorption region, known

as H-UPD (0.1 – 0.35 V_{RHE}), which remains almost unaltered for the several pH values presented (versus the RHE), the double layer region (0.35 – 0.55 V_{RHE}), and the hydroxyl adsorption-desorption region (0.6 – 0.8 V_{RHE}). The reduction current registered between 0.05 V_{RHE} and -0.1 V_{RHE} corresponds to the hydrogen evolution. We observe that the onset potential for the HER in alkaline solutions exhibits a shift towards negative potentials as the pH value increases. Hydrogen evolution clearly has the lowest overpotential at pH 1, even though there is only a small shift in the H-UPD region in comparison to alkaline media. We conclude from Figure 1 that a pH-dependent shift in the H-binding energy (if any) cannot explain the significant pH dependence of the HER overpotential on Pt(111).
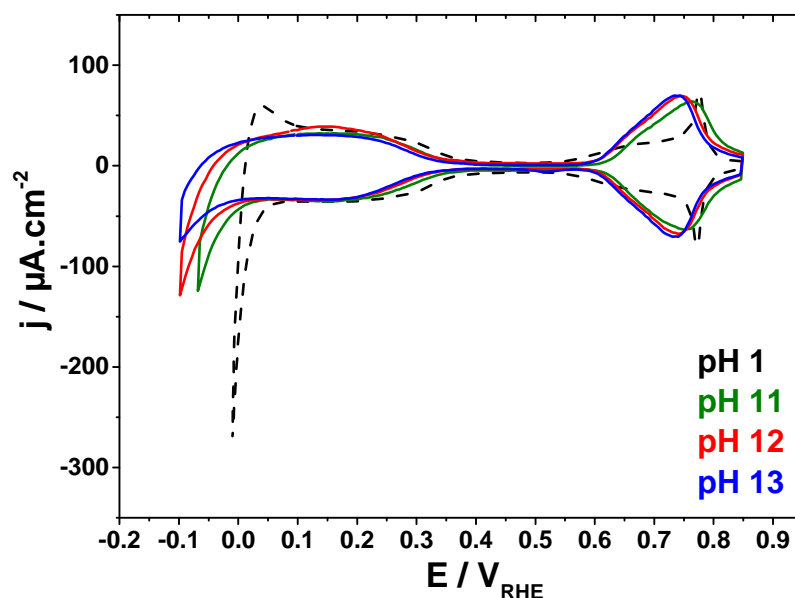

Figure 1. Cyclic voltammetries for Pt(111) in 0.1 M perchloric acid **(pH 1)**; 0.001 M NaOH + 0.099 M NaClO₄ **(pH 11)**; 0.01 M NaOH + 0.09 M NaClO₄ **(pH 12)**; 0.1 M NaOH **(pH 13).** Scan rate: 50 mV.s^{-1}.

To demonstrate that the pH also affects the rate of hydrogen adsorption in the H-UPD region, we studied the kinetics of hydrogen adsorption in the 0.1-0.3 V potential window. Figure 2 summarizes the measurements made by means of electrochemical impedance spectroscopy as a function of potential and pH. The experimental admittance spectra were fitted using the equivalent electric circuit (EEC[9c, 16]) presented in Figure 2a. This EEC corresponds to a simple heterogeneous adsorption step, forming an adsorbed intermediate without diffusion limitation. The charge transfer resistance, R_{ct}, is inversely proportional to the rate of the corresponding hydrogen adsorption reaction, i.e. $H^+ + e^- \rightarrow H_{ads}$ in acidic media, and $H_2O + e^- \rightarrow H_{ads} + OH^-$ in alkaline media. R_{sol} stands for the resistance of the solution, whereas C_{DL} and C_{AD} represent the capacitance of the double layer and the pseudo-capacitance of the adsorbed hydrogen, respectively. Figure 2b shows the admittance plots, measured at 0.2 V_{RHE} in solutions of 0.1 M ionic strength at different pH values. The data collected for the entire H-UPD region were fitted to the EEC shown in Figure 2a and can be found in Figure B1 in the Appendix B. From the Nyquist plots presented in Figure 2b we notice that for alkaline pH we observe two semicircles. The first semicircle at low frequencies (left side of each diagram) is related to the charge transfer resistance. For acidic media, only a single semicircle in the admittance plane is observed (not shown, see ref. 26), meaning that the H-UPD charge transfer process is too fast to be measured in acidic media[9c]. Therefore, not only the HER is slower in alkaline media, but also the H-UPD adsorption is slower, even if the thermodynamic driving force for hydrogen adsorption is the same (as all potentials are referred to the RHE scale and there is no observable pH dependence of the H-binding energy).

The R_{ct} measurements were performed for solutions with different pH value for the H-UPD region and are shown in Figure 2c. The R_{ct} for pH 7 is shown for comparison with the alkaline pH values (pH 7 was measured in a phosphate buffer, but since there is no phosphate adsorption in the H-UPD region[17], we do not expect an impact of phosphate on the hydrogen adsorption rate). From the figure we observe that the charge transfer is both pH- and potential-dependent. The

reaction becomes slower for higher pH values, pointing out that there is a reaction barrier for hydrogen adsorption that increases with pH. This effect cannot be described in terms of a presumed pH-dependent H-binding energy and must therefore have another origin.
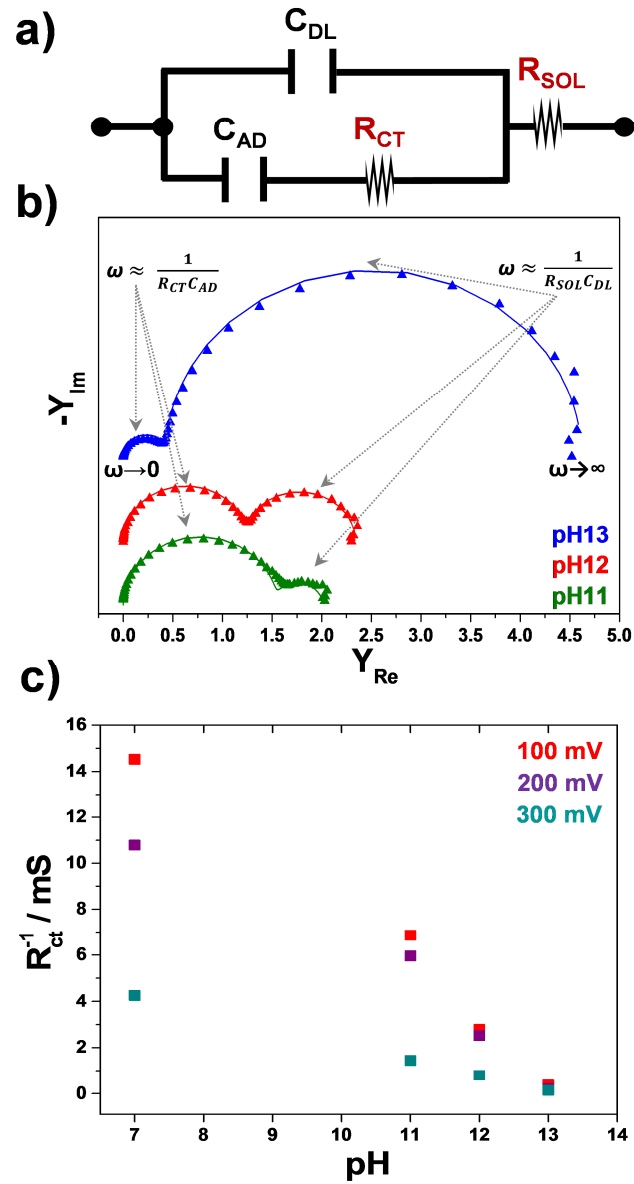
Figure 2. a) Equivalent electric circuit for H-UPD region, featuring the double layer capacitance, C_{DL}, the capacitance associated to the hydrogen adsorption, C_{AD}, the charge-transfer resistance for hydrogen adsorption, R_{CT}, and the solution resistance, R_{SOL}. b)

Admittance Nyquist plots for Pt(111) in 0.1 M solutions for different pH values, measured with frequencies ranging from 10 kHz to 0.1 Hz and an amplitude of 5 mV, at 0.2 V_{RHE}: the dots represent the experimental data points collected, while the solid lines correspond to the fit obtained using the EEC. The arrows point out how the components from the EEC in Fig. 2a are related to each semi-circle. The data for the entire H-UPD region can be found in Figure A1, in the Appendix B. c) Inverse of the charge transfer resistance as a function of the pH value. The R_{ct} was obtained from the fitting parameters for the admittance plots, collected for Pt(111) in 0.1 M solutions with different pH value. The different colors represent the potential at which the data was collected (see legend).

The mechanism for the hydrogen evolution at each pH value can be derived from the relationship between the current density and overpotential, known as Tafel plots. In order to estimate the Tafel slopes, we recorded polarization curves at 10 mV.s^{-1} under argon atmosphere, using 0.1 M solutions with pH values of 1, 1.8, 2.5, 4.3, 7, 9.1, 9.8, 11, 12 and 13, respectively. The polarization curves for these solutions are shown in Figure B2 in the Appendix B. Figure 3 shows the Tafel slopes as a function of pH, revealing the tendency of the slope to increase with pH, as reported previously[9b, 18] for pre-activated polycrystalline platinum electrodes. The significant conclusion from the combination of Figures 1 and 2 is that not only the rate of HER on Pt(111) changes with pH, but also the mechanism.

The relation of the rate-determining step in the mechanism to Tafel slope analysis has been described elsewhere[19]. Experimental reports[18b, 20] on polycrystalline and low-index single-crystal platinum electrodes under hydrodynamic conditions, exhibit Tafel slopes of ca. 30 mV.dec^{-1} for acid solutions and ca. 120 mV.dec^{-1} for alkaline solutions. Previous reported values of the Tafel slope for the HER on Pt(111) in acidic media are 31 mV.dec^{-1} in perchloric acid by Seto *et al.*[20] and 35 mV.dec^{-1} in sulphuric acid by Kita *et al.*[21] The interpretation of the measured Tafel slope is as follows. A value around 120 mV.dec^{-1} implies that the first electron transfer step (ET) is rate-determining (RDS), meaning that in alkaline media the so-called Volmer step $H_2O + e^- \rightarrow H_{ads} + OH^-$ is the slowest reaction step. A Tafel slope of ca. 40-30 mV.dec^{-1} implies that either the second ET

step is the RDS or the RDS is a chemical step preceded by two ETs, indicating that in acidic media the mechanism involves the Volmer step $H^+ + e^- \leftrightarrow H_{ads}$ in equilibrium, followed by a rate-determining Tafel step $2H_{ads} \rightarrow H_2$ or a rate-determining Heyrovsky step $H^+ + e^- + H_{ads} \rightarrow H_2$. These mechanistic implications are consistent with the observation that in alkaline solutions the hydrogen adsorption reaction is a slow reaction, whereas in acidic media this step is fast and in equilibrium.
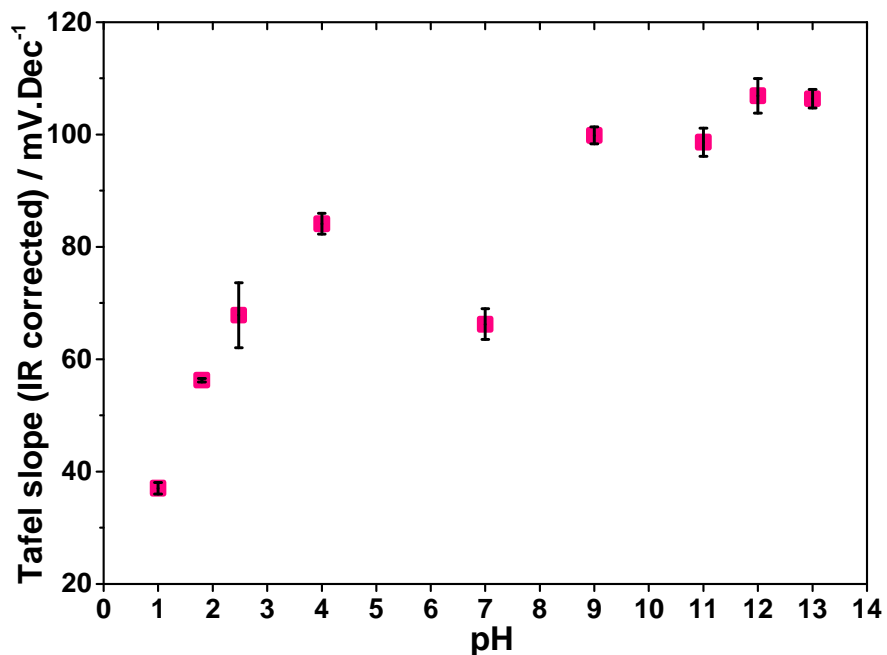
Figure 3. Tafel slopes measured for the hydrogen evolution reaction in 0.1 M solutions, in a wide pH range: 1, 1.8, 2.5, 4, 7, 9.1, 9.8, 11, 12 and 13 respectively. The description of the solutions used can be found in the experimental section.

Figure 4 compares the rate of hydrogen adsorption, as evaluated by EIS, and the rate of hydrogen evolution at pH 13 on bare Pt(111) and on Pt(111) in presence of a small amount of $Ni(OH)_2$. The Tafel plots for the HER (Fig. 4a) and

the inverse of the R_{ct} for H-UPD (Fig. 4b) for Pt(111)/Ni(OH)$_2$ show a clear enhancement of both rates in alkaline media, as compared to Pt(111). The HER rate enhancement was already reported in previous works[10b, 10d] by Marković *et al*.; the novelty here is that this enhancement *also* applies to the rate of H-UPD formation. From the Tafel plots in Figure 4a we can observe that the rate for hydrogen evolution in the presence of Ni(OH)$_2$ is now in between that for pH 13 and pH 1 on pure Pt(111), with a corresponding change in Tafel slope. This would suggest that the role of Ni(OH)$_2$ is to lower the barrier for the hydrogen adsorption reaction, rather than to change the energetics of the hydrogen intermediate or the mechanism.
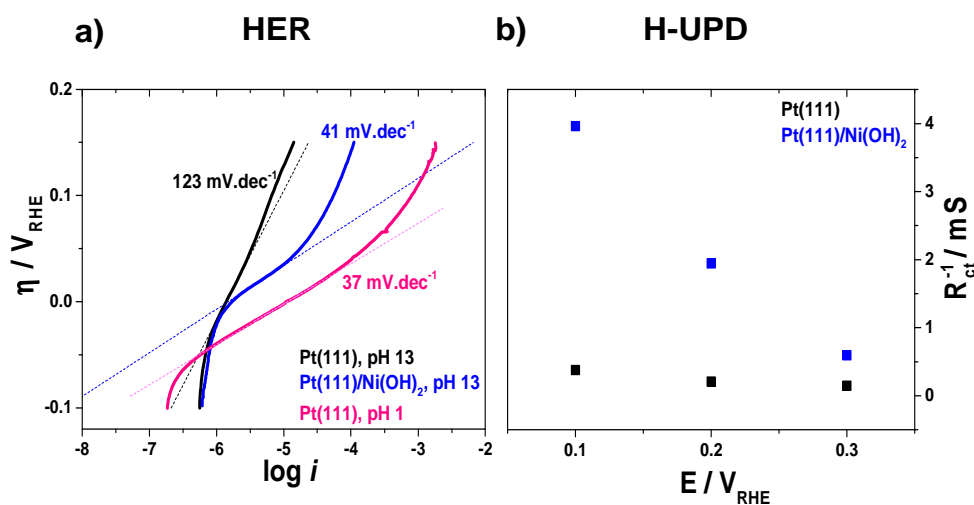
Figure 4. a) Tafel plots for HER on for Pt(111) at pH 1 and pH 13 and on a Pt(111) electrode decorated with 0.1 ML of Ni(OH)$_2$ in 0.1 M NaOH (pH 13), under argon atmosphere. The polarization curves were registered at a scan rate of 10 mV.s^{-1}. b) The inverse of the charge transfer resistance as a function of potential for Pt(111) (black squares) and Pt(111) electrode decorated with ~0.14 ML of Ni(OH)$_2$ in 0.1 M NaOH, pH 13 (blue squares); argon atmosphere. The R_{ct} was obtained from the fitting parameters for admittance plots (see Figure B3 in the Appendix B).

82

Our suggestion here is that the rate of hydrogen adsorption (and hence of hydrogen evolution if hydrogen adsorption is rate-determining) has a pH dependent barrier because the interfacial water structure at the Pt(111) electrode is pH dependent. During the hydrogen adsorption reaction, charge has to move through the interfacial double layer (H^+ in acid and OH^- in alkaline). The rate of such a charge transfer reaction depends on the extent to which the solvation environment (i.e. the water) can accommodate this charge migration. If the interfacial water is easily reorganized, charge transfer through the double layer will be rapid; if the interfacial water is rigid and difficult to reorganize, charge transfer through the double layer will be slow. An important parameter to influence the extent to which the interfacial water can be reorganized is the interfacial electric field. The latter is determined by the charge separation between the metal electrode and the electrolyte solution, which in turn, is dependent on the position of the pzc. In the presence of adsorption reactions, distinction should be done between total and free charges[22]. While the latter represents the true charge determining the electric field at the interface, the total charge, which includes also the charge stored in the bond of adsorbed species, is the only available parameter from electrochemical measurements. To obtain the true pzc (potential of zero free charge, pzfc), additional measurements and assumptions are necessary to separate adsorption reactions from the true capacitive processes[23]. In the absence of a strong interfacial electric field, i.e. close to the potential of zero (free) charge (pzc), water is relatively free to reorient and hence easy to reorganize. In the presence of a strong interfacial electric field, i.e. further away from the pzc, water is much more rigid and hence more difficult to reorganize. As has been shown by previous work[23-24], while the pzfc cannot be directly measured, an estimation can be obtained from values of CO displaced charge. This is achieved by extrapolating the charge in the double layer region either into the hydrogen adsorption region (acid solutions) or into the hydroxyl adsorption region (alkaline solutions). In this way, a relatively constant value of pzfc is obtained, independent of pH in the SHE scale. This means that pzfc changes from the double layer region (0.34 V_{RHE}) in acidic

83

solutions to the onset of the surface oxidation (ca. 1.0 V_{RHE}) in alkaline solutions[23]. As a consequence, at a given potential on the RHE scale, the strength of the electric field and the energy associated with the (re)organization of interfacial solvent molecules will depend on pH. Since the H-UPD region is far from the pzc of Pt(111) in alkaline media, the hydrogen adsorption reaction is slow in alkaline solutions. In this model, a way to compensate this strong electric field is to use surface modifiers, such as nickel, that bring the pzc closer to the equilibrium potential of the hydrogen evolution reaction.

To assess whether such a shift in pzc and the associated energy of reorganization of the interfacial water could indeed explain the promoting effect of $Ni(OH)_2$, we have employed the laser-induced temperature jump method. This technique uses short laser pulses to increase the temperature of the solvent at the interface for a very brief period of time[25]. During the relaxation at open circuit, the temporal change in potential induced by the temperature perturbation is registered. The sign of the transient gives information about the average orientation of the interfacial solvent that existed at the potential before the potentiostatic control was removed and the short laser pulse was applied. In this interpretation, it is implied that adsorption processes are not fast enough to respond to the temperature perturbation. Specifically, the potential for which the polarity of the transient changes is identified as the potential of maximum entropy (pme), which is expected to be closely related to the pzfc. Previous comparisons[25b] between the pme and pzfc of Pt(111) in acidic solution indeed show a close correspondence between the two quantities.

Details regarding the laser-induced temperature jump method can be found in the literature[25b]. The method was used to determine the pme of the Pt(111) interface at pH 13, as well as the effect of a submonolayer amount of $Ni(OH)_2$ deposited on the Pt(111) surface on the pme. The results of the measurements are shown in Figure 5. We present the cyclic voltammetries for the bare and decorated electrode in Figure 5a. The transients for Pt(111) at pH 13 in Figure 5b are

negative at 0.5 $V_{RHE.}$ At that potential, the interfacial water molecules are oriented with their hydrogens pointing towards the electrode surface. We observe a change in polarity of the interfacial species at 0.675 V_{RHE}. Assuming that the hydroxyl adsorption is not fast enough to contribute to the potential transient, this change in polarity suggests that from this potential the water molecules have an average orientation with the hydrogens pointing away from the electrode surface. The potential of maximum entropy, is therefore located close to 0.675 V_{RHE} (some 25 mV lower than the pzc) at potentials above which the average orientation of the hydrogens in the water molecules are pointing away from the electrode surface (see Fig. 5). In this case, the difference between the pme and the extrapolated value of the pzfc[23] would be a consequence of the hydroxyl adsorption on the water orientation and the double layer capacitance. What is clear is that pme and pzfc are both located above 0.6 V RHE, i.e., well above the value in acid solutions.

The laser-induced coulostatic potential transients collected for the Pt(111) electrode decorated with ~0.2 ML of $Ni(OH)_2$, at pH 13, are shown in Figure 5c. Negative transients are observed for 0.60 V_{RHE}. From 0.645 V_{RHE} we observe a change in polarity of the transient, suggesting that the pme has shifted ca. 30 mV negatively with respect to the bare Pt(111). This shift in pme/pzc is in accordance with our model for the enhancement of the H-UPD and hydrogen evolution by the presence of $Ni(OH)_2$ on the surface as proposed above, relating the hydrogen adsorption and hydrogen evolution rates to the energy required for the water reorganization in the electrode interface. While the interpretation of the t-jump experiment is subject to some uncertainty regarding the interference of hydroxyl adsorption to the measured potential transient, previous results with other adatoms clearly demonstrated that the presence of electropositive adatoms at the electrode interface decrease significantly the value of the pme, and therefore the pzfc[26], supporting our interpretation.

Our model for the role of interfacial solvent reorganization in the hydrogen adsorption reaction bears some resemblance to a model for electrochemical proton

transfer suggested many years ago by Pecina and Schmickler[27]. Using Monte Carlo simulations they showed that the activation energy for proton transfer increases at high interfacial fields due to the effect referred to above (at low field, the activation energy in their simulations in fact lowers due to a favourable configurational effect). More recently, Rossmeisl *et al.*[28] also considered models for the pH dependence of electrochemical proton transfer barriers, and emphasized the pH dependent contribution of the configurational entropy of the proton as the origin of the pH dependent kinetics. Our model emphasizes, on the other hand, the pH dependent enthalpy of interfacial water reorganization, as related to the pH dependent potential of zero charge of Pt on the RHE scale.
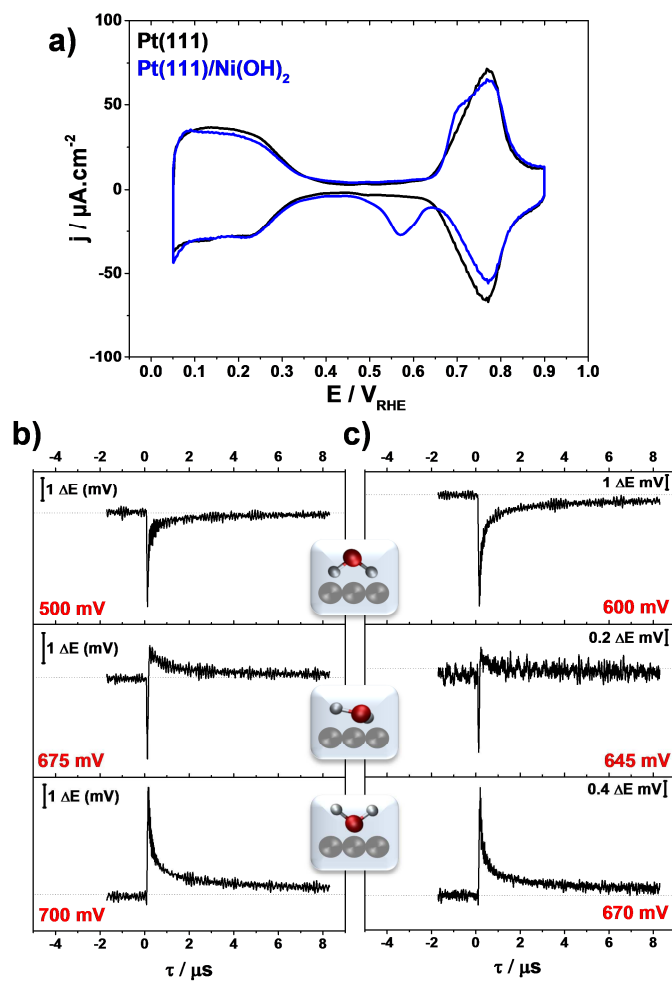
Figure 5. a) Cyclic voltammograms for Pt(111) in 0.1 M NaOH under argon atmosphere, registered at a scan rate of 50 mV.s^{-1}: The black line shows the blank of the bare electrode, whereas the blue line shows the Pt(111) electrode decorated with 0.17 ML of Ni(OH)$_2$, growth with instant deposition from a solution containing 5 mM Ni(NO$_3$)$_2$ (Ni^0) and 3 cycles in the 0.1 M NaOH solution. b) Laser-induced coulostatic potential transients collected for the Pt(111) electrode. c) Laser-induced coulostatic potential transients collected for the Pt(111) electrode decorated with 0.17 ML of Ni(OH)$_2$. Dotted lines mark zero mV. The cartoons illustrate the average orientation of water molecules in the interface.

4.4. Conclusions

Given the experimental evidence presented in this paper, we conclude that a pH-dependent shift in the H-binding energy does not explain the significant pH dependence of the HER overpotential on Pt(111). We have studied its kinetic origin by a thorough interpretation of combined impedance measurements, Tafel plot analysis and laser-induced temperature jump experiments of interfacial solvent reorganization. We showed that not only the HER is slower in alkaline media, but also the H-UPD adsorption is slower, even if the thermodynamic driving force is the same for the different pH values on the RHE scale. Also the rate-determining step in the mechanism for the hydrogen evolution reaction is affected by the pH, in agreement with the observation that hydrogen adsorption becomes a kinetically hindered step in alkaline media.

We explain our observations by introducing a new model for the HER highlighting the role of interfacial water reorganization in the hydrogen adsorption step. This model is based on the experimental result that in acidic media, the H-UPD and HER occur close to the potential of zero charge, whereas in alkaline media, the H-UPD and the hydrogen evolution occur far from the potential of zero (total) charge. This would imply that in alkaline media the interfacial water network at the potential of H-UPD and HER interacts strongly with the strong interfacial electric field and is therefore more rigid and more difficult to reorganize during the charge transfer through the electrical double layer. This causes the hydrogen step to be slow in alkaline media. The presence of $Ni(OH)_2$ in submonolayer amounts improves the H-UPD charge transfer and the hydrogen evolution kinetics in alkaline pH by inducing a shift in the potential of total zero charge toward the HER equilibrium potential, as confirmed by laser-induced temperature jump experiments. In this new model, $Ni(OH)_2$ promotes the hydrogen evolution reaction by lowering the energy barrier necessary for the reorganization of the interfacial water network, allowing a more efficient proton/hydroxide transfer through the double layer. Importantly, the new model also implies that the hydrogen binding

energy is not the sole descriptor for the HER kinetics. The strength of the interfacial electric field, as determined by the distance of the potential of zero (total) charge (or the potential of maximum entropy) from the equilibrium potential of the reaction to be catalysed, impacts on the rate of hydrogen adsorption by influencing the energetic barrier associated with the reorganisation of interfacial water during charge transfer.

4.5. Acknowledgments

4.6. References

1. (a) Morgan, E. R.; Acker, T. L., Practical Experience With a Mobile Methanol Synthesis Device. *Journal of Solar Energy Engineering* **2015,** *137* (6), 064506-064506; (b) Hotz, N., Hybrid Solar System for Decentralized Electric Power Generation and Storage. *Journal of Solar Energy Engineering* **2012,** *134* (4), 041010-041010; (c) Liu, C.-j.; Burghaus, U.; Besenbacher, F.; Wang, Z. L., Preparation and Characterization of Nanomaterials for Sustainable Energy Production. *ACS Nano* **2010,** *4* (10), 5517-5526; (d) Goldemberg, J., Ethanol for a Sustainable Energy Future. *Science* **2007,** *315* (5813), 808-810; (e) Hoffert, M. I.; Caldeira, K.; Benford, G.; Criswell, D. R.; Green, C.; Herzog, H.; Jain, A. K.; Kheshgi, H. S.; Lackner, K. S.; Lewis, J. S.; Lightfoot, H. D.; Manheimer, W.; Mankins, J. C.; Mauel, M. E.; Perkins, L. J.; Schlesinger, M. E.; Volk, T.; Wigley, T. M. L., Advanced Technology Paths to Global Climate Stability: Energy for a Greenhouse Planet. *Science* **2002,** *298* (5595), 981-987.

2. (a) Turner, J. A., Sustainable Hydrogen Production. *Science* **2004,** *305* (5686), 972-974; (b) Edwards, P. P.; Kuznetsov, V. L.; David, W. I. F.; Brandon, N. P., Hydrogen and fuel cells: Towards a sustainable energy future. *Energy Policy* **2008,** *36* (12), 4356-4362; (c) Momirlan, M.; Veziroglu, T. N., The properties of hydrogen as fuel tomorrow in sustainable energy system for a cleaner planet. *International Journal of Hydrogen Energy* **2005,** *30* (7), 795-802; (d) Bockris, J. O. M., The origin of ideas on a Hydrogen Economy and its solution to the decay of the environment. *International Journal of Hydrogen Energy* **2002,** *27* (7–8), 731-740.

3. (a) Kudo, A.; Miseki, Y., Heterogeneous photocatalyst materials for water splitting. *Chemical Society Reviews* **2009,** *38* (1), 253-278; (b) Bolton, J. R., Solar photoproduction of hydrogen: A review. *Solar Energy* **1996,** *57* (1), 37-50; (c) Ni, M.; Leung, M. K. H.; Leung, D. Y. C.; Sumathy, K., A review and recent developments in photocatalytic water-splitting using for hydrogen production. *Renewable and Sustainable Energy Reviews* **2007,** *11* (3), 401-425.

4. Van Hook, J. P., Methane-Steam Reforming. *Catalysis Reviews* **1980,** *21* (1), 1-51.

5. Barnhart, C. J.; Benson, S. M., On the importance of reducing the energetic and material demands of electrical energy storage. *Energy & Environmental Science* **2013,** *6* (4), 1083-1092.

6. (a) H. Hashemi, S. M.; Modestino, M. A.; Psaltis, D., A membrane-less electrolyzer for hydrogen production across the pH scale. *Energy & Environmental Science* **2015,** *8* (7), 2003-2009; (b) Zou, X.; Zhang, Y., Noble metal-free hydrogen evolution catalysts for water splitting. *Chemical Society Reviews* **2015,** *44* (15), 5148-5180; (c) Huang, Q.; Ye, Z.; Xiao, X., Recent progress in photocathodes for hydrogen evolution. *Journal of Materials Chemistry A* **2015,** *3* (31), 15824-15837.

7. (a) Man, I. C.; Su, H.-Y.; Calle-Vallejo, F.; Hansen, H. A.; Martínez, J. I.; Inoglu, N. G.; Kitchin, J.; Jaramillo, T. F.; Nørskov, J. K.; Rossmeisl, J., Universality in

Oxygen Evolution Electrocatalysis on Oxide Surfaces. *ChemCatChem* **2011,** *3* (7), 1159-1165; (b) Calle-Vallejo, F.; Díaz-Morales, O. A.; Kolb, M. J.; Koper, M. T. M., Why Is Bulk Thermochemistry a Good Descriptor for the Electrocatalytic Activity of Transition Metal Oxides? *ACS Catalysis* **2015,** *5* (2), 869-873.

8. (a) Diaz-Morales, O.; Ledezma-Yanez, I.; Koper, M. T. M.; Calle-Vallejo, F., Guidelines for the Rational Design of Ni-Based Double Hydroxide Electrocatalysts for the Oxygen Evolution Reaction. *ACS Catalysis* **2015,** *5* (9), 5380-5387; (b) Park, J. H.; Kim, S.; Bard, A. J., Novel Carbon-Doped TiO2 Nanotube Arrays with High Aspect Ratios for Efficient Solar Water Splitting. *Nano Letters* **2006,** *6* (1), 24-28; (c) Suntivich, J.; May, K. J.; Gasteiger, H. A.; Goodenough, J. B.; Shao-Horn, Y., A Perovskite Oxide Optimized for Oxygen Evolution Catalysis from Molecular Orbital Principles. *Science* **2011,** *334* (6061), 1383-1385; (d) Friebel, D.; Louie, M. W.; Bajdich, M.; Sanwald, K. E.; Cai, Y.; Wise, A. M.; Cheng, M.-J.; Sokaras, D.; Weng, T.-C.; Alonso-Mori, R.; Davis, R. C.; Bargar, J. R.; Nørskov, J. K.; Nilsson, A.; Bell, A. T., Identification of Highly Active Fe Sites in (Ni,Fe)OOH for Electrocatalytic Water Splitting. *Journal of the American Chemical Society* **2015,** *137* (3), 1305-1313.

9. (a) Bockris, J. O. M.; Potter, E. C., The Mechanism of the Cathodic Hydrogen Evolution Reaction. *Journal of The Electrochemical Society* **1952,** *99* (4), 169-186; (b) Conway, B. E.; Bai, L., State of adsorption and coverage by overpotential-deposited H in the H2 evolution reaction at Au and Pt. *Electrochimica Acta* **1986,** *31* (8), 1013-1024; (c) Schouten, K. J. P.; van der Niet, M. J. T. C.; Koper, M. T. M., Impedance spectroscopy of H and OH adsorption on stepped single-crystal platinum electrodes in alkaline and acidic media. *Physical Chemistry Chemical Physics* **2010,** *12* (46), 15217-15224.

10. (a) Subbaraman, R.; Tripkovic, D.; Chang, K.-C.; Strmcnik, D.; Paulikas, A. P.; Hirunsit, P.; Chan, M.; Greeley, J.; Stamenkovic, V.; Markovic, N. M., Trends in activity for the water electrolyser reactions on 3d M(Ni,Co,Fe,Mn) hydr(oxy)oxide

catalysts. *Nat Mater* **2012,** *11* (6), 550-557; (b) Subbaraman, R.; Tripkovic, D.; Strmcnik, D.; Chang, K.-C.; Uchimura, M.; Paulikas, A. P.; Stamenkovic, V.; Markovic, N. M., Enhancing Hydrogen Evolution Activity in Water Splitting by Tailoring Li+-Ni(OH)2-Pt Interfaces. *Science* **2011,** *334* (6060 %U http://www.sciencemag.org/content/334/6060/1256.abstract), 1256-1260; (c) Danilovic, N.; Subbaraman, R.; Strmcnik, D.; Chang, K.-C.; Paulikas, A. P.; Stamenkovic, V. R.; Markovic, N. M., Enhancing the Alkaline Hydrogen Evolution Reaction Activity through the Bifunctionality of Ni(OH)2/Metal Catalysts. *Angewandte Chemie* **2012,** *124* (50), 12663-12666; (d) Strmcnik, D.; Uchimura, M.; Wang, C.; Subbaraman, R.; Danilovic, N.; van der, V.; Paulikas, A. P.; Stamenkovic, V. R.; Markovic, N. M., Improving the hydrogen oxidation reaction rate by promotion of hydroxyl adsorption. *Nat Chem* **2013,** *5* (4), 300-306.

11. (a) Marković, N. M.; Sarraf, S. T.; Gasteiger, H. A.; Ross, P. N., Hydrogen electrochemistry on platinum low-index single-crystal surfaces in alkaline solution. *Journal of the Chemical Society, Faraday Transactions* **1996,** *92* (20), 3719-3725; (b) Sheng, W.; Gasteiger, H. A.; Shao-Horn, Y., Hydrogen Oxidation and Evolution Reaction Kinetics on Platinum: Acid vs Alkaline Electrolytes. *Journal of The Electrochemical Society* **2010,** *157* (11), B1529-B1536; (c) Sheng, W.; Zhuang, Z.; Gao, M.; Zheng, J.; Chen, J. G.; Yan, Y., Correlating hydrogen oxidation and evolution activity on platinum at different pH with measured hydrogen binding energy. *Nature communications* **2015,** *6*, 5848; (d) Greeley, J.; Jaramillo, T. F.; Bonde, J.; Chorkendorff, I.; Norskov, J. K., Computational high-throughput screening of electrocatalytic materials for hydrogen evolution. *Nat Mater* **2006,** *5* (11), 909-913.

12. (a) Laursen, A. B.; Varela, A. S.; Dionigi, F.; Fanchiu, H.; Miller, C.; Trinhammer, O. L.; Rossmeisl, J.; Dahl, S., Electrochemical Hydrogen Evolution: Sabatier's Principle and the Volcano Plot. *Journal of Chemical Education* **2012,** *89* (12), 1595-1599; (b) Skúlason, E.; Tripkovic, V.; Björketun, M. E.; Gudmundsdóttir, S.; Karlberg, G.; Rossmeisl, J.; Bligaard, T.; Jónsson, H.; Nørskov, J. K., Modeling

the Electrochemical Hydrogen Oxidation and Evolution Reactions on the Basis of Density Functional Theory Calculations. *The Journal of Physical Chemistry C* **2010,** *114* (42), 18182-18197; (c) Nørskov, J. K.; Bligaard, T.; Logadottir, A.; Kitchin, J. R.; Chen, J. G.; Pandelov, S.; Stimming, U., Trends in the Exchange Current for Hydrogen Evolution. *Journal of The Electrochemical Society* **2005,** *152* (3), J23-J26.

13. Durst, J.; Siebel, A.; Simon, C.; Hasche, F.; Herranz, J.; Gasteiger, H. A., New insights into the electrochemical hydrogen oxidation and evolution reaction mechanism. *Energy & Environmental Science* **2014,** *7* (7), 2255-2260.

14. van der Niet, M. J. T. C.; Garcia-Araez, N.; Hernández, J.; Feliu, J. M.; Koper, M. T. M., Water dissociation on well-defined platinum surfaces: The electrochemical perspective. *Catalysis Today* **2013,** *202*, 105-113.

15. Climent, V.; Garcia-Araez, N.; Compton, R. G.; Feliu, J. M., Effect of Deposited Bismuth on the Potential of Maximum Entropy of Pt(111) Single-Crystal Electrodes. *The Journal of Physical Chemistry B* **2006,** *110* (42), 21092-21100.

16. Morin, S.; Dumont, H.; Conway, B. E., Evaluation of the effect of two-dimensional geometry of pt single-crystal faces on the kinetics of upd of h using impedance spectroscopy. *Journal of Electroanalytical Chemistry* **1996,** *412* (1–2), 39-52.

17. Gisbert, R.; García, G.; Koper, M. T. M., Adsorption of phosphate species on poly-oriented Pt and Pt(1 1 1) electrodes over a wide range of pH. *Electrochimica Acta* **2010,** *55* (27), 7961-7968.

18. (a) Schuldiner, S., Hydrogen Overvoltage on Bright Platinum: II . pH and Salt Effects in Acid, Neutral, and Alkaline Solutions. *Journal of The Electrochemical Society* **1954,** *101* (8), 426-432; (b) Conway, B. E.; Bai, L., Determination of adsorption of OPD H species in the cathodic hydrogen evolution reaction at Pt in

93

relation to electrocatalysis. *Journal of Electroanalytical Chemistry and Interfacial Electrochemistry* **1986,** *198* (1), 149-175.

19. (a) Shinagawa, T.; Garcia-Esparza, A. T.; Takanabe, K., Insight on Tafel slopes from a microkinetic analysis of aqueous electrocatalysis for energy conversion. *Scientific Reports* **2015,** *5*, 13801; (b) D. Pletcher, R. G., R. Peat, L. M. Peter, J. Robinson, *Instrumental Methods in Electrochemistry*. Woodhead Publishing Limited: Cambridge, UK, 2010; p 666.

20. Seto, K.; Iannelli, A.; Love, B.; Lipkowski, J., The influence of surface crystallography on the rate of hydrogen evolution at Pt electrodes. *Journal of Electroanalytical Chemistry and Interfacial Electrochemistry* **1987,** *226* (1), 351-360.

21. Hoshi, N.; Asaumi, Y.; Nakamura, M.; Mikita, K.; Kajiwara, R., Structural Effects on the Hydrogen Oxidation Reaction on n(111)–(111) Surfaces of Platinum. *The Journal of Physical Chemistry C* **2009,** *113* (39), 16843-16846.

22. Climent, V.; Climent, V.; García Araez, N.; Herrero, E.; Feliu, J., Potential of zero total charge of platinum single crystals: A local approach to stepped surfaces vicinal to Pt(111). *Russian Journal of Electrochemistry* **2006,** *42* (11), 1145-1160.

23. Rizo, R.; Sitta, E.; Herrero, E.; Climent, V.; Feliu, J. M., Towards the understanding of the interfacial pH scale at Pt(1 1 1) electrodes. *Electrochimica Acta* **2015,** *162*, 138-145.

24. Garcia-Araez, N.; Climent, V.; Herrero, E.; Feliu, J. M.; Lipkowski, J., Thermodynamic approach to the double layer capacity of a Pt(1 1 1) electrode in perchloric acid solutions. *Electrochimica Acta* **2006,** *51* (18), 3787-3793.

25. (a) Sebastián, P.; Sandoval, A. P.; Climent, V.; Feliu, J. M., Study of the interface Pt(111)/ [Emmim][NTf2] using laser-induced temperature jump experiments. *Electrochemistry Communications* **2015,** *55*, 39-42; (b) Garcia-Araez,

94

N.; Climent, V.; Feliu, J., Potential-Dependent Water Orientation on Pt(111), Pt(100), and Pt(110), As Inferred from Laser-Pulsed Experiments. Electrostatic and Chemical Effects. *The Journal of Physical Chemistry C* **2009,** *113* (21), 9290-9304.

26. García-Aráez, N.; Climent, V.; Feliu, J. M., Evidence of Water Reorientation on Model Electrocatalytic Surfaces from Nanosecond-Laser-Pulsed Experiments. *Journal of the American Chemical Society* **2008,** *130* (12), 3824-3833.

27. Pecina, O.; Schmickler, W., A model for electrochemical proton-transfer reactions. *Chemical Physics* **1998,** *228* (1–3), 265-277.

28. Rossmeisl, J.; Chan, K.; Skúlason, E.; Björketun, M. E.; Tripkovic, V., On the pH dependence of electrochemical proton transfer barriers. *Catalysis Today* **2016,** *262*, 36-40.

5. Summary

97

This thesis discusses the role of the solvent in the hydrogen oxidation and evolution reactions on platinum and gold. This novel approach contributes to the understanding of the molecular origins affecting the kinetics of the hydrogen evolution reaction, which is a model electrochemical reaction as well as a promising source of energy, in the era of sustainable energy production and storage.

Since the traditional approach focuses on the nature of the catalyst and the catalytic activity, an exploration of the electrolyte and, specifically, the role of the solvent in the electrocatalysis of hydrogen is much needed. The experimental work presented here was carried out using linear sweep voltammetry and cyclic voltammetry, *in situ* Fourier-Transform InfraRed spectroscopy and Surface-Enhanced Raman spectroscopy, Electrochemical Impedance spectroscopy and the Laser-Induced Temperature Jump method. These techniques were key to elucidate the molecular nature of the solvent-proton, solvent-electrolyte and solvent-electrode interactions taking place at the electrode-electrolyte interface.

In Chapter 2 we studied the hydrogen oxidation and evolution reactions on a polycrystalline platinum electrode in acetonitrile. We started the study by comparing systems in presence of two different cations; namely, a metallic, hydrophilic cation and a lipophilic, organic cation. With this comparison we tried to establish the sensitivity of the reaction to the nature of the cation and we found no direct correlation. However, the kinetics happened to be sensitive to the presence of water in the organic-based electrolytes, since the interaction of the cation with water-traces was found to be different for each system. We used *in situ* FTIR to monitor these interactions and we observed that protons and small cations are preferentially solvated by water. On the other hand, the SERS measurements showed that platinum oxides are not involved in the catalysis of hydrogen evolution and oxidation in acetonitrile. Furthermore, these experiments confirmed that under hydrogen oxidation conditions, water solvates the protons preferentially and together they migrate from the electrode surface towards the bulk. These findings

impact on the hydrogen evolution and oxidation reaction, as we found out that these reactions are mediated by water. Hence, it is difficult to establish a reference electrode for organic solvents due to the sensitivity of the reaction to trace amounts of water. Our conclusions can be extended to several non-protic electrolytes used as test systems for molecular catalysts. Additionally, the sensitivity of these systems to trace amounts of water hinders the possibility of establishing consistent comparisons between systems with a different solvent, leading to an inaccurate comparison of the catalytic activity for the different (molecular) catalysts.

For the sake of completeness, we present a study on the influence of water on the hydrogen evolution reaction on a polycrystalline gold electrode in acetonitrile, which is found in Chapter 3. In this chapter we used *in situ* FTIR as spectroelectrochemical technique which allowed us to follow the migration of ions and water in and out of the interface. Our study reveals that water accumulates at the interface in presence of protons, exhibiting preferential solvation, in agreement with the observations discussed in Chapter 2. These findings endorse the relevance of the electrolyte conditions in the hydrogen electrocatalysis in non-protic solvents, as well as the importance of water in the hydrogen oxidation and evolution reactions. A Tafel plot analysis on polycrystalline gold and platinum in acetonitrile electrolytes shows that the hydrogen evolution presents the same rate-determining step for both metals; i.e. the first electron transfer along with the adsorption of atomic hydrogen on the electrode surface. This mechanism resembles the observations reported for hydrogen evolution in alkaline solutions, reinforcing the hypothesis that the solvent has a significant influence in the hydrogen electrocatalysis.

In Chapter 4 we present a thorough spectroelectrochemical study of the kinetics of hydrogen evolution and H-UPD formation in aqueous electrolytes. The study covers a wide pH range, and the electrode used is a Pt(111) single crystal. We start by measuring the charge transfer resistance in the H-UPD region, and our experiments show that not only the hydrogen evolution in alkaline solutions is

slower, but also the H-UPD formation is. Tafel slopes in the wide pH region (from pH 1 to pH 13) showed how the mechanism for hydrogen evolution changes, implying a major contribution of the solvent as we moved towards higher pH values. Next, we decorated the Pt(111) surface with submonolayer amounts of nickel and generated nickel hydroxide on the surface to monitor the improvement of the hydrogen kinetics in presence of this electropositive metal as a promoter. Once again, impedance spectroscopy and Tafel plot analysis were used. Our observations suggest that the presence of $Ni(OH)_2$ lowers the hydrogen adsorption reaction barriers, since it was found that not only the HER kinetics change, but also the charge transfer resistance kinetics for the UPD region happens to be faster in presence of the promoter. From these observations we propose a new kinetic model based on the energetic penalty paid for the reorganization of the interfacial water, since the rate of hydrogen adsorption has a pH dependent barrier because the interfacial water structure at the Pt(111) electrode is pH dependent. Therefore, the kinetics of charge transfer would be faster if water were easily reorganized (low pH values), and slower if the water network is rigid (high pH values), as determined by the potential of maximum entropy, which is closely related to the potential of zero free charge (pzfc). The latter is determined by the charge separation between the metal electrode and the electrolyte solution, which in turn, is dependent on the position of the pzfc. The temperature jump technique experiments showed how a submonolayer amount of nickel hydroxide shifts the pzfc closer to the equilibrium potential of the hydrogen evolution, impacting on the energy penalty associated to the movement of charges through the double layer. In consequence, the study elucidates the molecular origin of the slow reaction rates for the hydrogen evolution reaction in alkaline solutions.

In brief, this thesis showed the importance of the solvent in the hydrogen electrocatalysis, specifically, water, by settling its role as a solvent, as a proton donor, and by preferential proton solvation, ultimately clarifying a long-existing debate regarding the pH dependence of the hydrogen evolution, setting a path for

future exploration of solvent-electrode interfaces for tailoring electrocatalytic reactions.

6. Samenvatting

Dit proefschrift bespreekt de rol van het oplosmiddel voor de waterstof oxidatie en waterstof evolutie reactie (HER) op platina en goud. Deze nieuwe benadering draagt bij aan het inzicht van de moleculaire processen die van invloed zijn op de kinetiek van de waterstof evolutie reactie. De waterstof evolutie reactie zelf is een elektrochemische model reactie, maar ook een veelbelovende potentiele bron van energie in dit tijdperk van duurzame productie en opslag van energie.

Aangezien de traditionele aanpak is gericht op de aard van de katalysator en de katalytische activiteit, was een onderzoek naar de rol van het elektrolyt en van het oplosmiddel in de elektrokatalyse van waterstof hard nodig. Het experimentele werk in dit proefschrift werd uitgevoerd met behulp van lineaire sweep voltammetrie en cyclische voltammetrie, *in situ* Fourier-transformatie infrarood spectroscopie en Surface Enhanced Raman spectroscopie, Elektrochemische Impedantiespectroscopie en de Laser-Induced Temperature Jump methode. Deze technieken waren de sleutel om de moleculaire aard van de interacties tussen het proton, elektrolyt ionen, elektrode en oplosmiddelmoleculen die plaatsvinden in het elektrode-elektrolyt grensvlak te verklaren.

In hoofdstuk 2 bestudeerden we de waterstof oxidatie en de evolutie reacties op een polykristallijne platina-elektrode in acetonitril. We begonnen de studie door systemen te vergelijken in de aanwezigheid van twee verschillende kationen; namelijk een metaal hydrofiel kation en een lipofiel, organisch kation. Met deze vergelijking probeerden we de gevoeligheid van de reactie voor de aard van het kation vast te stellen, maar uiteindelijk vonden we geen directe correlatie. De kinetiek bleek echter gevoelig te zijn voor de aanwezigheid van water in de organische elektrolyten, omdat de interactie van het kation met de sporen water in de oplossing verschillend bleek te zijn voor ieder systeem. We gebruikten *in situ* FTIR om deze wisselwerkingen te monitoren en we constateerde dat protonen en kleine kationen bij voorkeur worden gesolvateerd door water. Anderzijds, de SERS metingen toonden aan dat platina oxiden niet betrokken zijn bij de katalyse van waterstof evolutie en oxidatie in acetonitril. Bovendien bevestigden deze

experimenten dat onder waterstof oxidatie omstandigheden water bij voorkeur de protonen solvateert waarna ze samen migreren van het elektrode-oppervlak naar de bulk. Deze bevindingen hebben invloed op de waterstof evolutie en waterstof oxidatie reactie, omdat we erachter kwamen dat deze reacties worden gemedieerd door water. Daarom is het moeilijk om een referentie-elektrode voor organische oplossingen vast te stellen, vanwege de gevoeligheid van deze reactie voor sporen van water in deze type oplossing. Onze conclusies kunnen worden uitgebreid naar verscheidene niet-protische elektrolyten die worden gebruikt als testsystemen voor moleculaire katalysatoren. Daarnaast belemmert de gevoeligheid sporen van in deze systemen de mogelijkheid tot het vaststellen van consistente vergelijkingen tussen systemen met een ander oplosmiddel. Dit leidt tot een onnauwkeurige vergelijking van de katalytische activiteit van de verschillende (moleculaire) katalysatoren.

Voor de volledigheid presenteren wij in hoofdstuk 3 een onderzoek naar de invloed van water op de waterstof evolutie reactie op een polykristallijne goud elektrode in acetonitril. In dit hoofdstuk gebruikten wij *in situ* FTIR als spectroelektrochemische techniek waardoor wij de migratie van ionen en water in uit en naar het grensvlak konden volgen. Onze studie laat zien dat het water zich ophoopt op het grensvlak wanneer protonen die preferentiële solvatatie laten zien aanwezig zijn. Dit is in overeenstemming met de waarnemingen in hoofdstuk 2. Deze bevindingen onderschrijven de relevantie van de elektrolyt omstandigheden in de waterstof elektrokatalyse in niet-protische oplosmiddelen en het belang van water in waterstof oxidatie en evolutie reacties. Een Tafel plot analyse van polykristallijn goud en platina in acetonitril elektrolyten toont aan dat de waterstof evolutie dezelfde snelheidsbepalende stap heeft voor beide metalen; d.w.z. de eerste elektronenoverdracht samen met de adsorptie van waterstof atomen op het elektrodeoppervlak. Dit mechanisme lijkt op de gerapporteerde waarnemingen voor waterstof evolutie in alkalische oplossingen, wat de hypothese versterkt dat het oplosmiddel een significante invloed heeft op de elektrokatalyse van waterstof.

105

In hoofdstuk 4 presenteren we een grondige spectroelektrochemische studie van de kinetiek van waterstof evolutie en H-UPD in waterige elektrolyten. Het onderzoek omvat een breed pH gebied met een vorming éénkristalijn Pt(111) als gebruikte elektrode. We begonnen met het meten van de ladingsoverdracht weerstand in de H-UPD regio. Uit onze experimenten bleek dat niet alleen de waterstof evolutie in alkalische oplossingen langzamer verloopt, maar ook dat de H-UPD formatie langzamer is. Tafel hellingen in het brede pH gebied (van pH 1 tot pH 13) lieten zien hoe het mechanisme voor de waterstof evolutie verandert, wat impliceert dat het oplosmiddel een belangrijke bijdrage levert als er naar hoge pH-waarden gegaan wordt. Daarna hebben we het Pt (111) oppervlak bedekt met een submonolaag nikkel hydroxide op het oppervlak om de verbetering van de waterstof kinetiek in de aanwezigheid van deze elektropositieve metalen als promotor inzichtelijk te maken. Opnieuw werden impedantie spectroscopie en Tafel plot analyses gebruikt. Onze waarnemingen suggereren dat de aanwezigheid van Ni(OH)$_2$ de waterstof adsorptie reactie barrières verlaagt, omdat het bleek dat niet alleen de HER kinetiek verandert, maar ook de ladingsoverdracht kinetiek van de UPD regio sneller is in aanwezigheid van de promotor. Uit deze observaties stellen wij een nieuw kinetisch model voor dat gebaseerd is op de energetische barrière die door de reorganisatie van het grensvlak water wordt gecreëerd. Aangezien de snelheid van waterstofadsorptie een pH afhankelijke barrière heeft, betekent dit dat de waterstructuur aan het Pt (111) –elektrolyt grensvlak pH afhankelijk is. Daarom zou de kinetiek van ladingsoverdracht sneller zijn als water gemakkelijk wordt gereorganiseerd (lage pH-waarden) en langzamer als het waternetwerk minder mobiel is (hoge pH-waarden). Dit wordt ook bepaald door de potentiaal van maximale entropie, die nauw verwant is met de *potential of zero free charge* (pzfc). Dit laatste wordt bepaald door de ladingsscheiding tussen de metaal elektrode en de elektrolyt oplossing, die op zijn beurt afhankelijk is van de positie van de pzfc. De temperatuur sprong techniek experimenten toonden aan hoe een submonolaag nikkel hydroxide de pzfc dichter bij het evenwicht potentiaal van de waterstof evolutie kan brengen, Dit heeft invloed op de energetische barrière die samengaat

met de beweging van lading door de dubbellaag. Deze studie verduidelijkt dus de moleculaire processen en de langzame reactiesnelheden voor de waterstof evolutie reactie in alkalische oplossingen.

Dit proefschrift laat het belang zien van het oplosmiddel in waterstof elektrokatalyse, met een specifieke focus op water. Hierbij hebben we haar rol als oplosmiddel en als protondonor laten zien en verduidelijken we uiteindelijk het lang lopende probleem van de pH-afhankelijkheid van waterstof evolutie aan platina. Dit proefschrift maakt de weg vrij voor toekomstige verkenningen van oplosmiddel-electrode grensvlaken en voor het op maat maken van elektrokatalytische reacties.

7. List of publications

- I. Ledezma-Yanez, W.D.Z. Wallace, P. Sebastián-Pascual, V. Climent, J.M. Feliu, M.T.M. Koper, "Enhancement of hydrogen evolution rates on platinum electrodes by controlling interfacial water reorganization" (submitted).

- I. Ledezma-Yanez, M.T.M. Koper, "Influence of water on the hydrogen evolution reaction on a gold electrode in acetonitrile solution" (submitted).

- I. Ledezma-Yanez, Elena Pérez Gallent, M.T.M. Koper, F. Calle-Vallejo, "Structure-sensitive electroreduction of acetaldehyde to ethanol on copper and its mechanistic implications for CO and CO_2 reduction". *Catalysis Today,* 262 (2016) 90-94.

- M. C. Figueiredo, I. Ledezma-Yanez, M.T.M. Koper, "*In situ* spectroscopic study of CO_2 electroreduction at copper electrodes in acetonitrile", ACS Catalysis, 6 (2016) 2382–2392.

- I. Ledezma-Yanez, O. Díaz-Morales, M. C. Figueiredo, M.T.M. Koper, "Hydrogen oxidation and hydrogen evolution on a platinum electrode in acetonitrile" *ChemElectroChem,* 2 (2015) 1612-1622.

- O. Diaz-Morales, I. Ledezma-Yanez, M.T.M. Koper and F. Calle-Vallejo, "Guidelines for the rational design of Ni-based double hydroxide electrocatalysts for the oxygen evolution reaction", *ACS Catalysis*, 5 (2015) 5380–5387.

- J. Shen, R. Kortlever, R. Kas, Y. Birdja, O. Diaz-Morales, Y. Kwon, I. Ledezma-Yanez, K. J. Schouten, G. Mul and M.T.M. Koper, "Electrocatalytic reduction of carbon dioxide to carbon monoxide and methane at an immobilized cobalt protoporphyrin in aqueous solution", *Nature Communications* 6 (2015) 8177.

- Lenys Fernández, <u>I. Ledezma</u>, Carlos Borrás, Luis Alfredo Martínez, Hermes Carrero, "Horseradish peroxidase modified electrode based on a film of Co-Al layered double hydroxide modified with sodium dodecylbenzenesulfonate for determination of 2-chlorophenol" *Sensors and Actuators B*, 182 (2013) 625-632.

8. Curriculum Vitae

Isis was born in Barquisimeto, Venezuela, in January 1983. She moved to Caracas to pursue studies at Simón Bolívar University when she was 15 years old, and spent six years reading about world-class literature, philosophy and Latin-American history, striving between a humanistic career (Literature) and a scientific career (Chemistry). In 2007, Isis started teaching basic chemistry courses, which motivated her to start working in the Electroanalysis lab and, later, in the Solid State Physics lab of the university *(ad honorem)*. In her Master thesis, Isis worked on the synthesis and characterization of a family of double layered hydroxides, known as hydrotalcites, as the catalytic support for a biosensor based in an immobilized enzyme. Ultimately she built and tested a biosensor for the detection of halogenated pollutants from wastewaters, based on immobilized horseradish peroxidase. She finished her Chemistry studies in 2011 and moved to The Netherlands, to work in a PhD project under the supervision of Professor Marc Koper. The project was aimed to understand the role of the solvent in the hydrogen oxidation and evolution reactions. In her PhD project, she demonstrated the preferential solvation of protons in not-completely-dry acetonitrile solutions and elucidated the origin of the slow kinetics of the hydrogen evolution on platinum in aqueous alkaline electrolytes. The results of her work are presented in this thesis.

Appendix A: Supplementary Material for Chapter 2
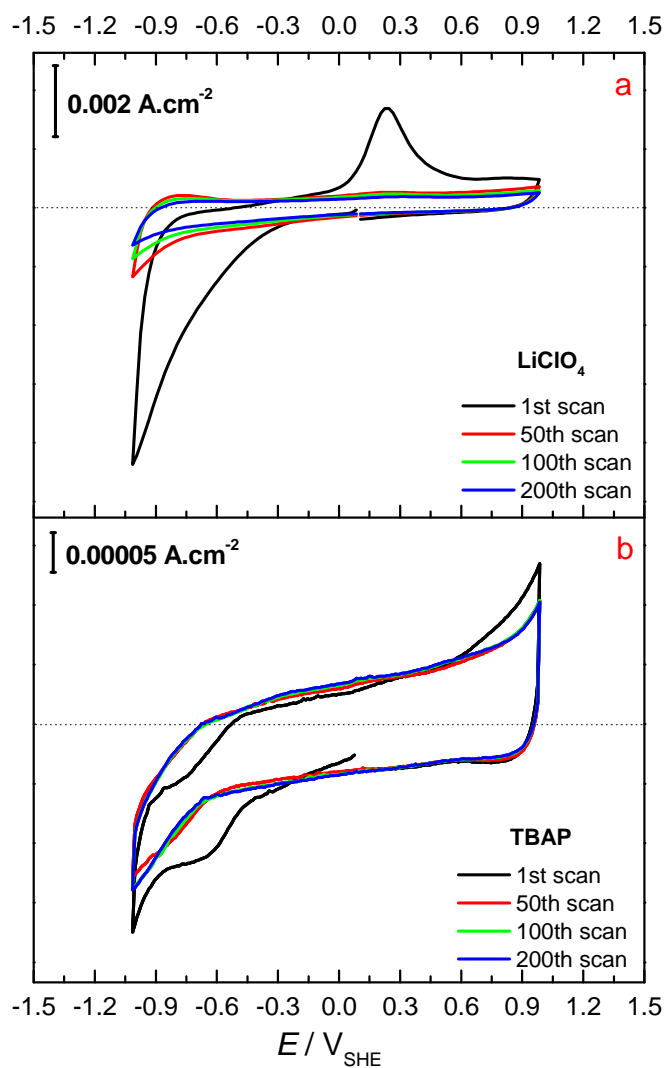
Figure A1. Cyclic voltammetries for a polycrystalline platinum wire in acetonitrile, containing: a) 100 mM LiClO₄ or b) 100 mM TBAP, as supporting electrolytes, under argon atmosphere. Scan rate: 500 mV/s. The horizontal dotted lines mark zero current.

116

Figure A1 shows the evolution in time of the blank voltammetries for polycrystalline platinum in acetonitrile, using $LiClO_4$ (Figure A1a) or TBAP (Figure A1b) as supporting electrolytes, in presence of argon. The scans were taken from 0.1 V_{SHE} towards cathodic potentials and back towards the anodic end potential. The background current for the solution with $LiClO_4$ is two orders of magnitude larger compared with the solution containing TBAP. For the $LiClO_4$ electrolyte, the interfacial water reduction starts at ca. -0.350 V_{SHE}, and in the anodic sweep shows a corresponding oxidation peak at ca. 0.050 V_{SHE}. It is noteworthy mentioning that the peaks observed in the first scan disappear from the second scan on (not shown), and that the system shows a similar double layer from the second till the last scan registered. For the TBAP electrolyte, we observe a redox couple at ca. -0.450 $V_{SHE,}$ assigned to the water reduction and oxidation, and the shape of the first scan disappears from the second scan on, adopting the shape shown in the consecutive scans.
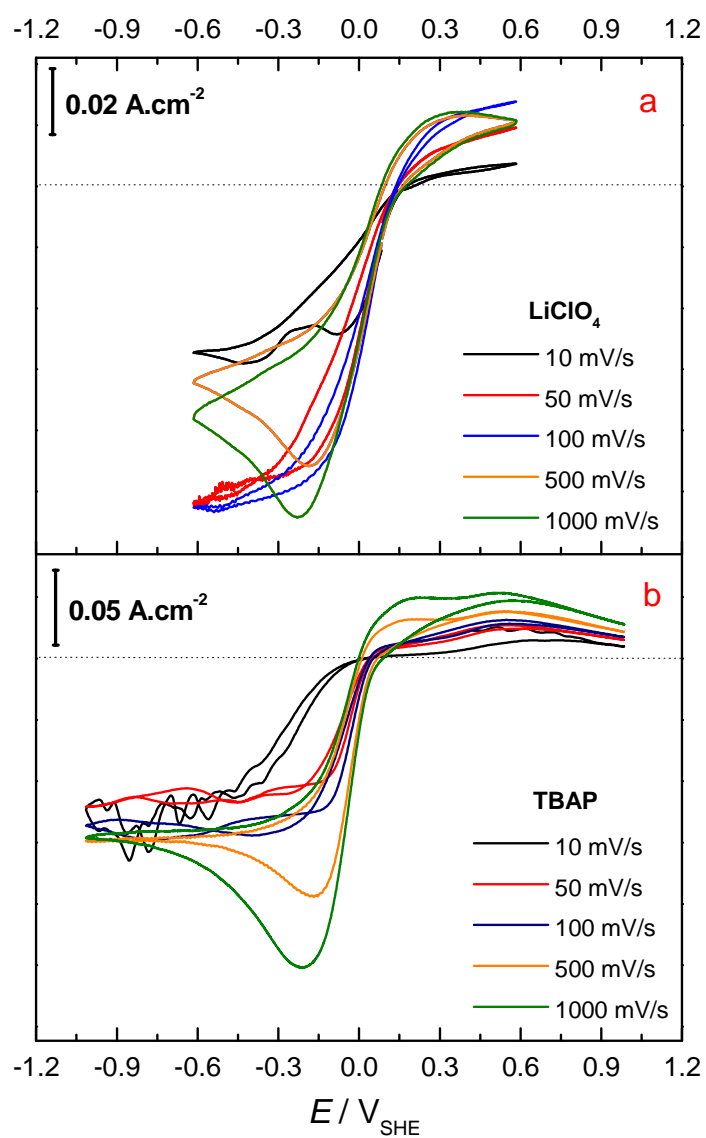
Figure A2. Cyclic voltammetries for a polycrystalline platinum wire in acetonitrile, in presence of 10 mM $HClO_4$, under hydrogen atmosphere. The second cycle is shown for each scan rate. a) 100 mM $LiClO_4$ or b) 100 mM TBAP, as supporting electrolytes. The horizontal dotted lines mark zero current.

Figure A2 shows the voltammetric response towards scan rate variations for polycrystalline platinum in acetonitrile, containing 10 mM $HClO_4$ and saturated with hydrogen, using $LiClO_4$ (Figure A2a) or TBAP (Figure A2b) as supporting electrolytes. The potential window for the measurements in Figure A2a was shortened to avoid formation and adsorption of lithium hydroxide on the electrode surface at low scan rates. The scans were taken from 0.1 V_{SHE} towards cathodic potentials and back towards the anodic end potential. Subfigures A2a and A2b depict an increase in current as a function of scan rate. As a general remark, we point out the fact that the voltammetries tend to get steeper with the increase in scan rate.

Figures A3 and A4 depict the SER spectra for the acetonitrile-$LiClO_4$ and acetonitrile-TBAP respective characteristic bands, under argon atmosphere, hydrogen atmosphere and after the addition of 10 mM of acid, under hydrogen atmosphere. From left to right, all three figures show the δ-C-CN, the ν-C-C, the δ-C-H and the ν-CN modes from the solvent as main features.
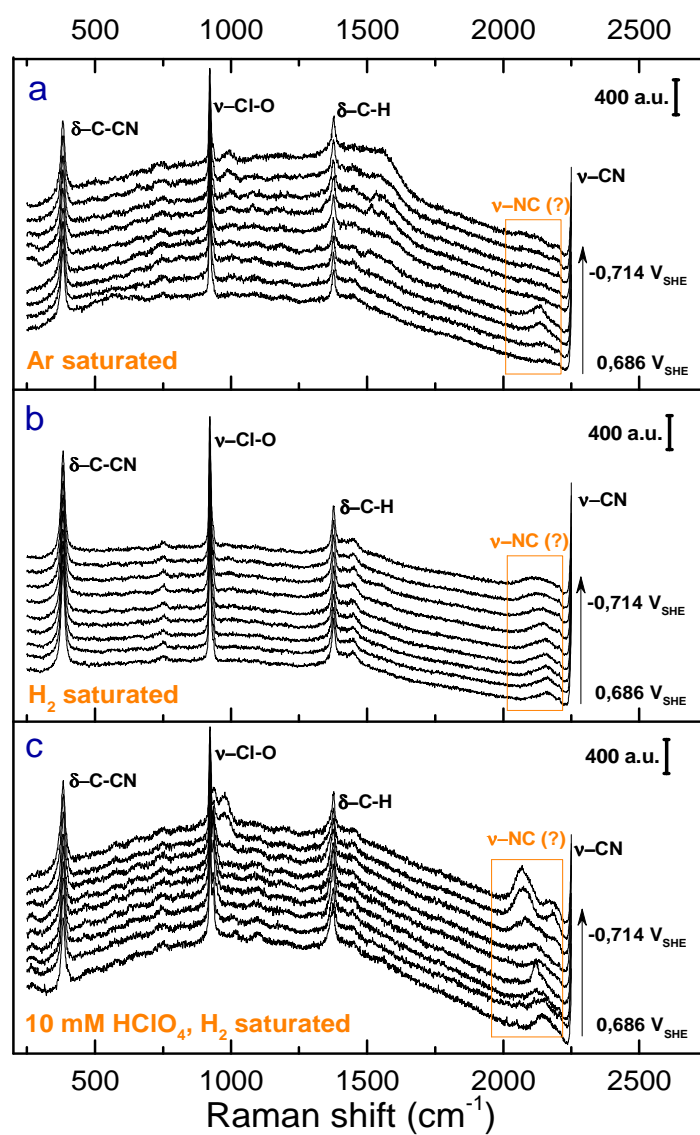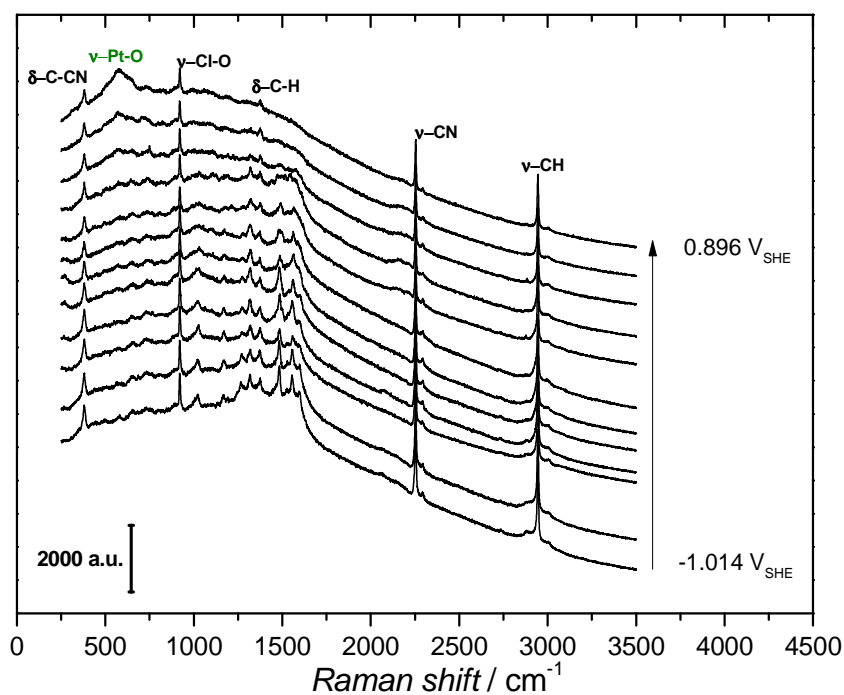
Figure A3. SERS spectra for acetonitrile, containing 100 mM LiClO₄ as supporting electrolyte.
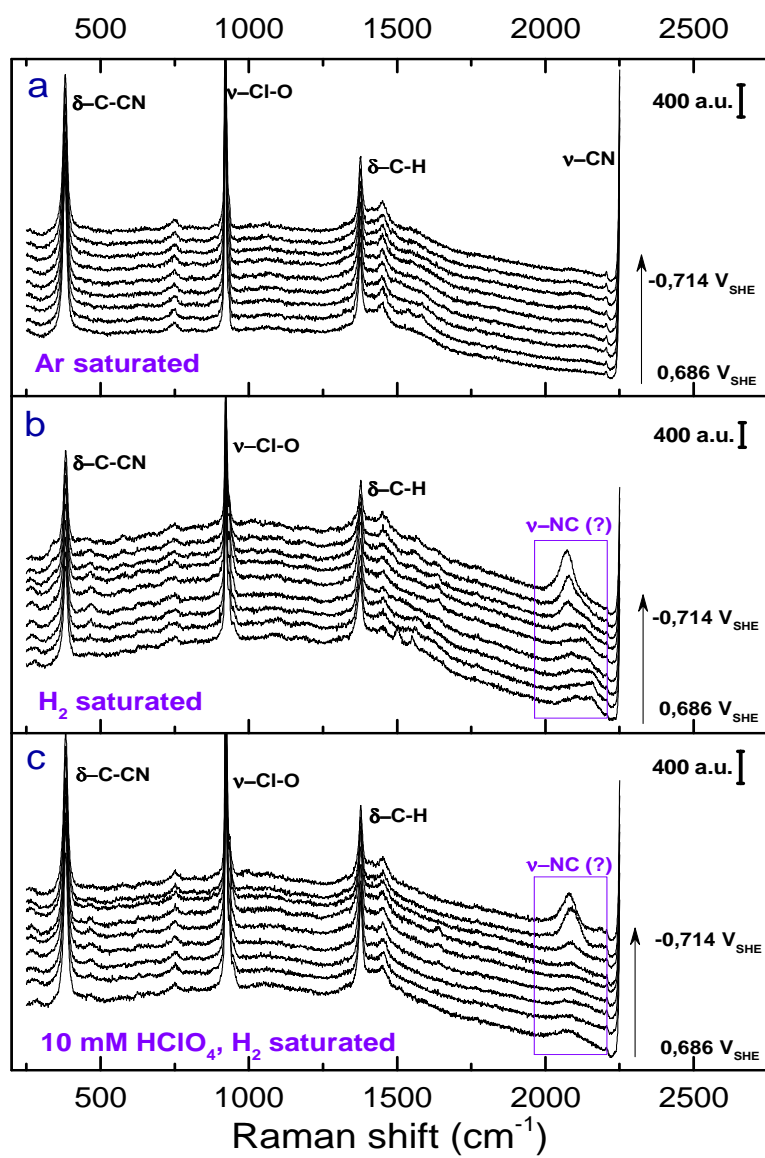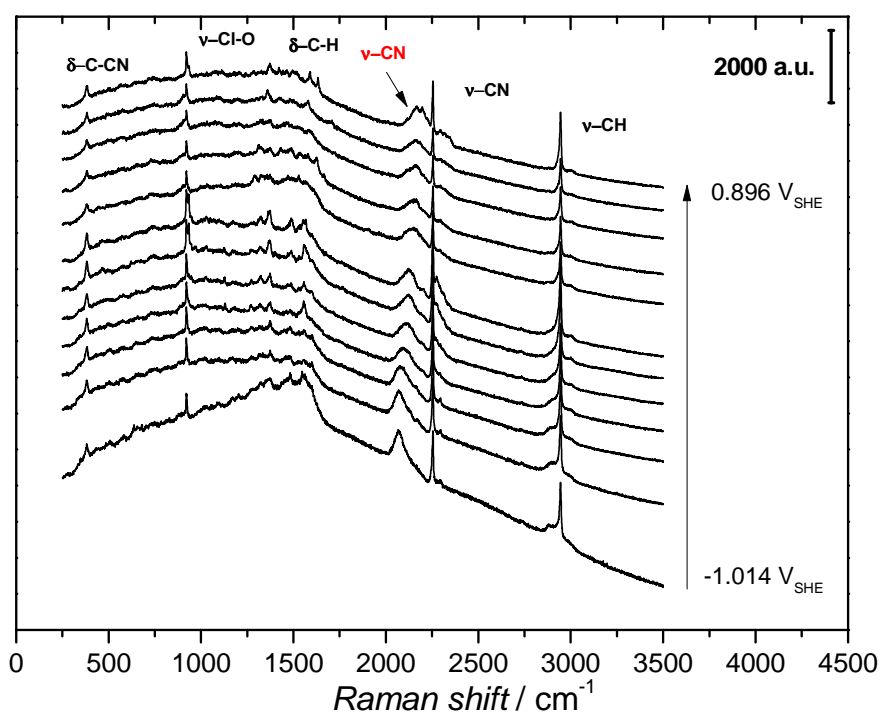
Figure A4. SERS spectra for acetonitrile, containing 100 mM TBAP as supporting electrolyte.

Figure A5 shows the SER spectra for 100 mM of TBAP in presence of acetonitrile and 50 mM of water, under argon atmosphere. We observe the characteristic bands for acetonitrile, and the ν-Cl-O mode for the perchlorate anion from the electrolyte. The spectra were collected from cathodic towards anodic potentials, starting at -1.014 V_{SHE} till 0.896 V_{SHE}, every 0.2 V. As a remarkable feature, we point out the formation of Pt-O around 0.496 V_{SHE}, at 520 cm^{-1}. Interestingly, the band from the ν-NC mode is weak and present only at positive potentials.

Figure A5. SERS spectra for acetonitrile, containing 100 mM TBAP as supporting electrolyte, after adding 50 mM H_2O. Argon atmosphere.

Figure A6 shows the SER spectra for 100 mM of TBAP in presence of acetonitrile and 50 mM of water, saturated with molecular hydrogen. This spectra also shows the characteristic bands for acetonitrile, and the ν-Cl-O mode for the perchlorate anion from the electrolyte. The spectra were collected using the same procedure as described for Figure A5. However, there is no evidence for the formation of Pt-O in presence of hydrogen, and the band corresponding to the ν-NC mode is present in the whole potential range studied.

**Figure A6.** SERS spectra for acetonitrile, containing 100 mM TBAP as supporting electrolyte, after adding 50 mM H_2O. Hydrogen atmosphere.

Appendix B: Supplementary Material for Chapter 4
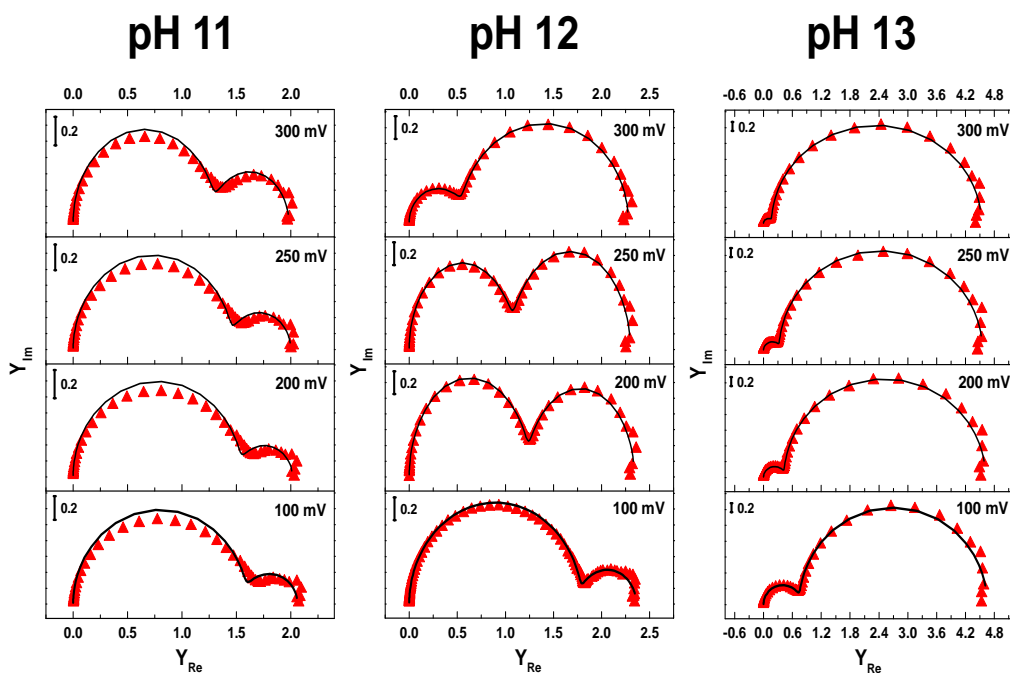
Figure B1. Admittance Nyquist plots for Pt(111) in 0.1 M solutions for different pH values, measured with frequencies ranging from 10 kHz to 0.1 Hz and an amplitude of 5 mV, at 0.1, 0.2, 0.25 and 0.3 V_{RHE}: the dots represent the experimental data points collected, while the solid lines correspond to the fit obtained using the EEC.
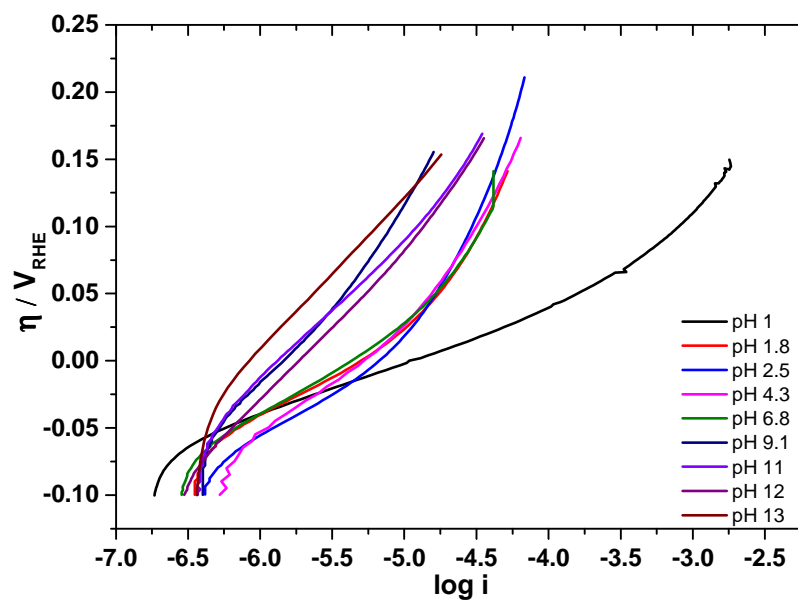
Figure B2. Tafel plots for Pt(111) in solutions with 0.1 M ionic strength and different pH values (see legend). Scan rate: 10 mV.s^{-1}.
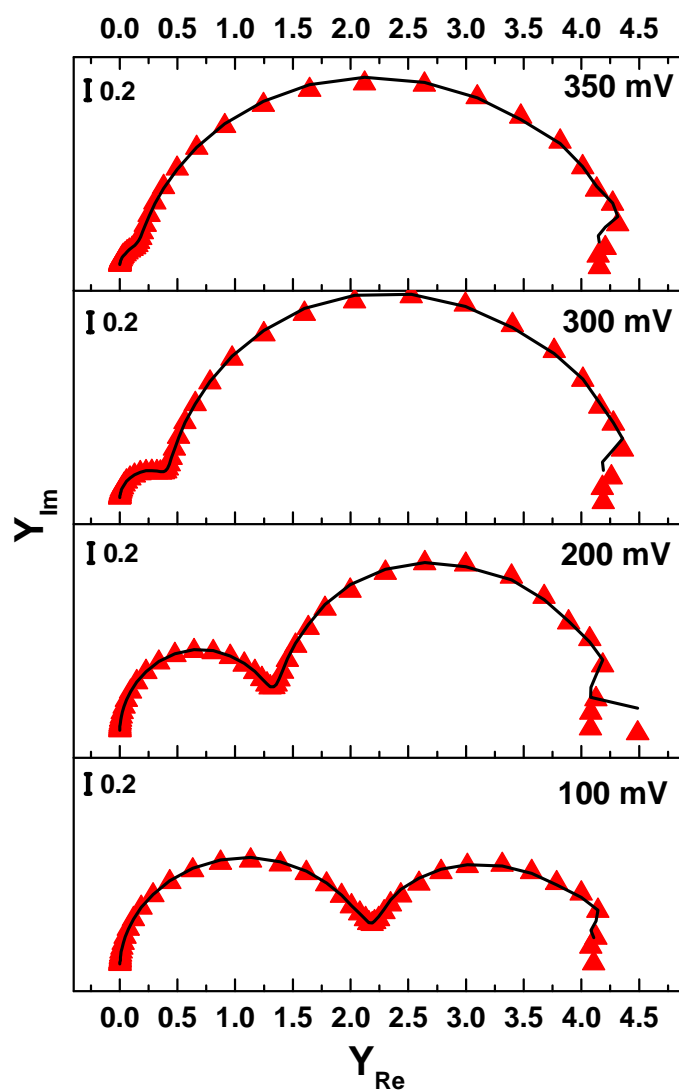
Figure B3. Admittance Nyquist plots for Pt(111) decorated with 0.14 ML of Ni(OH)$_2$ in 0.1 M NaOH (pH 13), measured with frequencies ranging from 10 kHz to 0.1 Hz and an amplitude of 5 mV, at 0.1 V$_{RHE}$: the dots represent the experimental data points collected, while the solid lines correspond to the fit obtained using the EEC.